The metalloproteinase inhibitor Reck is essential for zebrafish DRG development

Andrew Prendergast

A dissertation submitted in partial fulfillment of the requirements for the degree of

Doctor of Philosophy

University of Washington

2013

Reading Committee:

David Raible, Chair

Rachel Wong

Tom Reh

Program Authorized to Offer Degree:

Neurobiology and Behavior

University of Washington

Abstract

The metalloproteinase inhibitor Reck is essential for zebrafish DRG development

Andrew Prendergast

Chair of the Supervisory Committee:

Professor David Raible

Department of Biological Structure

Embryonic development can be viewed as a series of fate choice events in which multipotent cells divide and adopt more specialized function and morphology. The vertebrate neural crest is an example of a multipotent cell population that undergoes this process, ultimately becoming an array of different cell types, including the neurons of the peripheral nervous system. The factors that influence neural crest to make these decisions is still not well-understood. The work presented herein establishes the metalloproteinase inhibitor Reck as a key factor in the development of the dorsal root ganglia, one element of the peripheral nervous system derived from neural crest.

Table of Contents

Chapter I: A review of the neural crest and its contribution to neurogenesis in the peripheral nervous system 1

Chapter abstract 1

Overview 1

Definition of trunk neural crest 2

Divergent neural crest migratory pathways reflect fate restriction of the trunk neural crest 2

Neural crest fate restriction begins long before the observation of overt differentiation markers 3

Factors that specify the neural crest continue to modify neural crest fate proliferation, survival, and fate choice 4

The survival and multipotency of trunk neural crest is maintained by several transcription factors expressed during migration 6

Sox10 promotes neural crest survival, supports glial development, and maintains neural crest multipotency. 6

ErbB/Neuregulin signaling supports neural crest migration and glial development 7

Neural crest are instructed to develop as autonomic neurons by BMP signals emanating from the dorsal aorta 9

BMPs directly promote neuronal fates. 9

BMPs trigger changes in trophic factor dependence. 12

The transcriptional cascade leading to autonomic nervous system differentiation is extensively cross-regulatory 14

Autonomic differentiation begins with the expression of Ascl1. 14

Expression of the Phox2 transcription factors is essential for the continued development of the sympathetic ganglia. 15

Insm1 is activated downstream of Phox2b and promotes proliferation in nascent sympathetic ganglia. 17

HAND1 and 2 mediate specific aspects of noradrenergic differentiation. 17

GATA transcription factors are situated near the end of the sympathogenic transcriptional cascade. 18

Lessons learned from the autonomic transcription factor cascade. 19

Dorsal root ganglia formation occurs in overlapping waves of neurogenesis that can be followed using the Trk receptor family as markers of cell fate 20
DRG neurogenesis is traditionally understood to occur in distinct waves. 20
Ablation of TrkC signaling causes the loss of large-diameter neurons. 21
Loss of TrkB function causes loss of a subset of DRG neurons. 23
Removal of TrkA and its ligand cause loss of most small-diameter neurons. 23
Trk receptor studies are complicated by the fact that Trk receptor expression is not exclusive. 24
The DRG transcriptional cascade is hierarchical and sorts cells into subtypes 25
The neurogenins are the top-tier transcription factors in the DRG transcriptional cascade. 25
The subsequent expression of other transcription factors is essential to dorsal root ganglia development and maintenance 27
Brn3a and Islet1 are initiated after the Neurog factors and cooperate to regulate many targets. 27
Runx transcription factors further refine the dorsal root ganglion sensory neuron population 28
Common features in autonomic and sensory neuronal development 30
Figures 32
Chapter II: The metalloproteinase inhibitor Reck is essential for zebrafish DRG development 40
Chapter abstract 40
Introduction 40
Materials and methods 42
Zebrafish husbandry 42
Transgenic lines 42
Immunohistochemistry 43
Genetic screen 43
Mutation identification 43
Morpholino oligonucleotide knockdown 44
Angiograms 44
mRNA injection 44
In situ hybridization 44

Metalloproteinase activity 45
Transplants 45
Neural crest migration measurements 45
Time-lapse microscopy and cell tracking 46
Drug experiments 46
TUNEL staining 47
Results 47
Sdp is a recessive phenotype involving the loss of DRG neurons 47
All sdp alleles have sequence polymorphisms in the reck gene 48
Metalloproteinases are upregulated in sdp embryos 49
Morpholino oligonucleotide knockdown of reck transcript phenocopies the DRG phenotype observed in sdp 49
Expression of reck rescues DRG in sdp embryos 50
Expression of reck is consistent with a role in the development of neural crest derivatives 50
MO-injected embryos exhibit vasculature defects 51
The requirement for reck in DRG development is cell-autonomous 51
Altered neural crest migration after perturbation of reck 52
Discussion 54
Figures 59
Tables 81

Chapter III: Attempts to identify metalloproteinases subject to Reck inhibition and observation of putative perdurant adult DRG stem cells 85
Chapter abstract 85
Introduction 85
Materials and methods 87
Fluorescence activated cell sorting 87
Zebrafish embryo extract 87
Cell culture 87
Immunohistochemistry 88
Quantitative real-time PCR 88
Morpholino knockdown of metalloproteinase transcripts 88
In situ hybridization 88

Generation of Reck fusion proteins 89
mRNA injection 89
Photoconversion and lineage tracing 89
Results 90
Generation of photoconvertible transgenic embryos for the study of neural crest and examination of cell lineage in DRG 90
Neural crest cells are efficiently isolated from Tg(sox10:eos) embryos using fluorescence activated cell sorting 91
Comparative quantative RT-PCR identifies metalloproteinases that may be of high relevance to neural crest development 91
Morpholino oligonucleotide knockdown of individual candidate MMPs does not rescue sdp 92
Reck fusion proteins are fully functional and suggest that zebrafish Reck is a GPI-linked protein 92
A latent sox10+/neuroD- stem cell exists in the DRG and contributes to later DRG growth 94
Discussion 95
Figures 98
Chapter IV: Summary and future directions 109
Chapter abstract 109
Future experiments to address the Reck signaling mechanism 109
Future experiments to address migratory behavior in neural crest 112
Future experiments to address persistent stem cell function in DRG 112
References 114

Chapter I: A review of the neural crest and its contribution to neurogenesis in the peripheral nervous system

Chapter abstract

Much of the peripheral nervous system (PNS) is derived from trunk neural crest. Trunk neural crest is an initially multipotent cell population that must migrate and undergo cell fate decisions in order to generate the diversity of cell types that exists in the PNS. Here, we discuss the generation of the sympathetic chain ganglia and the dorsal root ganglia from neural crest, specifically focusing on the gene regulatory network that contributes to their devlopment. Neural crest is induced to develop as sympathetic neurons by BMP emanating from the aorta. This initiates a transcription factor cascade beginning with Ascl1. This network involves extensive cross-regulation terminating in the expression of tyrosine hydroxylase and dopamine-β-hydroxylase. DRG are induced to develop by unknown signals; expression of the Neurogenin transcription factors initiates a more sequential cascade ending in the expression of Trk receptors, which are restricted to neuronal subtypes carrying different sensory modalities.

Overview

The majority of the peripheral nervous system originates from the so-called “trunk neural crest.” After the neurulation is complete, the trunk neural crest is situated at the dorsalmost aspect of the neural tube. It must then colonize more ventral aspects of the body by migrating great distances and subsequently undergoing overt differentiation. The timing of these events relative to other major developmental milestones is outlined in Figure 1 for mouse, chicken, and zebrafish embryos. Here, we will primarily discuss neurogenesis in the sympathetic chain ganglia or paravertebral ganglia as well as in the dorsal root or spinal sensory ganglia. The anatomy of these structures and some of their projections is illustrated in Figure 2.

Definition of trunk neural crest

Trunk neural crest is variably defined, but can generally be understood to encompass all neural crest posterior to the hindbrain. Nonetheless, fate mapping studies performed with different techniques in different model organisms have generated an array of boundary definitions and led investigators to propose additional subdivisions. The most prevalent of these is the compartmentalization of the trunk neural crest into vagal, trunk, and sacral neural crest. The rough segment boundaries for these compartments are outlined in Figure 3 for zebrafish and chick embryos (Le Douarin; Martinsen, 2005; Sato and Yost, 2003; Schilling and Kimmel, 1994; Shepherd, 2012; Vaglia and Hall, 1999). These compartments reflect distinct developmental outcomes: in amniotes and mammals, vagal and sacral neural crest both contribute to the enteric nervous system (Pomeranz and Gershon, 1990; Serbedzija et al., 1991) while in fish, the vagal neural crest is the only known source for the enteric nervous system (Shepherd, 2004).

Divergent neural crest migratory pathways reflect fate restriction of the trunk neural crest

Trunk neural crest is specified at the lateral edges of the neuroectoderm; following the completion of neurulation, it exists as a mesenchymal population between the dorsal neural tube and the overlying non-neural epithelium. These cells then migrate to colonize their ultimate targets, along migratory pathways illustrated in Figure 4. Trunk neural crest migrates along two generally recognized pathways—a ventromedial migration that occurs first, and a dorsolateral pathway, into which crest cells enter with some delay (the timing of these events are summarized in Figure 1). However, some investigators refer to other migratory patterns, including intersomitic migration in chick embryos (Le Douarin), as well as multiple ventral migratory streams in both the mouse and chick (Bronner-Fraser, 1986b; Serbedzija et al., 1990).

In all species considered here, the ventromedial migratory stream gives rise to sympathetic neurons, sensory neurons of the dorsal root ganglia, and the glia associated with these neurons (Le Douarin). As a result, the trunk peripheral nervous system across vertebrate taxa is probably derived solely from cells that enter this migratory route. However, the nature of this migration differs somewhat from species to species. In chick and in mouse embryos, this stream passes in part through the sclerotome (a medial subdivision of the somite) (Bronner-Fraser, 1986a; Rickmann et al., 1985; Serbedzija et al., 1990) with fewer cells invading the sclerotome in mice than in chick. In teleost embryos, ventromedially migrating cells travel exclusively between the neural tube and somite (Eisen and Weston, 1993; Lamers et al., 1981; Morin-Kensicki and Eisen, 1997; Raible et al., 1992). Ventromedial migration is segmented such that one distinct stream of migrating neural crest is present in each somite. In mouse and chick embryos, this migration is restricted to the anterior half of each somite (Bronner-Fraser, 1986a; Rickmann et al., 1985); in the zebrafish, this migration is instead restricted to the middle of each somite (Eisen and Weston, 1993; Raible et al., 1992).

Neural crest fate restriction begins long before the observation of overt differentiation markers

Neural crest is essentially homogenous with respect to marker expression both before and during its migration. Does this reflect a general homogeneity of developmental potential? Some evidence suggests that neural crest cells exhibit considerable fate plasticity throughout their migration. Labeled premigratory neural crest cells in chick embryos yield mixed derivatives when examined later (Bronner-Fraser and Fraser, 1988; Frank and Sanes, 1991), although some fate bias is apparent, as neuron-only clones still occur with great frequency (Frank and Sanes, 1991). Lineage labeling experiments performed *in vivo* in zebrafish (Raible and Eisen, 1994) and chick embryos (Krispin et al., 2010) suggest fate restriction occurs early, possibly prior to the initiation of migration in most cases. Experiments in which cultured neural crest is ablated prior to differentiation

selectively depletes particular colony types, verifying this early fate commitment (Sieber-Blum and Sieber, 1984).

Heterochronic transplants—that is, experiments in which cells are transplanted between two different developmental stages—suggest that neural crest fate restriction cannot be overcome by returning those cells to a less differentiated environment (Bronner-Fraser et al., 1980; Le Lievre et al., 1980; Schweizer et al., 1983) though some transplant experiments suggest lineage restriction may not be consistent over developmental time (Baker et al., 1997; Weston and Butler, 1966). Experiments in quail (Baroffio et al., 1988; Dupin et al., 1990; Henion and Weston, 1997; Sieber-Blum and Cohen, 1980) or mouse (Ito and Sieber-Blum, 1993) clonal cultures generally support these experiments, as clones predominantly give rise to a restricted set of cell types and not the full complement of trunk neural crest derivatives. Taken together, the data suggest that neural crest exhibits some commitment and this commitment may occur surprisingly early in development.

Factors that specify the neural crest continue to modify neural crest fate proliferation, survival, and fate choice

Many signaling factors involved in the initial specification of the neural crest from ectoderm have been identified, amongst them: BMPs, FGFs, retinoic acid, and Wnts (reviewed recently in (Milet and Monsoro-Burq, 2012) and elsewhere in this volume). As in many tissues, these signals are reused later in development to influence other aspects of tissue morphogenesis. Consider BMPs, which contribute to neural crest specification through a morphogen gradient/threshold and/or cooperative signaling. Following this initial function, BMPs regulate neural crest delamination and survival. BMPs later play a pivotal role in the specification of sympathetic neurons, and this will be discussed in detail below.

Wnt signaling is known to influence the specification (Chang and Hemmati-Brivanlou, 1998; García-Castro et al., 2002; LaBonne and Bronner-

Fraser, 1998; Saint-Jeannet et al., 1997), delamination (Burstyn-Cohen et al., 2004; Chalpe et al., 2010; De Calisto et al., 2005; Shoval et al., 2006), and migration (Banerjee et al., 2011; Matthews et al., 2008) of neural crest cells (reviewed more extensively in (Klymkowsky et al., 2010)), but it also influences fate choice in trunk neural crest. Wnt1 expression is apparent in neural crest at E8.5 in mouse embryos (Parr et al., 1993) and is maintained for some time after, suggesting that it may continue to influence neural crest development. Conditional inactivation of Wnt signaling in mouse neural crest cells results in loss of melanocyte and sensory neuron lineages (Hari et al., 2002). Hyperactivation of Wnt signaling using a constitutively active beta-catenin expressed in mouse neural crest induces ectopic sensory neuron formation at the expense of other cell types (Lee et al., 2004). However, zebrafish neural crest cells injected with beta-catenin mRNA assume a pigment cell fate at the expense of neurons and glia (Dorsky et al., 1998). Coincident with the latter result, treatment of chick neural crest explants with Wnt3a-conditioned media results in a preponderance of melanocytes at the expense of neurons and glia (Jin et al., 2001). It is likely that the timing of Wnt signaling regulates the potential disparate roles of this signaling pathway in cell lineage specification, as temporal disruption of Wnt signaling results in distinct deficits (Hari et al., 2012; Lewis, 2004).

Retinoic acid, a derivative of vitamin A/retinol, appears to initially regulate whether cells develop as anterior neural plate or neural crest (Villanueva et al., 2002). Later expression from ventral neural tube is positioned appropriately to influence neural crest to develop as neurons (Wagner et al., 1992), possibly via enhanced precursor proliferation. Both isoforms of cellular retinoic acid binding protein (CRABP), an intracellular molecule that binds and transports retinoic acid, and at least one of the retinoic acid receptors (RXRs), RXRα, are expressed in both neural crest and DRG (Dencker et al., 1990; Maden et al., 1991; Maden et al., 1990; Maden et al., 1989; Rowe et al., 1991; Ruberte et al., 1991; Ruberte et al., 1992; Vaessen et al., 1990). Experiments to determine the effect of retinoic acid on cultured quail (Henion and Weston, 1994) and mouse (Ito and Morita,

1995) neural crest cells suggest retinoic acid is both mitogenic and influences cells to develop as sympathetic neurons.

The survival and multipotency of trunk neural crest is maintained by several transcription factors expressed during migration

Sox10 promotes neural crest survival, supports glial development, and maintains neural crest multipotency.

The Sox (SRY-related, HMG box-containing) family of transcription factors contains several members expressed in neural crest (the SoxE subfamily): Sox8, Sox9, and Sox10 (discovered in (Wright et al., 1993) and reviewed in (Haldin and Labonne, 2010)). Of these, Sox10 is notable amongst the SoxE family for its continued expression throughout migration and glial differentiation (McKeown et al., 2005). Sox10 expression is initiated in the neural crest as early as E8.5 in mice (Britsch et al., 2001; Kuhlbrodt et al., 1998a), HH 7/8 in chick (Cheng et al., 2000), St 12 in *Xenopus* (Honoré et al., 2003), and 5SS in fish (Dutton et al., 2001). Its expression is maintained in Schwann cells and satellite glia of the DRG, though in crest-derived sensory neurons, Sox10 is downregulated concurrent with differentiation (Britsch et al., 2001; Cheng et al., 2000; Kim et al., 2003; Kuhlbrodt et al., 1998a; Paratore et al., 2001).

Perturbation of Sox10 function (due to haploinsufficiency) in humans causes Waardenburg-Hirschsprung disease (Kuhlbrodt et al., 1998b; Pingault et al., 1998). This disorder is characterized by phenotypes consistent with aberrant neural crest development: pigment disorders, deafness, and dysfunction of the gastrointestinal tract due to a lack of enervation. Mouse Sox10 mutants have been isolated both by targeted inactivation (Britsch et al., 2001; Paratore et al., 2001; Schreiner et al., 2007; Sonnenberg-Riethmacher et al., 2001) and serendipitous discovery (Herbarth et al., 1998; Kelsh and Eisen, 2000; Southard-Smith et al., 1998). These mutants exhibit pigment deficits, absence of peripheral glia, and they are generally unviable. Surprisingly, DRG in Sox10 mutant mice initially develop normally, but these DRG degenerate over several days, probably

because they lack glial support (Britsch et al., 2001; Sonnenberg-Riethmacher et al., 2001). Other reports suggest that undifferentiated progenitors in the DRG die by apoptosis (Paratore et al., 2001). Work in zebrafish suggests migrating neural crest cells require Sox10 for survival (Carney et al., 2006; Dutton et al., 2001; Kelsh and Eisen, 2000). These results can be reconciled by a model in which Sox10 promotes the survival of a subset of neural crest directly and thereby also indirectly promotes the survival of DRG neurons.

In addition to ensuring the survival of neural crest, Sox10 also appears to maintain neural crest in an undifferentiated, proliferative state. Constitutive activation of Sox10 in cultured neural crest stem cells confers resistance to the differentiating factors BMP2 and TGFβ (Kim et al., 2003). Electroporation of Sox10 into chick neural tube produces cells which migrate and express the crest marker HNK-1, but fail to express other markers of differentiation (McKeown et al., 2005). A limited body of evidence also suggests that Sox10 acts as a top-level, positive regulator of transcription factors in the gene networks leading to both sympathetic ganglia differentiation (Figure 5A-D) and DRG differentiation (Figure 5A, E-G).

ErbB/Neuregulin signaling supports neural crest migration and glial development

The ErbB family of tyrosine kinase receptors contains four members in mammals and are receptors of varying affinity for neuregulin (Nrg) (reviewed in (Citri and Yarden, 2006)). Neuregulin itself comes in multiple isoforms, each of which is generated by alternative splicing from four mammalian loci; of these, Nrg1 appears to be most important to neural crest development (Busfield et al., 1997; Harari et al., 1999; Higashiyama et al., 1997; Marchionni et al., 1993; Steinthorsdottir et al., 2004; Zhang et al., 1997). Signaling through ErbB receptors involves the formation of receptor dimers; these can be homodimers or heterodimers (reviewed in (Citri and Yarden, 2006)). Although ErbB3/B2 and ErbB4/B2 heterodimers are believed to be the functional Neuregulin receptor

complexes, ErbB4/2 function seems to be confined to cardiac development (Gassmann et al., 1995; Kramer et al., 1996; Lee et al., 1995; Meyer and Birchmeier, 1995). While ErbB2 is not itself a high affinity receptor for neuregulin, it remains of interest as its heterodimerization with ErbB3 increases ErbB3's affinity for neuregulin (Sliwkowski et al., 1994). ErbB3 is expressed in mouse DRG as early as E10 (Meyer et al., 1997). The expression of neuregulin splice variants is tissue-specific, with Nrg1 type III expression initiating in the DRG at E10 and remaining strong thereafter (Meyer et al., 1997). ErbB2/3 and Nrg1 type III are therefore the most important ErbB-related factors implicated in neural crest development.

Neuregulin/ErbB signaling appears to serve multiple functions in neural crest development. Though some researchers find no evidence of DRG hypotrophy following Nrg inactivation (Kramer et al., 1996; Meyer and Birchmeier, 1995), others do (Britsch et al., 1998), probably because DRG neurons degenerate between E10.5 and E14.5 in the absence of neuregulin and the effect must therefore be observed at later time points. Zebrafish exhibit somewhat different Nrg requirements—they posses three known Nrg genes; of these, both Nrg1 and Nrg2a appear to be important for normal neural crest development (Honjo et al., 2008).

Targeted deletion of ErbB2, ErbB3, or the Nrg1 locus causes neural crest to pile up in the dorsal root ganglia anlage rather than migrate to its normal ventralmost extent (Britsch et al., 1998); consequently sympathetic ganglia fail to develop (Britsch et al., 1998; Honjo et al., 2008). Migratory phenotypes are also observed in zebrafish ErbB2 and ErbB3b mutants (Honjo et al., 2008). However, in contrast to the results obtained in mouse embryos, neural crest migration is highly disorganized and perhaps excessive in this context. Although the sensory neurons of the DRG initially form normally in mouse mutants of both ErbB3 (Riethmacher et al., 1997) and ErbB2 (Morris et al., 1999; Woldeyesus et al., 1999), these neurons are rapidly lost due to apoptosis. In the comparable zebrafish alleles, DRG do not appear to form at all, though apoptosis is not

excluded as a mechanism for this phenotype (Honjo et al., 2008). Viewed in conjunction with the divergent observations pertaining to neural crest migration and neuregulin dependence, these results suggest ErbB/Nrg signaling may have somewhat different effects in zebrafish than in mammals. However, in either model, ErbB/Nrg signaling is probably involved in neural crest migration and is certainly essential to the development of DRG neurons.

The most reliably occurring phenotype across all alleles of ErbB studied is a failure of peripheral glial development, an outcome that occurs in every studied mutation of ErbB2, ErbB3, or neuregulin (Britsch et al., 1998; Kramer et al., 1996; Lyons et al., 2005; Meyer and Birchmeier, 1995; Meyer et al., 1997; Morris et al., 1999; Riethmacher et al., 1997; Woldeyesus et al., 1999). Nrg1 type III appears to be specifically required for the formation of these glia, as replacing the endogenous locus with an Nrg cassette in which the Ig domain has been disrupted (yielding an Nrg type III analogue that is not susceptible to alternative splicing) is sufficient to rescue loss of Nrg1 function with respect to the glial defect (CITE). ErbB signaling appears to be necessary for several steps in glial development, including fate acquisition (Shah et al., 1994), proliferation of glial progenitors (Lyons et al., 2005), and migration to target (Lyons et al., 2005). Whether the defects observed in DRG neurons following the disruption of ErbB/Nrg signaling are secondary to the glial phenotypes remains an interesting question.

Neural crest are instructed to develop as autonomic neurons by BMP signals emanating from the dorsal aorta

BMPs directly promote neuronal fates.

In mice, neural crest derivatives appear to differentiate overtly roughly in the order with which they terminate their migration (Serbedzija et al., 1990). Under this model, autonomic derivatives are the first to form, followed by dorsal root ganglia (which are situated more dorsally). Melanocytes, derived from the later dorsolateral migratory stream, are the last to develop. It should be noted

that some experiments in chick embryos contradict this order of differentiation, finding instead that DRG neurons and sympathetic ganglia differentiate more or less simultaneously (George et al., 2010; Serbedzija et al., 1989); but other experiments in chick do support the ventral-to-dorsal differentiation sequence model (Krispin et al., 2010). We will discuss the formation of the peripheral nervous system derivatives of the neural crest in the order with which they are classically believed to form, beginning with the development of the sympathetic ganglia and following with the development of the DRG.

The autonomic nervous system is a broad category of peripheral nerves and ganglia subdivided into parasympathetic and sympathetic systems. Parasympathetic nerves project from the central nervous system, synapsing on ganglia located close to or within target organs (Le Douarin). Sympathetic neurons are generally situated as a segmented strip of bilaterally symmetric ganglia lying ventral to and flanking the spinal cord. These are known as the sympathetic chain ganglia or the paravertebral ganglia. These ganglia also receive CNS enervation from preganglionic fibers; the postganglionic fibers then project long distances to enervate target organs (Le Douarin).

A large body of evidence now exists to suggest that exposure to BMPs during dorsoventral neural crest migration specifies the autonomic lineage. However, the role of BMPs in this process appears to be quite complicated. It is clear that several BMPs are expressed by the dorsal aorta, including BMP2 (Lyons et al., 1995; Shah et al., 1996), BMP4 (McPherson et al., 2000; Reissmann et al., 1996), and BMP7 (Reissmann et al., 1996). All three BMPs are capable of increasing the incidence of either neuronal morphologies or autonomic markers such as tyrosine hydroxylase (TH) in culture (Liu et al., 2005; Morrison et al., 1999; Reissmann et al., 1996; Shah et al., 1996; Varley and Maxwell, 1996; Varley et al., 1998; Varley et al., 1995; Wu and Howard, 2001) and these effects are comparable to those observed when neural crest is co-cultured with dorsal aorta explants (Reissmann et al., 1996). Viral expression of a constitutively active BMPR1A receptor in neural crest exerts similar effects

(Varley et al., 1998) and administration of the BMP antagonist Noggin (Schneider et al., 1999) or a dominant negative BMP receptor (Parlier et al., 2008) blocks autonomic specification both in vitro and in vivo.

By what mechanism does BMP treatment increase the density of presumptive autonomic neurons? It does not appear to accelerate the proliferation of autonomic precursors, as BrdU+ neurons are not more prevalent following BMP treatment (Liu et al., 2005; Varley and Maxwell, 1996); furthermore, BMPs neither induce apoptosis directly, nor promote the survival of a committed subset of neural crest cells (Lo et al., 1997; Morrison et al., 1999; Varley and Maxwell, 1996). After implantation with Noggin-soaked agarose beads, chick embryos exhibit colonization of the sympathogenic anlage (as assessed by expression of Sox10), but the expression of markers of noradrenergic fate is not initiated (Howard et al., 2000; Schneider et al., 1999). A nearly identical result is observed when BMPR1A is conditionally deleted from neural crest (Morikawa et al., 2009). These results suggest that although neural crest survives and migrates appropriately, the program of sympathetic neuron differentiation is never induced in the absence of BMP. BMP therefore appears to directly instruct neural crest to adopt autonomic fates.

The conditions under which this instruction can occur appear to be somewhat narrow however, and this has led to confusing results. Neural crest cultures respond to BMP concentrations in a non-monotonic fashion, with lower doses of BMP2 and BMP4 strongly promoting autonomic differentiation. However, this effect falls off dramatically at higher doses (Reissmann et al., 1996; Varley and Maxwell, 1996). Conversely, BMP7 is less potent than BMP2 or BMP4, and exhibits a monotonic relationship between concentration and autonomic induction (Reissmann et al., 1996). There also may be a narrow temporal window in which neural crest is responsive to BMPs as cells treated after some time in vitro or isolated from older embryos are less responsive to attempts to induce autonomic differentiation (Ernsberger et al., 2000; Lo et al., 1997; Reissmann et al., 1996; Varley and Maxwell, 1996; Varley et al., 1995;

Varley et al., 1998). Consequently, neural crest seems to have a very narrow susceptibility to BMP-mediated autonomic specification.

Several investigators have attempted to further characterize the BMP-activated signal cascades affecting sympathetic nervous system development. BMP receptor activation leads to phosphorylation of the R-Smads 1, 5, and 8, which are typically shuttled to the nucleus by Smad4; this is known as canonical BMP signaling (recently reviewed in (Mueller and Nickel, 2012)). Smad4 conditional knockout mouse embryos exhibit normal sympathetic ganglia initially, but by E16.5, ganglion size is reduced as a consequence of reduced proliferation (Morikawa et al., 2009). Surprisingly, R-Smads translocate to the nucleus in sympathetic ganglia even after Smad4 deletion, suggesting that another, as of yet undescribed mechanism may mediate other aspects of BMP-induced sympathetic neurogenesis. Non-canonical BMP signaling is also implicated in noradrenergic differentiation via MAPK and PKA-dependent mechanisms (Liu et al., 2005; Wu and Howard, 2001). We can conclude, perhaps unsurprisingly, that BMP's influence on neural crest is mediated by multiple, partially redundant arms of the BMP signaling pathway.

BMPs trigger changes in trophic factor dependence.

In contradiction with the above evidence, some investigators observe only transient increases in TH+ cell density (Pisano et al., 2000) or extensive apoptosis following BMP administration (Gomes and Kessler, 2001; Song et al., 1998). These findings may reflect the narrowness of the window in which BMPs can promote autonomic fates, but it is perhaps more likely that they reflect changes in neurotrophic factor dependence that BMP enforces as a consequence of its pro-autonomic function. During the development of the vertebrate nervous system, far more neurons are generated than can be retained in the adult organism. In one of the most widely appreciated studies in all of developmental biology, Levi-Montalcini, Hamburger, and investigators following their work established that whether neurons live or die is predicated on their

acquisition of limited growth factors called neurotrophins (reviewed in (Barde, 1989; Levi-Montalcini, 1987)). A variety of neurotrophins and their cognate receptors have now been identified, including the high affinity neurotrophin receptors TrkA, TrkB, and TrkC. As we shall see, these neurotrophin receptors are essential components of all aspects of peripheral nervous system development and serve as some of the earliest indicators of neuronal subtype in both autonomic and sensory lineages.

One consequence of adopting a neuronal fate is an acquired dependence on the neurotrophic factors that bind the Trk receptors. NGF, BDNF, and NT-3 are primarily (but not exclusively) ligands for the TrkA, TrkB, and TrkC receptors, respectively (Hempstead et al., 1991; Hosang and Shooter, 1985; Kaplan et al., 1991a; Kaplan et al., 1991b; Lamballe et al., 1991; Radeke and Feinstein, 1991; Soppet et al., 1991; Squinto et al., 1991). Genetic inactivation of the neurotrophins and their cognate receptors rapidly revealed that sympathetic ganglia rely on neurotrophic signaling throughout their development. TrkA and NGF knockout mice both exhibit reductions in the size of sympathetic ganglia (Crowley et al., 1994; Smeyne et al., 1994); in the case of NGF-/- mice, sympathetic ganglia cannot be identified in dissection by P14 (Crowley et al., 1994). TrkC and NT-3 knockout mice exhibit comparable phenotypes that can be duplicated using NT-3 antiserum injection (ElShamy et al., 1996; Ernfors et al., 1994b; Fariñas et al., 1994; Zhou and Rush, 1995). Signaling through TrkA and TrkC therefore appear to be critical to the maintenance of the autonomic nervous system.

Surprisingly, cells in the sympathetic ganglia exhibit varying reliance on these neurotrophic factors at different developmental timepoints. Initially, cultured sympathetic neurons survive only in response to NT-3, but cultures derived from postnatal ganglia exhibit a significantly stronger survival response to NGF than NT-3 (Birren et al., 1993; DiCicco-Bloom et al., 1993). This switch in neurotrophin requirements coincides with the expected changes in Trk receptor expression, with TrkC expression declining over developmental time and being replaced in

sympathetic ganglia by TrkA (Birren et al., 1993; DiCicco-Bloom et al., 1993). How is this transition initiated? BMP appears to induce TrkC expression either directly or indirectly and suppress TrkA expression (Kobayashi et al., 1998). Since BMP is only transiently available in the sympathetic anlage, it is likely that BMP confers dependence on NT-3/TrkC signaling for trophic maintenance. This dependence is later transferred to NGF/TrkA, perhaps as a consequence of cessation of BMP exposure.

The transcriptional cascade leading to autonomic nervous system differentiation is extensively cross-regulatory

Until this point, we have restricted the discussion of peripheral neurogenesis primarily to signaling molecules and survival factors. However, as in other tissues, these factors inevitably cooperate to activate a transcriptional cascade that in turn establishes the functional and morphological changes that are coincident with differentiation. For the remainder of this chapter, we will discuss the transcriptional networks responsible for the generation of the autonomic and sensory lineages.

Autonomic differentiation begins with the expression of Ascl1.

Achaete-scute homolog 1 (Ascl1) is a proneural, bHLH transcription factor and the first indicator of neuronal differentiation in the autonomic lineage; it is in fact excluded from all other neural crest derivatives (Johnson et al., 1990; Lo et al., 1991). A great deal of evidence suggests that Ascl1 expression is a direct outcome of BMP signaling. The onset of Ascl1 expression coincides with the first exposure of neural crest to BMPs at the dorsal aorta, occurring at 10.5 in mouse (Lo et al., 1991) and HH15 in chick embryos (Ernsberger et al., 1995). The domain of BMP and Ascl1 expressions overlap spatially in the sympathetic anlage and cultured neural crest stem cells express Ascl1 following BMP treatment (McPherson et al., 2000; Shah et al., 1996). Abrogation of BMP signaling using Noggin-soaked beads implanted in the path of migrating neural crest (Schneider et al., 1999) or by knocking out Smad4 in neural crest

(Morikawa et al., 2009) sharply reduces Ascl1 expression. Ascl1 expression also persists when sympathogenic neural crest is deprived of axial signals, a property other genes in the sympathetic program do not share (Groves et al., 1995). Ascl1 appears to occur earlier than any other marker of the autonomic lineage and is dependent on BMP signaling.

Ascl1 is therefore situated to act as a master proneural gene for the specification of the sympathetic lineage. Consistent with this hypothesis, neural crest explants from Ascl1-/- mice fail to form neurons in culture (Sommer et al., 1995) and forced expression of Ascl1 in neural crest stem cells (Lo et al., 1998) or in Xenopus embryos (Parlier et al., 2008) is sufficient to induce neuronal markers. However, studies of targeted inactivation of Ascl1 in an in vivo context yield results inconsistent with this model. Although many markers of sympathetic neurogenesis (such as Phox2a, TH, and DβH) are absent at early stages of autonomic development, others (such as c-Ret, or the neurofilament proteins) are present (Sommer et al., 1995), and more caudal sympathetic ganglia express the full complement of sympathetic markers within a few days (Guillemot et al., 1993; Hirsch et al., 1998; Pattyn et al., 2006). One implication of these results is that Ascl1 is one of a set of at least partially redundant proneural factors and is merely the first to appear. Therefore, in its absence, sympathetic ganglia either fail to form or are hypertrophic due to delayed neuronal differentiation or altered proliferation of precursors.

Expression of the Phox2 transcription factors is essential for the continued development of the sympathetic ganglia.

Ascl1 is perhaps then best considered not as a master regulatory gene, but rather, as a component in a transcriptional network that utilizes extensive cross-regulation and functional overlap rather than one in which an orderly sequence of gene expression leads to differentiation. The paired homeobox Phox2 genes are the next transcription factors expressed in the sympathetic anlage, and their relationship to Ascl1 and other sympathogenic genes typifies

this complexity. Phox2b is expressed in sympathetic ganglia at the earliest stages of ganglion formation and precedes that of Phox2a or later noradrenergic markers (Ernsberger et al., 2000; Pattyn et al., 1997; Pattyn et al., 1999). Targeted inactivation of Phox2b does not impair Ascl1 expression and Ascl1 deletion does not affect Phox2b expression, so initiation of either gene is clearly independent of initiation of the other (Pattyn et al., 1999; Pattyn et al., 2006). Despite this apparent redundancy, the consequences of Phox2b loss-of-function are dire—although neural crest migrates appropriately, colonizes the sympathetic anlage, and expresses Ascl1, by E13.5, all prospective sympathetic neurons are lost due to apoptosis and the sympathetic ganglia are consequently not maintained (Pattyn et al., 1999). Despite its later expression then, Phox2b appears to be hierarchically equivalent to Ascl1.

By contrast, Phox2a is the first transcription factor in the autonomic cascade that seems to depend on prior factors. Phox2a was discovered first, though it is expressed slightly later than Phox2b, being initiated at E10.5 in mouse embryos and HH18 in chicken embryos (Groves et al., 1995; Tiveron et al., 1996; Valarché et al., 1993). Phox2a expression appears to be entirely dependent on Phox2b-mediated activation (Pattyn et al., 1999), although its expression can be induced in culture via forced expression of Ascl1 (Lo et al., 1998). Multiple in vitro studies have established that Phox2a directly binds and activates the promoters for DβH and TH (Kim et al., 1998; Yang et al., 1998; Zellmer et al., 1995), and forced expression of Phox2a in culture or in vivo confirms these results (Lo et al., 1999; Stanke et al., 1999), though these results may depend on the type of cell line employed and whether other signaling factors such as cAMP are present in sufficient quantity (Lo et al., 1998). Taken together, these results show that Phox2a is initiated by first-tier factors and contributes directly to sympathetic differentiation. This behavior will be observed in many of the transcription factors discussed subsequently.

Insm1 is activated downstream of Phox2b and promotes proliferation in nascent sympathetic ganglia.

Insm1 is a zinc-finger transcription factor expressed as early as E9.5 in the sympathetic anlage, making it one of the earliest-expressed genes implicated in sympathetic neuron development (Wildner et al., 2008). Targeted deletion of Insm1 impairs neither Ascl1 nor Phox2b expression, suggesting it is situated downstream of both genes (Wildner et al., 2008). Knockdown at the transcript level in Xenopus embryos reduces the expression of later sympathetic markers (Parlier et al., 2008); similar deficits are initially observed in Insm1 knockout mice, but the expression of these other markers are eventually restored, again reflecting the extensive redundancy of the sympathogenic gene regulatory network (Wildner et al., 2008). Insm1 loss-of-function does permanently reduce the size of sympathetic ganglia, and this is coincident with a reduction in proliferating cells (Wildner et al., 2008). Furthermore, in the absence of Insm1, Ascl1 expression is upregulated; this suggests an important role for Insm1 in terminating Ascl1 expression (Wildner et al., 2008). Insm1 therefore represents a second-tier factor that regulates proliferation and shuts off earlier factors in the network; the latter is a function that is surprisingly rare in the autonomic cascade.

HAND1 and 2 mediate specific aspects of noradrenergic differentiation.

The Hand transcription factors are bHLH transcription factors that appear to mediate the adoption of a restricted set of noradrenergic characteristics. Hand2 is expressed first of the two Hand factors, coming on at E10.5 in mouse embryos in sympathetic ganglion precursors (Cserjesi et al., 1995; Morikawa et al., 2005); both genes are expressed in chick embryos by HH17 (Howard et al., 1999). Both Hand1 and 2 appear to predominantly lie downstream of the other factors discussed in the transcriptional network leading to sympathetic neuron differentiation, but as with most other genes in this network, evidence exists to suggest they also regulate upstream elements. It is difficult to place Hand2 in the hierarchy of the sympathogenic transcriptional regulatory network due to

contradictory evidence. All studies agree that expression of TH and DβH are lost following Hand2 deletion (Hendershot et al., 2008; Lucas et al., 2006; Morikawa et al., 2007; Schmidt et al., 2009) and expanded following Hand2 overexpression (Howard et al., 1999; Howard et al., 2000); there is additionally significant evidence to show that Hand2 directly binds the DβH promoter and activates it (Rychlik et al., 2003; Rychlik et al., 2005; Vincentz et al., 2012).

It is somewhat less clear whether any of the other transcription factors in the network are susceptible to manipulation of Hand2 levels, but the weight of the evidence suggests Hand2 expression is situated later in the hierarchy (Hendershot et al., 2008; Howard et al., 2000; Lucas et al., 2006; Morikawa et al., 2005; Morikawa et al., 2007; Schmidt et al., 2009), with perhaps only Hand1 being wholly dependent on Hand2 function (Morikawa et al., 2007). Hand1 in fact may itself be wholly dispensable for sympathetic neuron formation, as knockouts appear to have normal TH and DβH expression. Investigations as to the mechanism by which Hand2 contributes to sympathetic ganglion development are also murky. Some investigators find reduced proliferation as a consequence of Hand expression (Howard et al., 1999), suggesting Hand promotes cell cycle exit, but other groups have come to the opposite finding (Hendershot et al., 2008). The role of the Hand genes in sympathetic neuron development therefore remains a fertile field of inquiry.

GATA transcription factors are situated near the end of the sympathogenic transcriptional cascade.

Although transcription factor expression in the sympathetic lineage is hardly sequential, the Gata factors appear to be expressed the latest of the genes discussed here. The Gata family of genes contain 6 members in mammals, all of which are zinc-finger transcription factors (Yamamoto et al., 1990). Two of these, Gata2 and Gata3, exhibit specific expression in the sympathetic ganglia and appear to influence their development. Gata2 expression in the sympathetic lineage begins at HH18 (Groves et al., 1995)

appearing slightly later than that of Phox2b, Hand2, and Phox2a (Tsarovina et al., 2004). Gata2 expression is dependent on BMP signaling, and abrogation of Gata2 expression using dominant negative constructs reduces TH staining and causes hypertrophy in sympathetic ganglia (Tsarovina et al., 2004). Surprisingly, the same authors find that Gata2 overexpression does not itself lead to the expression of any other sympathetic marker, but does induce expression of other pan-neuronal markers (Tsarovina et al., 2004). Paradoxically, the function of Gata3 in sympathetic ganglia appears to vary depending on the model organism employed. Gata3 expression is initiated in sympathetic ganglia at E11.5 in mouse embryos (Embryonic expression and cloning of the murine GATA-3 gene, 1994) but apparently is never expressed in the sympathetic ganglia of chick embryos (Tsarovina et al., 2004) and therefore may only be relevant to mammalian sympathetic ganglia development. Targeted deletion of Gata3 in mouse embryos leads to reductions in sympathetic ganglia volume and TH expression (Lim et al., 2000; Moriguchi, 2006). Taken together, the Gata factors appear to be positioned last in the gene regulatory sequence, being primarily responsible for activating the enzymes in the catecholamine biosynthetic pathway or other neuronal differentiation genes.

Lessons learned from the autonomic transcription factor cascade.

What can we glean from this detailed investigation of the autonomic gene regulatory network? The network is initiated by the expression of the top-tier factors Ascl1 and Phox2b at the sympathetic anlage, and this initiation appears to be wholly dependent on BMP signaling emanating from the dorsal aorta. The expression of second-tier factors (defined as those dependent on expression of Ascl1 and Phox2b) follows.

These later factors (Phox2a, Insm1, and Hand2) extensively activate one another and promote the continued expression of the top-tier factors. At the same time, they promote the expression of noradrenergic markers. The autonomic cascade is notable for its lack of negative regulation and its relative

egalitarianism amongst factors. This may reflect the relative simplicity of the sympathetic lineage, which does not exhibit the cell type diversity observed in the DRG. As we shall see, that network is far more hierarchical and less compressed in developmental time.

Dorsal root ganglia formation occurs in overlapping waves of neurogenesis that can be followed using the Trk receptor family as markers of cell fate

As in the autonomic lineage, the sensory neurons of the DRG must acquire neurotrophic factors to survive. In the autonomic lineage, Trk receptor dependence is more or less equivalent across all cells but varies with developmental time. By contrast, Trk receptor requirements in DRG appear to vary primarily with cell subtype. The sensory neurons of the dorsal root ganglia convey several sensory modalities from the periphery to the central nervous system; these are: proprioception, mechanoreception, thermoreception, and nociception. Each sensation is conveyed by distinct neuronal subtypes (reviewed in (Marmigère and Ernfors, 2007)) and consequently, the undifferentiated neural crest must undergo fate decisions to give rise to this neuronal diversity. The expression of each individual neurotrophin receptor is associated with a different sensory modality carried by DRG. Trk expression is complicated by the fact that DRG neurons initially exhibit somewhat broad expression of these receptors, which is then segregated as development progresses.

DRG neurogenesis is traditionally understood to occur in distinct waves.

In chick and mouse embryos, large-diameter, mechanoreceptive and proprioceptive neurons are the first to be born (Frank and Sanes, 1991; Lawson and Biscoe, 1979). These cells express the neurotrophin receptors TrkB and TrkC (Kashiba et al., 2003; Klein et al., 1989; McMahon et al., 1994; Mu et al., 1993). Proprioceptive neurons later downregulate TrkB whereas mechanoreceptive neurons express various combinations of TrkB, TrkC, and Ret before downregulating TrkC (Chen et al., 2006a; Kramer et al., 2006). Mechanoreceptors are therefore often referred to as TrkB+ and proprioceptors as

TrkC+; this is an oversimplification, however, as some coexpression of Trk receptors clearly persists postnatally (Liebl et al., 1997; Rifkin et al., 2000). In a slightly delayed but overlapping phase of neurogenesis, small-diameter, nociceptive neurons are born (Frank and Sanes, 1991; Lawson and Biscoe, 1979). These cells initially express TrkA, although this expression will be later downregulated in the subset of cells that differentiate as non-peptidergic nociceptors (Averill et al., 1995; Chen et al., 2006b; Kashiba et al., 1996; Yoshikawa et al., 2007) (and see (Kobayashi et al., 2005) for a study of TRP/Trk receptor coexpression).

What is the source of this second wave of neurogenesis? Between E10.75 and E13.5 in mouse embryos, Krox20/Egr2+ boundary cap cells located at the dorsal root proliferate and infiltrate the DRG (Maro et al., 2004). Ultimately, these cells will contribute to the Schwann glia of the dorsal root, satellite glia adjacent to TrkB/C+ large-diameter neurons, and a subset of the TrkA+ nociceptive neuronal population (Maro et al., 2004). Investigators working in chick embryos have also observed an additional wave of contralateral neural crest migration into the nascent DRG between HH18-22 (George et al., 2007). As with boundary cap cells, these late-infiltrating cells primarily differentiate as TrkA+ nociceptive neurons (George et al., 2007). Subsequent work by the same authors found that the peripheral layer of the chick DRG, present as early as HH21 (itself partially derived from the contralaterally-migrating cells already described) divide, infiltrate the DRG core, and differentiate primarily as TrkA+ neurons (George et al., 2010). Therefore, this second wave of neurogenesis is probably derived from multiple spatially distinct but lineally related progenitor populations. It is perhaps inappropriate, then, to consider it a single “wave” except insofar as TrkA+ neurons tend to arise later than TrkB/C+ neurons.

Ablation of TrkC signaling causes the loss of large-diameter neurons.

Genetic ablation or other perturbation of a given Trk receptor or its prevalent ligand generally leads to the loss of the neurons conveying the sensory

modality with which its expression is correlated, suggesting that each Trk receptor supports the survival of the submodality with which it is associated. TrkC, the high affinity receptor for NT-3, is the first Trk receptor expressed in DRG, potentially appearing in some migrating neural crest even prior to overt neuronal differentiation (Henion et al., 1995; Kahane and Kalcheim, 1994; Pinco et al., 1993; Rifkin et al., 2000; Tessarollo et al., 1993) although this claim is disputed (Fariñas et al., 1998). Mice in which the TrkC receptor has been genetically ablated (Klein et al., 1994) or disrupted using anti-TrkC antibodies (Lefcort et al., 1996) exhibit significant loss of DRG neurons—about 20% following receptor knockout and about 50% following antibody treatment. In both cases, this loss falls most heavily on large-diameter proprioceptive neurons. Genetic ablation of the TrkC ligand NT-3 leads to a much more severe defect with investigators observing between 50-80% fewer neurons in mutants than in wild type mice (ElShamy and Ernfors, 1996; Ernfors et al., 1994b; Fariñas et al., 1994; Fariñas et al., 1996; Liebl et al., 1997; Tessarollo et al., 1994; Tojo et al., 1995). Clearly, TrkC/NT-3 signaling is essential for the retention of large-diameter neurons.

Yet although proprioceptors are obviously lost following this manipulation (Klein et al., 1994; Kucera et al., 1995), the magnitude of neuronal loss is incompatible with a model where only postmitotic TrkC+ proprioceptors are dependent on NT-3. This discrepancy can be explained if NT-3 is required to support a cycling progenitor population, and indeed some investigators observe a role for NT-3 in maintenance of actively cycling DRG neuronal progenitors *in vivo* (ElShamy and Ernfors, 1996; Memberg and Hall, 1995) or in various culture models (DiCicco-Bloom et al., 1993; Kalcheim et al., 2004). However, others find no evidence that Trk+ cells divide or that progenitors are depleted following NT-3 inactivation (Fariñas et al., 1996; Fariñas et al., 1998). It is likely that NT-3 supports the maintenance of other neuronal subtypes via weaker interactions at the TrkA and TrkB receptors; indeed, apoptotic TrkB neurons are observed following NT-3 loss-of-function (Fariñas et al., 1998) and double knockouts of BDNF and NT-3 do not have an additive effect on neuron loss, suggesting

overlap in their neurotrophin requirements (Liebl et al., 1997). NT-3 may also directly promote or accelerate the adoption of neural or glial fates by undifferentiated neural crest (Chalazonitis et al., 1994; Wright et al., 1992). The requirement for NT-3 is broader than at TrkC+ neurons alone.

Loss of TrkB function causes loss of a subset of DRG neurons.

Interpreting experiments concerning the dependence of nascent DRG on TrkB/BDNF is somewhat more straightforward than for TrkC/NT-3. TrkB knockout mice do not respond to painful stimuli and exhibit approximately 30% fewer DRG neurons than wild-type controls (Klein et al., 1993); knocking out BDNF has a comparable effect on DRG neuron density (Ernfors et al., 1994a; Jones et al., 1994). As is the case for NT-3, BDNF may additionally act as a mitogenic factor on neuronal precursors (Memberg and Hall, 1995) or as a maturation factor (Wright et al., 1992). TrkB/BDNF signaling therefore appears to be somewhat more tightly restricted to cell type than is observed for NT-3.

Removal of TrkA and its ligand cause loss of most small-diameter neurons.

As TrkA is ultimately the most widely expressed of the Trk receptors and since it supports the maintenance of nociceptive neurons (themselves the most prevalent of the DRG neurons), it is perhaps unsurprising that knocking out TrkA leads to massive losses in DRG volume. Following TrkA loss-of-function, mice DRG are reduced 70-90% of wild-type size (Minichiello et al., 1995; Silos-Santiago et al., 1995; Smeyne et al., 1994) The distribution of surviving neurons is increased in cell diameter and surviving embryos do not respond to a variety of painful stimuli, suggesting nociceptors are specifically lost. Reducing or ablating NGF function using antibodies administered or induced in utero (Carroll et al., 1992; Goedert et al., 1984; Johnson et al., 1980; Ruit et al., 1992), or through targeted gene inactivation (Crowley et al., 1994) parallel the results of TrkA loss-of-function almost exactly. As with TrkB/BDNF, then, TrkA signaling appears to correlate with a single cell type—in this case, the small-diameter, nociceptive neurons.

Trk receptor studies are complicated by the fact that Trk receptor expression is not exclusive.

To what extent DRG neuron progenitors are committed to their fates as they express multiple Trk receptor subtypes is somewhat unclear. TrkB+/TrkC+ cells are frequently observed at early stages of DRG development, though their expression eventually resolves into two largely distinct populations by E14.5 in mouse embryos (Fariñas et al., 1998; Kramer et al., 2006). TrkA expression is partially unsegregated from that of TrkB or TrkC expression at E11.5 in mice (Sun et al., 2008) and most TrkA+ or TrkB+ cells in chick embryos also initially express TrkC (Rifkin et al., 2000), though this coexpression disappears rapidly. And though the expression of each of the Trk receptors correlates strongly with the neuronal diameter in concordance with the sensory modality it purportedly represents (TrkC+/proprioceptors being larger than TrkB+/mechanoreceptors being larger than TrkA+/nociceptors (McMahon et al., 1994; Mu et al., 1993; Wright and Snider, 1995)), it must be noted that there is considerable overlap in the size distributions of TrkA-, TrkB-, and TrkC-expressing cells. This may mean that neuronal precursors are merely biased towards one subtype or another, rather than being exclusively restricted to the TrkB/C+ or TrkA+ waves as they are traditionally conceived. Alternatively, and arguably more plausibly, cells may commit to one fate or another long before Trk expression resolves, but express other Trk receptors anyway—perhaps because there is a general requirement for other neurotrophins earlier in their development. A closer dissection of the developmental potential of Trk-expressing cells therefore remains a productive field of inquiry.

Zebrafish embryos present an intriguing alternative strategy for the development of the DRG. Zebrafish DRG consist initially of only one or two crest-derived neurons, but the population of DRG neurons increases gradually over developmental time, apparently supported by local progenitors that express the neural crest/glial marker Sox10 (McGraw et al., 2012). It should be noted that the temporal dynamics of neuronal subtype generation have not yet been tested in

the zebrafish owing to the relatively poor quality of Trk receptor markers in fish relative to other models.

The DRG transcriptional cascade is hierarchical and sorts cells into subtypes

The neurogenins are the top-tier transcription factors in the DRG transcriptional cascade.

The expression of the bHLH transcription factors Neurog1 and Neurog2 in neural crest is correlated with the two major waves of DRG neurogenesis. In mice and chick embryos, Neurog2 is expressed in neural crest just before Neurog1 (Ma et al., 1999; Perez et al., 1999; Sommer et al., 1996), and Neurog1 knockout mice fail to develop nociceptive neurons but retain proprioceptive and mechanoreceptive neurons (Ma et al., 1999). However, Neurog2 is not itself a master proneural gene—Neurog2 knockout mice express Neurog1 with a lag of 12-18 hours and ultimately produce DRG (albeit delayed in their production of proprioceptive and mechanoreceptive neurons); it is only when both Neurog1 and Neurog2 are knocked out that DRG are fully lost (Ma et al., 1999). It is apparent then, that Neurog1 and Neurog2 exhibit some functional overlap, and that Neurog2 activates the early expression of Neurog1. Neurog1 itself seems to be required for the production of nociceptive neurons but is apparently competent to direct the development of proprioceptive and mechanoreceptive neurons as well. Neurog genes therefore appear to serve the role of Ascl1/Phox2b in the DRG cascade—that of the top-tier proneural factor.

Overexpression experiments involving neurogenins have outcomes consistent with the loss-of-function data; forced expression of Neurogenin mRNA greatly increases neurogenesis in Xenopus, zebrafish, and chick embryos. These neurons express sensory markers, and their preponderance comes at the expense of glia derived from the same lineages (Blader et al., 1997; Ma et al., 1996; Perez et al., 1999; Perron et al., 1999). Cultured cortical progenitors respond similarly following Neurog1 viral infection (Sun et al., 2001). Taken

together, these results indicate that Neurogenins not only promote a sensory neuron fate, but also actively suppress the adoption of glial fates.

The fate commitment imposed by Neurogenin expression is fairly strong, albeit not absolute. Zebrafish retain only a single neurogenin gene; knocking it down results in the loss of cranial sensory ganglia, DRG, and all sensory hair cell innervation (Andermann et al., 2002). In the case of zebrafish DRG, cells deficient in Neurogenin1 adopt a glial fate instead (McGraw et al., 2008). In mouse, Neurog2+ cells, while capable of adopting autonomic fates, differentiate as sensory neurons far more frequently than the progenitors from which they are derived (Zirlinger et al., 2002). Neurog2 is in fact capable of compensating for Ascl1 loss of function in specifying sympathetic ganglia (Parras, 2002). Challenging neural tube explants with BMP2, a factor that induces an autonomic fate from undifferentiated crest cells, does not eliminate the expression of Neurog1, Neurog2, or NeuroD in nascent sensory neurons (Greenwood et al., 1999). Due to their powerful proneural influence, Neurog transcription factors appear to be good candidates for top-tier sensory fate determinants.

In the sympathetic lineage, it is clear that BMPs act as a local instructive signal, imparting a neuronal fate on undifferentiated neural crest by initiating Ascl1 expression. Finding a similar signal in the initiation of Neurog expression has been challenging; however, studies in zebrafish suggest that neural crest migration itself might be somehow linked to the onset of Neurog1 expression. Embryos lacking Erbb3 or Erbb2 receptors fail to express Neurog1 in the DRG anlage despite their initially normal neural crest formation and migration (Honjo et al., 2008). Erbb mutants exhibit increasingly disorganized neural crest migration over time, with cells failing to colonize the DRG anlage. Similar results are obtained in observations of Sonic hedgehog (Shh) mutants. Neurog1 expression does not occur in mutants of the Hedgehog receptor Smoothened, and these also exhibit disorganized neural crest migration (Ungos et al., 2003). Neurog1 expression is also lost following inactivation of the gene Reck, which encodes an inhibitor of metalloproteinases (Prendergast et al., 2012). In culture systems,

cells become hypermigratory following Reck inhibition; presumably this is a consequence of elevated metalloproteinase activity increasing extracellular matrix permeability (Morioka et al., 2009). In zebrafish lacking Reck expression, neural crest is also hypermigratory (Prendergast et al., 2012). These results might indicate that migratory behavior itself can act as a key determinant of neuronal fate, perhaps by exposing cells to other, as of yet unknown proneural signals. However, previous data from zebrafish suggests that neural crest fate is set early, long before migration through the DRG anlage (Raible and Eisen, 1994). It therefore remains unclear exactly how Erbb signaling, Shh signaling, or Reck-mediated inhibition of MMPs contribute to DRG specification.

The subsequent expression of other transcription factors is essential to dorsal root ganglia development and maintenance

Brn3a and Islet1 are initiated after the Neurog factors and cooperate to regulate many targets.

Following the expression of the Neurogenin genes, the expression of a host of other proneural transcription factors is initiated in the nascent DRG, forming a complex hierarchical cascade of gene expression (illustrated in Figure 5). Brn3a is a class IV POU domain transcription factor expressed from E10.5 onward in mouse DRG, just as sensory neurons exit the cell cycle (Eng et al., 2001; Fedtsova and Turner, 1995; Zou et al., 2012). Elimination of Brn3a alone has no effect on DRG neuronal density prenatally; however, expression of the neuronal markers Brn3b and Brn3c is reduced and expression of all Trk receptors is reduced prenatally as DRG neurons gradually die (McEvilly et al., 1996; Xiang et al., 1996). Brn3a directly activates the transcription of many later markers of sensory neuron fate, including Runx1, Runx3, and Drg11 (Eng et al., 2007). Coincident with its expression at the end of sensory neuron precursor division, Brn3a also represses the proneural bHLH transcription factor NeuroD1 (Eng et al., 2007). It therefore seems to act as a transitional factor between initial specification and differentiation.

Expression of Brn3a coincides roughly with the onset of the LIM homeodomain transcription factor Islet1, another essential factor in the development of motor neurons (Pfaff et al., 1996). When conditionally deleted from neural crest in mouse embryos using a Wnt1-Cre/loxP-Isl1 transgenic strategy, DRG and sympathetic ganglia exhibit apoptotic degeneration between E11.5 and E14.5. Some investigators have shown that this neuronal loss falls primarily on TrkB- and TrkA-expressing neurons (Sun et al., 2008) while others observe a deficit in TrkC-expressing neurons (Zou et al., 2012). Isl1, like Brn3a, appears to activate later neuronal markers while inhibiting the expression of proneural genes that precede its expression—Runx1 expression is reduced in Isl1 knockout DRG, but NeuroD4 and Neurog1 exhibit increased expression (Sun et al., 2008).

Although neither is essential for initial DRG formation, both Brn3a and Isl1 appear to be critical for the maintenance of DRG neurons as development progresses. Brn3a and Isl1 are colocalized in E12.5 mouse DRG (Dykes et al., 2011). However, Brn3a and Isl1 do not appear to regulate each other's expression. Brn3a knockouts retain Isl1 expression (Dykes et al., 2011; McEvilly et al., 1996) and Isl1 knockouts retain Brn3a expression (Dykes et al., 2011; Sun et al., 2008). Both genes appear to regulate a number of transcripts in common. However, the effect of knocking out both Brn3a and Isl1 on a given transcript is less than the effects of either single knockout added together, suggesting extensive redundancy and cooperativity in their function (Dykes et al., 2011).

Runx transcription factors further refine the dorsal root ganglion sensory neuron population.

Although the Neurogenins exhibit limited specificity with respect to the segregation of DRG neuronal subtypes, the second-tier transcription factors Brn3a and Isl1 do not. We might then expect other transcription factors to promote differential expression of Trk receptors and their concomitant

commitment to proprioceptive, mechanoreceptive, and nociceptive fates. The Runx transcription factors appear to serve this function to a limited extent.

Runx3 is the first of these transcription factors to be expressed in DRG, beginning at E10.5 in mouse embryos (Levanon et al., 2002). Runx3 generally exhibits strong correlation with TrkC+ prospective proprioceptors but is excluded from essentially all TrkB+ cells even if those cells also express TrkC (Kramer et al., 2006; Sun et al., 2008). This expression pattern seems to reflect a direct suppression of TrkB transcription by Runx3. Expressing Runx3 under the control of the Isl1 promoter (making it essentially pan-neuronal in the nascent DRG) strongly suppresses TrkB cell-autonomously and Runx3$^{-/-}$ embryos exhibit an expanded TrkB+ population as well as greater coexpression of TrkB and TrkC (Inoue et al., 2007; Kramer et al., 2006). These results are supported by experiments in a neuroblastoma cell line that expresses TrkB in response to retinoic acid (RA) treatment. Transfection of these cells with Runx3 prior to RA administration occludes TrkB expression; the authors go on to show that Runx3 binds directly to TrkB regulatory elements (Inoue et al., 2007). In addition to suppressing TrkB expression, Runx3 is essential for the maintenance of TrkC+ neurons. TrkC expression is initiated in Runx3$^{-/-}$ mutant mouse DRG (although it is far weaker than in wt embryos), but this expression is rapidly lost (Inoue et al., 2007; Levanon et al., 2002). Runx3 therefore influences cells to assume a proprioceptive fate by inhibiting TrkB expression and promoting TrkC expression.

Runx1 expression is slightly delayed relative to Runx3, appearing at approximately E12.5 in mouse DRG; its expression is strongly correlated with that of TrkA (Kramer et al., 2006; Levanon et al., 2002; Sun et al., 2008). Runx1 loss-of-function only marginally affects the absolute number of neurons present in mouse DRG with investigators variably reporting both increases and decreases in neuronal volume, proliferation, and cell death depending on the developmental timepoint observed (Kobayashi et al., 2012; Yoshikawa et al., 2007). Runx1 does appear to unambiguously influence the expression of calcitonin gene related peptide (CGRP), a marker of peptidergic nociceptive

neurons. Runx1 expression is excluded from CGRP+ cells, and loss of Runx1 function leads to an excess of CGRP neurons (Kramer et al., 2006; Yoshikawa et al., 2007). Runx1 therefore diverts nociceptors towards a non-peptidergic fate at the expense of peptidergic cells.

Common features in autonomic and sensory neuronal development

When viewed in totality, the developmental processes of the autonomic and sensory lineages have much in common. An initially heterogeneous population consisting of committed and multipotent progenitors migrates in phases and along different routes to reach essential niches for their continued development. Signals emanating from sources located along the route of migration (the spinal cord in the case of the DRG and the dorsal aorta in the case of the autonomic lineage) further influence the development of this heterogeneous cell population.

The expression of bHLH neurogenic transcription factors is the earliest indicator of neuronal differentiation in both the DRG and autonomic lineages; DRG sensory neuron fate is indicated by expression of the Neurogenins, whereas autonomic neurons express Ascl1. These transcription factors then initiate a complex cascade of second-tier transcription factors—Brn3a and Isl1 in the case of DRG neurons and the Phox2 factors in autonomic cells. Although both networks exhibit sequential expression of transcription factors, both are characterized by a great degree of redundancy and cross-regulation. The DRG will ultimately produce multiple neuronal types carrying different sensory modalities; despite this, most transcription factors implicated in their development do not appear to exhibit cell-type specificity (with the notable exception of the Runx transcription factors and perhaps Drg11 (Rebelo et al., 2007; Saito et al., 1995)) . In sympathetic ganglia, the gene regulatory network is even more homogenous in its expression and redundant in its function. Each successive factor is expressed in essentially all neurons, and nearly every factor appears to exert positive regulatory effects on most other factors in the network.

Finally, neuronal survival is regulated by the expression and maintenance of a series of neurotrophic Trk receptors. The profile of Trk receptors changes over time in both contexts. In DRG sensory neurons, an initially broad pattern of Trk receptor expression is whittled down such that each Trk receptor defines a particular sensory modality. In contrast, in the autonomic lineage, there appears to be primarily a chronological sequence of Trk receptor expression, such that most cells are dependent on the same neurotrophins for brief developmental intervals.

Figures

Figure 1. Timing of developmental milestones in zebrafish, chick, and mouse embryos with a focus on dorsal root ganglia development. Important events in dorsal root ganglia development are highlighted in red and the timing of each event is expressed in terms of each organism's most commonly expressed staging system (rather than in absolute time). Developmental milestones are presented for **(A)** the zebrafish Danio rerio **(B)** the chicken Gallus gallus and **(C)** the mouse Mus musculus. The following works are cited as support for the intervals displayed in the figure: (1) (Kimmel et al., 1995), (2) (Raible et al., 1992), (3) (Hamburger and Hamilton, 1992), (4) (Schoenwolf and Smith, 1990), (5) (Yang et al., 2006), (6) (Serbedzija et al., 1989), (7) (Carr and Simpson, 1978), (8) (Hamburger et al., 1981), (9) (Downs and Davies, 1993), (10) (Theiler, 2007), (11) (Serbedzija et al., 1990), (12) (Lawson and Biscoe, 1979), (13) (Maro et al., 2004), (14) (Tamarin and Boyde, 1977), (15) (George et al., 2007).

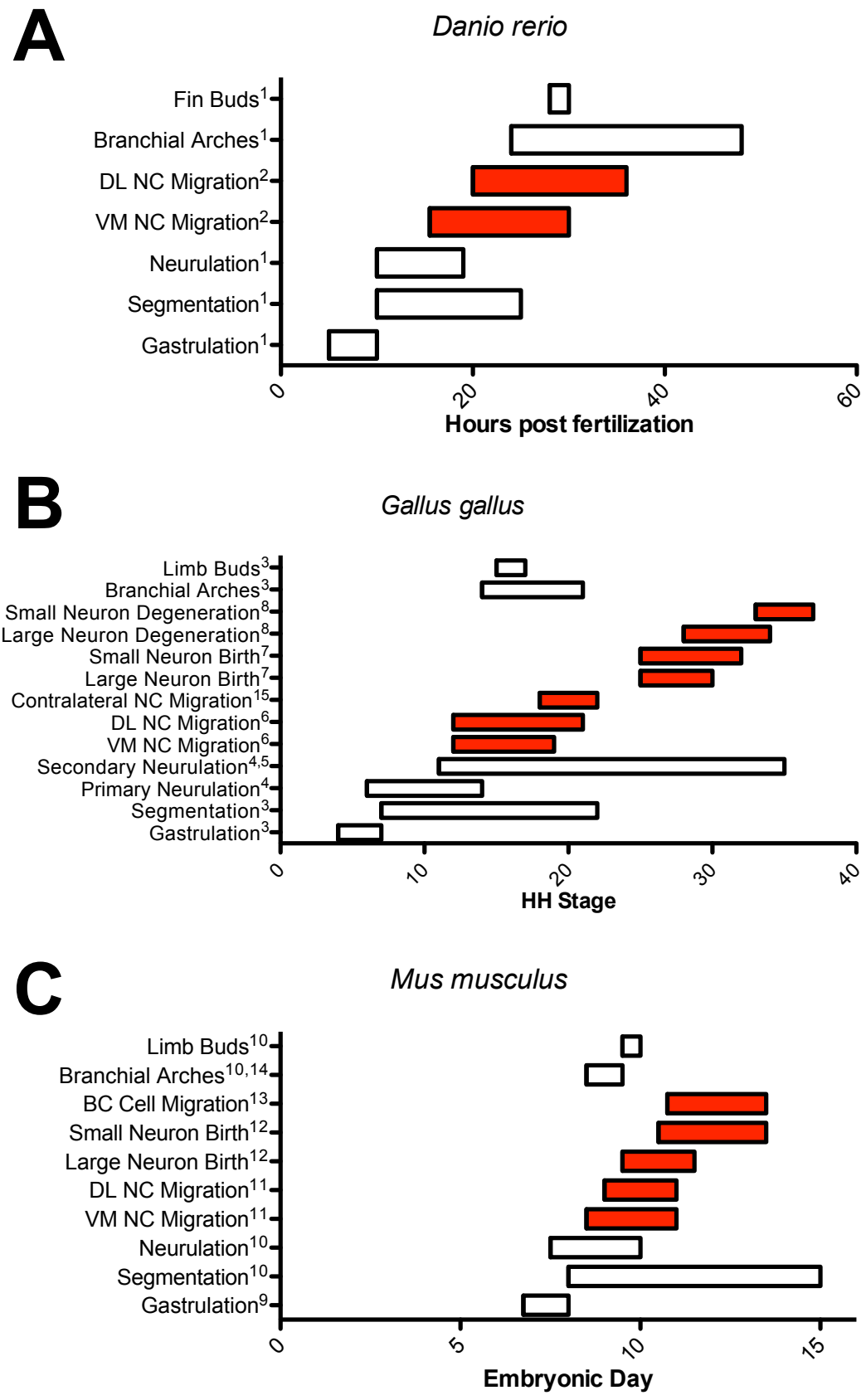
A
Danio rerio
Fin Buds[1]
Branchial Arches[1]
DL NC Migration[2]
VM NC Migration[2]
Neurulation[1]
Segmentation[1]
Gastrulation[1]
0
20
40
60
Hours post fertilization
B
Gallus gallus
Limb Buds[3]
Branchial Arches[3]
Small Neuron Degeneration[8]
Large Neuron Degeneration[8]
Small Neuron Birth[7]
Large Neuron Birth[7]
Contralateral NC Migration[15]
DL NC Migration[6]
VM NC Migration[6]
Secondary Neurulation[4,5]
Primary Neurulation[4]
Segmentation[3]
Gastrulation[3]
0
10
20
30
40
HH Stage
C
Mus musculus
Limb Buds[10]
Branchial Arches[10,14]
BC Cell Migration[13]
Small Neuron Birth[12]
Large Neuron Birth[12]
DL NC Migration[11]
VM NC Migration[11]
Neurulation[10]
Segmentation[10]
Gastrulation[9]
0
5
10
15
Embryonic Day

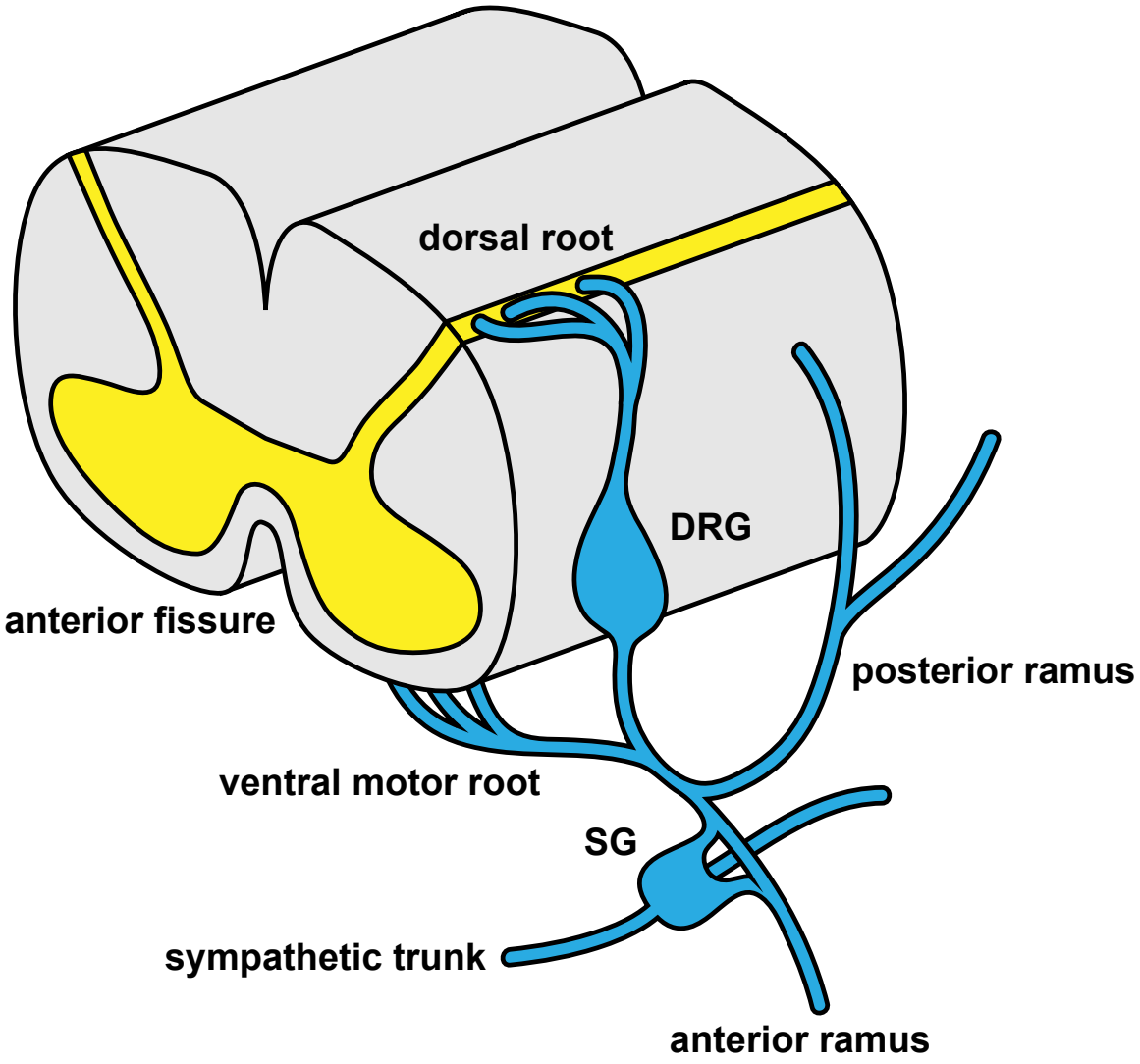

Figure 2. Some of the PNS derivatives of the trunk neural crest. A single segment of spinal cord is diagrammed along with one hemisegment of adjacent peripheral nervous system tissue. Based on images from (Goldstein, 2001) and modeled as mammalian tissue. Although the DRG and SG are derived entirely from neural crest, PNS nerves will also contain neuroectodermally-derived fibers (e.g. the ventral motor root).

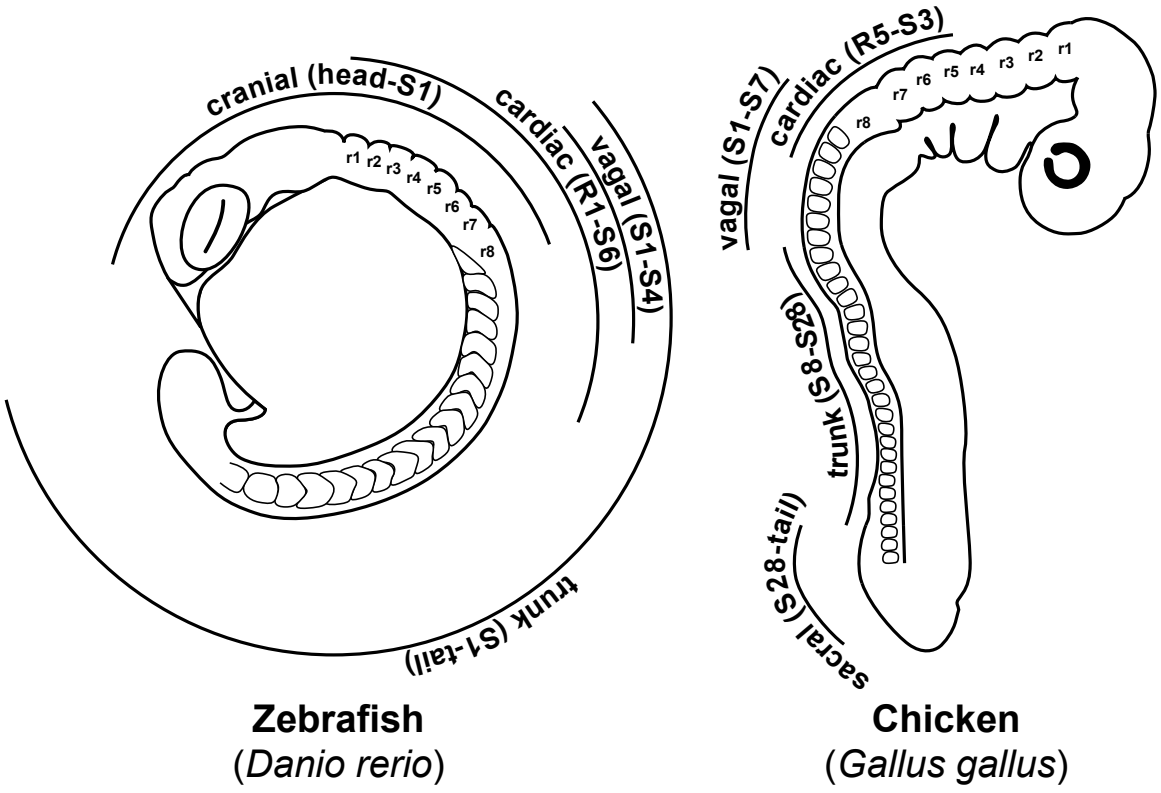

Figure 3. Regionalization of neural crest. A schematized 18SS zebrafish embryo is displayed at left and an HH18 chick embryo is displayed at right (based on images from (Kimmel et al., 1995) and (Hamburger and Hamilton, 1992), respectively).

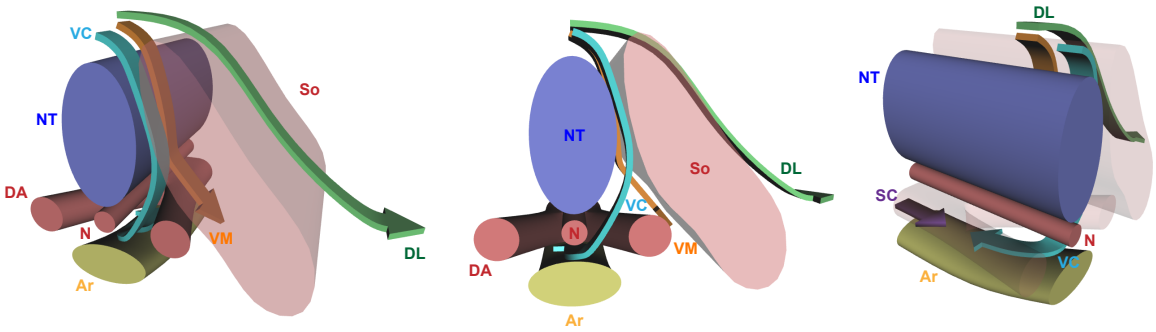

Figure 4. Migratory pathways of trunk neural crest. Trunk neural crest initially migrates along a ventromedial (VM) pathway. The exact route this pathway takes depends on the model organism—in mice and chicken embryos, these cells infiltrate the sclerotome while in fish, they travel between the neural tube and somite. This migratory stream gives rise to the autonomic lineage as well as the sensory neurons and glia of the DRG. A slightly delayed migratory stream travels between the somite and the overlying epidermis; this dorsolateral (DL) pathway gives rise to pigment cells. Also shown is the migratory pathway of the vagal neural crest (VC), which is exposed to inductive axial signals and then colonizes the developing gut.

Figure 5. Gene regulatory network leading to dorsal root ganglia differentiation, gliogenesis, and autonomic nervous system development. We summarize diverse sources of evidence in this figure, and it is possible that any given linkage may or may not be direct, since there is a relative paucity of studies that establish direct binding between transcription factors and their targets. We have cited each linkage and described the type of study done in support, so readers can draw their own conclusions as to the strength of the link. Thicker lines indicate direct binding studies. **(A)** The early/gliogenic component of the PNS transcriptional network. Sox10 directly activates the transcription of myelin-specific genes, but also activates top-tier autonomic and sensory transcription factors. **(B)** Initial signaling steps that specifies the neurons of the sympathetic ganglia. BMP2/4/7 signaling activates a transcriptional cascade leading to DβH and TH transcription via Ascl1 and Phox2b. **(C)** Second-tier transcription factors in autonomic specification. Note the extensive cross-regulation in this module. **(D)** Later events in autonomic specification. Gata and Hand transcription factors are the last to be expressed; DβH and TH indicate overt autonomic neuronal differentiation. **(E)** Initial steps in the gene regulatory network that specifies the neurons of the dorsal root ganglia. An unknown combination of signals initiates the expression of Neurogenins, which cooperate to activate downstream neurogenic factors. **(F)** Second-tier transcription factors in sensory specification. In contrast to the sympathetic gene regulatory network, the program for specification in DRG is more hierarchical and generates a diversity of cell types through the restricted expression of survival mechanisms and cell-type-specific transcription factors. **(G)** Later events in sensory specification. Runx transcription factors refine Trk receptor expression to help define particular neuronal subtypes. * There are several *neuroD* genes, each repressed by Isl1 and Brn3a to a different extent; here they are condensed to a single unit for clarity. ** This result was obtained in zebrafish, which has only one *neurog* gene—it is therefore difficult to extrapolate how this regulatory interaction would appear in mammals, which have two *neurog* genes. The following works are cited as support for the interactions displayed in the figure: (1) (Ma et al., 1999), (2) (Dykes et al., 2011), (3) (Sun et al., 2008), (4) (Eng et al., 2007), (5) (Kramer et al., 2006), (6) (Perez et al., 1999), (7) (Lee et al., 2008), (8) (Yoshikawa et al., 2007), (9) (Nakamura et al., 2008), (10) (Chen et al., 2006b), (11) (Pattyn et al., 1999), (12) (Schneider et al., 1999), (13) (Morikawa et al., 2009), (14) (Liu et al., 2005), (15) (Howard et al., 2000), (16) (Lo et al., 1998), (17) (Castro et al., 2011), (18) (Wildner et al., 2008), (19) (Yang et al., 1998), (20) (Parlier et al., 2008), (21) (Kim et al., 1998), (22) (Zellmer et al., 1995), (23) (Lo et al., 1999), (24) (Stanke et al., 1999), (25) (Tsarovina et al., 2004), (26) (Moriguchi, 2006), (27) (Morikawa et al., 2007), (28) (Hendershot et al., 2008), (29) (Rychlik et al., 2003), (30) (Rychlik et al., 2005), (31) (Vincentz et al., 2012), (32) (Schmidt et al., 2009), (33) (Lucas et al., 2006), (34) (Xu et al., 2003), (35) (Peirano et al., 2000), (36) (Britsch et al., 2001), (37) (Peirano and Wegner, 2000), (38) (Kim et al., 2003), (39) (McKeown et al., 2005), (40) (Carney et al., 2006), (41) (Teng et al., 2008), (42) (Mundell and Labosky, 2011).


B
(38)
(38)
(38)
(38)
(38)
(14)
MAPK
(13)
Smad4
(18)
(12, 16)
(17, 18, 20)
BMP2/4/7
ascl1
A
(39)
(39, 41, 42)
(7)
(7)
(35, 37)
(7, 36, 38)
foxd3
sox10
erbb3
mpz
myelinating glia
plp
E
(40**)
(40**)
(4)
(3)
(6)
(1)
(6)
neurog2
neurog1
neuroD*
B
C
D
A
E
F
G

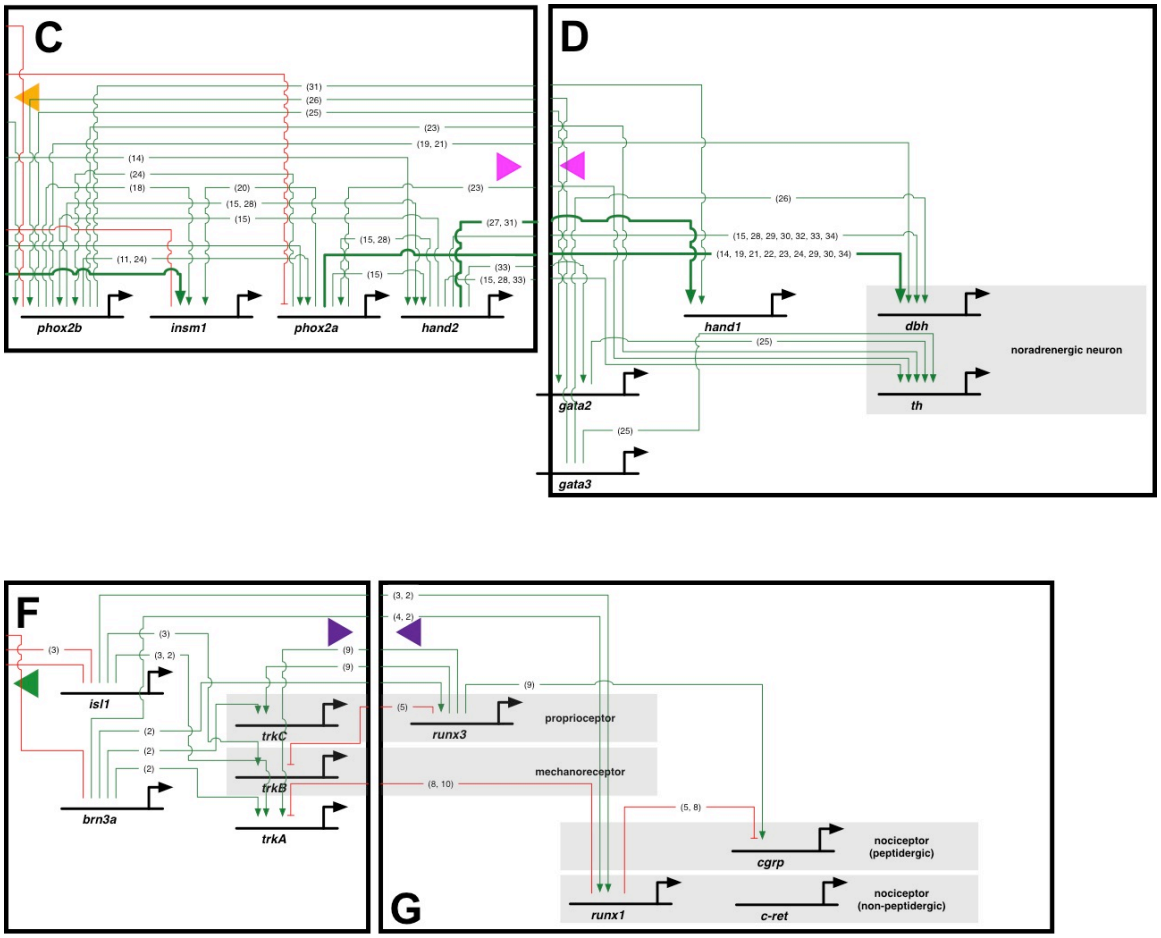
C
(31)
(26)
(25)
(23)
(19, 21)
(14)
(24)
(18)
(20)
(15, 28)
(15)
(23)
(27, 31)
(15, 28)
(11, 24)
(33)
(15, 28, 33)
(15)
phox2b
insm1
phox2a
hand2
D
(26)
(15, 28, 29, 30, 32, 33, 34)
(14, 19, 21, 22, 23, 24, 29, 30, 34)
hand1
dbh
noradrenergic neuron
(25)
gata2
th
(25)
gata3
F
(3)
(3)
(3, 2)
(9)
(9)
isl1
(2)
(2)
(2)
trkC
trkB
brn3a
trkA
G
(3, 2)
(4, 2)
(9)
(5)
runx3
proprioceptor
mechanoreceptor
(8, 10)
(5, 8)
cgrp
nociceptor
(peptidergic)
runx1
c-ret
nociceptor
(non-peptidergic)

Chapter II: The metalloproteinase inhibitor Reck is essential for zebrafish DRG development

Chapter abstract

The neural crest is a migratory, multipotent cell lineage that contributes to myriad tissues, including the sensory neurons and glia of the dorsal root ganglia (DRG). To identify genes affecting cell fate specification in neural crest, we performed a forward genetic screen for mutations causing DRG deficiencies. This screen yielded a mutant lacking all DRG; we named this mutant *sensory deprived* (*sdp*). We identified a total of four alleles of *sdp*, all of which possess lesions in the gene coding for reversion-inducing cysteine rich protein containing Kazal motifs (RECK). RECK is an inhibitor of metalloproteinases previously shown to regulate cell motility. We found *reck* function to be both necessary for DRG formation and sufficient to rescue the *sdp* phenotype. *Reck* is expressed in neural crest cells and is required in a cell-autonomous fashion for appropriate DRG sensory neuron formation. In the absence of proper *reck* function, sensory neuron precursors fail to migrate to the position of DRG formation, suggesting that this molecule is critical for proper migration and differentiation.

Introduction

During normal embryonic development, cells are often generated in locations far removed from where they must differentiate. Cell migration is important in the formation of many tissues, and the dysregulation of migration has drastic consequences for embryos and adult organisms alike. Neural crest is a transient cell lineage that gives rise to tissues including, but not limited to: cartilage and bone of the craniofacial skeleton, secretory neuroendocrine cells, pigment cells, and many of the neurons and glia of the peripheral nervous system (Le Douarin). Neural crest is specified as a limited cell population at the lateral border of neural and non-neural ectoderm; it must then migrate in regulated phases and expand to generate these derivatives. All vertebrate taxa

possess neural crest, and the mechanisms that distinguish neural crest from all other cell types are considered to have been critical in the origin and evolution of the vertebrate clade (Gans and Northcutt, 1983; Knecht and Bronner-Fraser, 2002).

The relationship between neural crest differentiation and migration is poorly understood. Most studies have identified molecules crucial to early events in migration, such as delamination from the neuroectoderm or maintenance of neural crest segmentation. However, little attention has been paid to the cues that terminate migration, an essential condition for appropriate neural crest cell differentiation. Furthermore, although studies have defined a handful of guidance factors and extracellular matrix cues that direct neural crest to its targets, it is unclear how these migratory cues interact with specific neural crest fate decisions.

Dorsal root ganglia (DRG) are a crest-derived, segmentally arrayed series of sensory neurons and their associated glia that detect pain, temperature, mechanical and proprioceptive stimuli. Expression of the *neurogenins (neurog)*, a family of bHLH transcription factors, is currently the earliest known indicator of DRG neuronal identity (Greenwood et al., 1999; Ma et al., 1999; Perez et al., 1999). In the zebrafish, *neurog1* is essential for the formation of DRG neurons (Andermann et al., 2002; Cornell and Eisen, 2002); in its absence, cells differentiate as myelinating Schwann cells (McGraw et al., 2008). Although *neurog* transcription factors clearly determine sensory neuron identity, the mechanism by which their expression is initiated is unclear.

To identify genes implicated in the initial cell fate decisions in DRG, we conducted a mutant screen in the zebrafish for mutants lacking DRG sensory neurons. We isolated a mutant, *sensory deprived* (*sdp*), in which neural crest derivatives form normally with the exception of the DRG. Subsequent work mapped the associated mutation to the gene encoding RECK (reversion-inducing, cysteine-rich protein containing Kazal motifs), an inhibitor of

metalloproteinases (Takahashi et al., 1998). *reck* has previously been implicated in the development of the mammalian cortex (Muraguchi et al., 2007) and circulatory system (Oh et al., 2001). In cell culture studies, loss of *reck* function is associated with a hypermigratory phenotype (Morioka et al., 2009; Silveira Corrêa et al., 2010), presumably because upregulated metalloproteinase activity allows cells to more easily permeate the extracellular matrix. This cell migratory behavior is reflected in studies of human cancers, which are more aggressive following RECK inactivation (Clark et al., 2007). Our results suggest a mechanistic link between termination of migration and initial differentiation of sensory neuron precursors from the neural crest.

Materials and methods

Zebrafish husbandry

Zebrafish were maintained at 28.5ºC on a 14h/10h light/dark cycle following established methods and IACUC standards (Westerfield). Embryos were maintained in E2 medium, and staged according to the standard manual (Kimmel et al., 1995). DRG were identified using Tg(*neurog1:egfp*)^{w61} (McGraw et al., 2008).

Transgenic lines

The 4.9 Kb *sox10* promoter (Carney et al., 2006), fluorescent protein Eos (Wiedenmann et al., 2004) (Evrogen) or nls-Eos, and a polyadenylation sequence (Kwan et al., 2007) were Gateway-cloned (Invitrogen) to generate pSox10:Eos/pSox10nls-Eos; clones were microinjected with Tol2 transposase to generate germline transgenics *Tg(sox10:eos)*^{w9} and *Tg(sox10:nlseos)*^{w18} as previously described (Fisher et al., 2006).

Immunohistochemistry

Embryos were stained with the antibodies mouse α-Elavl1 (Invitrogen), 1:500; rabbit α-GFP (Invitrogen) 1:1000; mouse α-acetylated tubulin (Sigma) 1:5000, mouse α-MF20 (Developmental Studies Hybridoma Bank, University of Iowa) 1:100, rabbit α-Sox10 (gift of Sarah Kucenas, University of Virginia) 1:500, as previously described (Westerfield) and imaged by confocal microscopy.

Genetic screen

We treated *AB males with 3 mM ethylnitrosourea (Solnica-Krezel et al., 1994). F_3 progeny were screened by immunostaining for Elavl1. *Sdp*^{w15} was identified in the *AB background during screening. Three additional alleles were identified: *sdp*^{w13} by complementation screening against *sdp*^{w15} carriers; *sdp*^{w12} and *sdp*^{w14} were isolated as novel mutations and later established as *sdp* alleles by complementation.

Mutation identification

sdp^{w12} heterozygotes were outcrossed to the Wik strain and F_2 progeny were subjected to bulked segregant analysis using SSLP markers followed by analysis of individuals, as described (Bahary et al., 2004). Zebrafish *reck* sequence was generated by alignment of ESTs identified by BLAST search using *M. musculus* RECK protein as the search string, and used as a template to clone the zebrafish cDNA by PCR. Staged embryos were homogenized in Trizol (Invitrogen), and total RNA was isolated by column purification (Qiagen). RNA was treated with DNAse I (Fermentas) to remove genomic DNA and reverse transcribed (Invitrogen). Amplicons were cloned into pCR4-TOPO (Invitrogen) and sequenced.

To identify *sdp*^{w12} mutant embryos, tissue was homogenized by overnight incubation in 200 µg/µL proteinase K. A 233 bp amplicon was PCR-amplified from genomic DNA using primers F: 5′-GAATCTCCACCCATCGCCAAGATG; R:

5′-GAATGTTAGCAGCTGTGAGGTTTG and digested with AvaII (NEB), which cuts the wildtype product.

Morpholino oligonucleotide knockdown

A splice-blocking morpholino oligonucleotide (MO) with the sequence CAGGTAGCAGCCGTCACTCACTCTC was generated based on prediction of efficacy by the manufacturer (GeneTools). This MO targets the *reck* exon 7/intron 7 boundary. Injected embryos were processed for cDNA as above. We designed primers flanking intron 7 (F: 5′-CATCAACAACTCACTACCAGGAGC, exon 7; R: 5′-GGGTGTAGTCTGGTGTAGTTCTCC, exon 8) to detect appropriately spliced *reck* transcript.

Angiograms

Tg(fli1a:egfp)^{y1} embryos (Lawson and Weinstein, 2002) were injected at 48 hpf in the sinus venosus with a 40% solution of Qdot fluorescent nanocrystals (Invitrogen) as previously described (Kamei et al., 2010; Weinstein et al., 1995) and imaged using an Olympus FluoView FV-1000 confocal microscope.

mRNA injection

Wildtype and *sdp*^{w12} *reck* coding sequences were ligated into pCS2p+, linearized with NotI and transcribed *in vitro* with SP6 polymerase to generate capped, polyadenylated mRNA (Ambion). A range of mRNA concentrations was injected into embryos derived from a cross between *Tg(neurog1:egfp)/sdp*$^{w12/+}$ parents. Data were analyzed using a two-factor ANOVA; post-hoc significance between conditions was determined using the Scheffé method.

In situ hybridization

Digoxigenin-labeled riboprobes for *crestin* (Rubinstein et al., 2000) and *neurog1* (Korzh et al., 1998) were generated as previously described. A 2.1 Kb fragment of *reck* was subcloned into pBluescript II SK, linearized with EcoRV and transcribed with T7 polymerase (Invitrogen) to generate digoxigenin-labeled

riboprobe. In situ hybridization was carried out as previously described (Thisse and Thisse, 2008). Fluorescent in situ hybridization was carried out as previously described (Vize et al., 2009). Embryos were then embedded in 4% agarose and sectioned at 100 μm on a Leica VT1000S vibratome. Colocalization of *reck* and *crestin* was analyzed by confocal imaging in single optical planes sampled every 7 μm. The anterior-posterior position of each section was determined by alignment to the section containing the yolk constriction.

Metalloproteinase activity

Tg(neurog1:egfp)/*sdp*$^{w12/+}$ parents were incrossed; the resulting embryos were sorted by phenotype at 48 hpf and homogenized in lysis buffer (150mM NaCl, 10mM HEPES, 2mM DTT, 0.1% Triton-X 100, pH 8.0). Protein concentration was normalized using the Bradford method. Lysate was incubated with DQ gelatin (Invitrogen) at room temperature; fluorescence was assayed using a fluorimeter (Tecan).

Transplants

Donor *Tg(neurog1:egfp)* embryos were injected with 1 nL 2.5% tetramethyl rhodamine dextran, 0.1M KCl and either 1.75 μg/μL *reck* MO or sterile water. Host *nacre*$^{w2/w2}$ embryos were injected at the one-cell stage with 1 nL 0.2% phenol red, 0.1M KCl, and either 1.75 μg/μL *reck* MO or sterile water. Donor and host embryos were dechorionated and mounted in 4% methylcellulose at sphere or dome stage (~3.5-4.5 hpf). Cells were aspirated into a pulled capillary glass needle and deposited into host embryos. Transplants were allowed to recover in E2 media supplemented with 100U penicillin/100 μg/mL streptomycin.

Neural crest migration measurements

Tg(sox10:eos)/sdp$^{w12/+}$ fish were incrossed; the resulting clutch was fixed at 24 hpf, immunostained for MF20, and imaged via confocal microscopy. Images were thresholded in Photoshop and subjected to a MatLab (Mathworks)

algorithm measuring the length of y-direction signal (i.e. first black pixel to last black pixel) for each x coordinate. This plot was smoothed by averaging over 10-point bins. Local maxima were detected by an iterative point-to-point comparison function (peakdet, http://billauer.co.il/peakdet.html).

Time-lapse microscopy and cell tracking

18s *Tg(sox10:nls-eos)* embryos and 30hpf *Tg(sox10:nls-eos)/Tg(neurod:tagrfp)*^{w69} embryos were immobilized in 1.5% Type VII agarose (Sigma) and imaged every 10 minutes using a 3i Marianas spinning disk confocal microscope system. Image files were processed using Slidebook (3i) and ImageJ (NIH) software. Movies from the early interval were initiated at the beginning of neural crest migration. Movies from the late interval were synchronized so that the lateral line crosses somite 16 at the same frame. Divisions were identified by resolution of mitotic figures; cell death determined by nuclear fragmentation.

Cell tracking was performed manually in ImageJ. Dorsoventral cell velocity was defined as the sum of y-axis displacements divided by the number of frames in which the cell was visible. Proliferative and apoptotic rates were defined by the following equation—

$$\left(\frac{x}{n_{cells} \times t_{frames}}\right) \times 144 \quad (1),$$

—where x is the number of events observed per time lapse, n_{cells} is the total number of cells tracked, and t_{frames} is the number of frames (each separated by 10 minutes). Multiplying by 144 yielded the number of events per cell-day.

Drug experiments

Tg(neurog1:egfp)/sdp^{w12} embryos were treated in drug dissolved in 1% DMSO/E2 medium from 16s-3dpf; drug solution was changed daily. Embryos were fixed, immunostained for Elavl1 and GFP. Drugs were administered at the following concentrations: GM6001 (Enzi Life Sciences), 100μM; batimastat

(Tocris Biosciences), 500μM; marimastat (Tocris Biosciences), 100μM; DAPT (Sigma), 100μM.

TUNEL staining

Fish were fixed at 30hpf and immunostained with rabbit α-Sox10 antibody. Embryos were permeabilized with 20μg/mL proteinase K (Sigma), and subjected to TUNEL labeling using fluorescein substrate (Roche). $TUNEL^{+}$ and $Sox10^{+}$ cells were counted from confocal stacks and the embryos were subsequently genotyped.

Results

Sdp is a recessive phenotype involving the loss of DRG neurons

To identify mutations that alter DRG development, we screened for perturbed expression of Elavl1 in the peripheral nervous system (Henion et al., 1996; Marusich et al., 1994; Szabo et al., 1991). We identified 4 alleles of a recessive mutation, *sensory deprived* (*sdp*). All mutant embryos completely lack DRG through 5 dpf (Figure 6, Figure 7). However, for all mutations all other neural crest derivatives appear to develop normally (Figure 8) including pigment cells, enteric neurons, lateral line glia, and sympathetic chain (Figure 8); while normal in morphology, the ceratohyal cartilage is displaced (Figure 8K-L′). Cranial ganglia, which have both neural crest and placode origin, appear normal (Figure 8), and have comparable cell counts (Figure 9). Fish homozygous for any of the *sdp* alleles die by day 12.

Mutant embryos display defects in DRG formation at the earliest stages of their development. *sdp* embryos exhibit no *neurog1* expression in DRG precursors as assessed by a *neurog1:egfp* transgenic line (Figure 6A-B′) and by *in situ* hybridization for *neurog1* transcript (Figure 6C-D′). In addition, no cells in the periphery ectopically express these markers, nor are any ectopic neurons revealed by Elavl1 staining, suggesting that the *sdp* phenotype is not caused by DRG displacement. By contrast, *neurog1* expression in the central nervous

system and cranial placodes appears normal. These results suggest that the *sdp* phenotype is a result of a defect occurring upstream of *neurog1*.

Neurons and glia of the zebrafish DRG are derived from a common subpopulation of neural crest (McGraw et al., 2008; Raible and Eisen, 1994). The *sdp* phenotype could be caused by a failure to specify this neuroglial lineage or by a later defect in neuronal differentiation. To address this question, we generated the transgenic line *Tg(sox10:eos)* in which the fluorophore Eos (Wiedenmann et al., 2004) is expressed under the control of the promoter for *sox10*, an SRY-box containing transcription factor expressed in neural crest and maintained in crest-derived glial cells (Carney et al., 2006). Schwann cells apposed to motor axons are retained in *sdp* embryos; however, satellite glia adjacent to DRG are notably absent (Figure 6E, E′). Schwann cells are also found in normal distribution along the lateral line nerve (Figure 8E, H). We conclude that DRG neuron formation is compromised in *sdp* rather than specification of the neuroglial lineage.

All sdp alleles have sequence polymorphisms in the reck gene

To identify the genomic location of *sdp* alleles, we used recombination mapping in an sdp^{w12}/Wik hybrid background. We identified a critical region of ~200 Kb on chromosome 24 associated with *sdp* (Figure 10A). Direct sequencing of sdp^{w12} cDNA corresponding to transcripts in this region identified a mutation in the exon 9 splice donor of *reck* that caused a 510 bp intron to be retained (Figure 10C). This intron contains a stop codon, which would truncate any translated protein to 309 amino acids. *Reck* encodes a 956 amino acid protein containing an N-terminal signal sequence and two Kazal motifs (Figure 10B); it is a GPI-linked inhibitor of metalloproteinases (Takahashi et al., 1998). All *sdp* alleles possessed perturbations in the *reck* sequence (Figure 10B-C′): a C38R missense mutation in a highly conserved residue (sdp^{w13}), a W252X premature stop mutation (sdp^{w14}), and a 0.5 Mb deletion of chromosome 24 that eliminates at least 4 other genes in addition to *reck* (sdp^{w15}). Although each *sdp* allele

possesses a different lesion in *reck*, they are equivalent with respect to the DRG phenotype (Figure 7). Complementation analysis reveals that the *w12*, *w13* and *w14* alleles are likely null since no additional phenotypes were observed when crossed to the *w15* deficiency (not shown). The severe swelling phenotype of the *w15* deficiency (Figure 7) is reduced by complementation, suggesting that this phenotype is affected by loss of additional genes found in the interval.

Metalloproteinases are upregulated in sdp embryos

RECK inhibits the maturation and activity of the metalloproteinases MMP-2, MMP-9, MMP-14, and ADAM10 (Muraguchi et al., 2007; Oh et al., 2001; Takahashi et al., 1998). We incubated protein extracts from 48 hpf $sdp^{w12/w12}$ and sibling embryos with a fluorescein/gelatin conjugate, and found that mutant embryos exhibited greater metalloproteinase activity than siblings (Figure 11). RECK therefore appears to be a major inhibitor of metalloproteinases in developing zebrafish embryos.

Morpholino oligonucleotide knockdown of reck transcript phenocopies the DRG phenotype observed in sdp

To confirm that *reck* loss-of-function is the cause of the DRG phenotype observed in *sdp*, we generated a splice-blocking MO directed against the exon7/intron7 boundary. Embryos injected with this MO failed to develop DRG (Figure 12A-D) despite the appropriate formation of cranial ganglia (Figure 12C), Schwann cells (Figure 12G), lateral line glia (Figure 12H), and pigment cells (Figure 12I), matching the phenotypes of *reck* mutants. DRG counts declined in a dose-dependent fashion (Figure 12E). We verified that *reck* expression was disrupted by this MO by subjecting cDNA to quantitative RT-PCR using primers flanking intron 7 (Figure 12F). These primers generate an amplicon of 366 bp when applied to appropriately-spliced transcript; we cannot detect this amplicon in cDNA from embryos injected with *reck* MO. These results confirm that DRG formation fails in the absence of *reck* function.

Expression of reck rescues DRG in sdp embryos

To show that reintroduction of *reck* was sufficient to rescue the *sdp* phenotype, we injected *wt* or sdp^{w12} mutant mRNA into embryos derived from $sdp^{w12/+}$ incrosses (Figure 12; Table 1). Injection of mutant mRNA had no effect on mutants or siblings (Figure 12J, L). Injection of *wt reck* mRNA restored DRG to wild-type levels in $sdp^{w12/w12}$ embryos (Figure 12M). Overexpression of *wt reck* mRNA failed to generate any observable phenotype on its own (Figure 12K). We conclude that *reck* loss-of-function is solely responsible for the DRG defect observed in *sdp*.

Expression of reck is consistent with a role in the development of neural crest derivatives

We examined *reck* expression by *in situ* hybridization to identify tissues in which *reck* might act to influence DRG development. *In situ* hybridization for *crestin* was used to identify neural crest. In the trunk, *crestin* is expressed adjacent to the dorsal neural tube and in cells migrating between neural tube and somite (Figure 13A, B, 14C, D, I-I‴), while *reck* is expressed primarily in ventral mesoderm, consistent with a role in vasculature development (Figure 13A, B, 14G, H, J-J‴). However, a band of dorsal *reck* expression appears at 22 hpf (Figure 13A, B, 14G, H, J-J‴). This dorsal expression is transient, disappearing by 30 hpf (Figure 13C, D)

To quantify the degree to which *reck* and *crestin* expression colocalize, embryos at 22 and 30 hpf were subjected to double fluorescent *in situ* hybridization followed by serial sectioning (Figure 13B, D). Cells were counted as $reck^{+}$, $crestin^{+}$, or $reck/crestin^{+}$ in each section. At 22 hpf, essentially all neural crest cells express *reck.* Although fewer neural crest cells are observed in posterior segments, we do not observe significant changes in *reck/crestin* colocalization (Figure 13E, G). By 30 hpf, however, the expression of *reck* and *crestin* has largely separated into two separate cell populations (Figure 13F, G);

however, a small subset of cells (approximately 3 cells per hemisegment) continues to express both *reck* and *crestin*.

MO-injected embryos exhibit vasculature defects

Mice with a targeted disruption of the *reck* locus display impaired vascular maturation and abdominal hemorrhage (Oh et al., 2001). To determine whether *reck*-deficient zebrafish embryos exhibit similar defects, we injected *reck* MO into *Tg(fli1a:egfp)* embryos, a transgenic reporter expressed in the endothelial cells of the vasculature (Lawson and Weinstein, 2002). Between 24-32 hpf, vasculature in MO-injected embryos is comparable to the vasculature of control embryos, if slightly delayed (Figure 15A-C, G-I, Table 2). However, by 48 hpf, moderate defects in circulation and vascular development are manifest. The parachordal vessel (PAV), a derivative of the caudal vein, often fails to form following *reck* knockdown (Figure 15D, J, Table 2). Additionally, although circulation initiates normally in MO-injected embryos, angiograms revealed poor perfusion in intersegmental vessels (Figure 15E, K) as well as significantly impaired axial circulation (Table 2). At 3 dpf, intracranial hemorrhage is apparent in *reck*-deficient embryos, suggesting that vascular integrity is also impaired (Figure 15F, L, Table 2). These results demonstrate that, as in mouse, loss of *reck* is associated with disruption of vasculature development.

The requirement for reck in DRG development is cell-autonomous

Previous work has demonstrated that RECK is a GPI-linked protein that inhibits metalloproteinases in *cis*, blocking activity in the same cell in which it is expressed (Muraguchi et al., 2007). *Reck* is expressed in both neural crest and the environment through which it migrates, including vascular precursors that themselves have defective development. Therefore, the failure of DRG to form in the absence of *reck* function could be attributed either to cell environment or incompetence in the neural crest itself. To differentiate between these possibilities, we performed transplants between MO- and mock-injected embryos.

Donor cells were derived from rhodamine-labeled, *Tg(neurog1:egfp)* embryos and transplanted into *nacre* host embryos (Lister et al., 1999); the resulting transplants were then immunostained for Elavl1. This allowed us to identify all donor cells incorporated into the transplant (rhodamine), donor cells which differentiated into sensory neurons (GFP), and all differentiated neurons in the transplant (Elavl1). Since *nacre* embryos lack trunk melanophores, we were able to verify whether donor cells had become neural crest by the appearance of donor-derived melanophores. Analysis was restricted to those embryos in which melanophores developed.

When cells from mock-injected embryos were deposited into mock-injected hosts, they were able to differentiate into DRG sensory neurons (Figure 16A, B; Table 3). However, when cells from MO-injected embryos were transplanted into mock-injected embryos, they never formed DRG neurons, despite the fact that donor cells frequently generated neural crest (Figure 16C, D). Conversely, when cells from mock-injected donors were transplanted into MO-injected hosts, they formed DRG neurons readily but were unable to induce host cells to form DRG neurons (Figure 16E, F). Therefore, we conclude that *reck* is required cell-autonomously in migrating neural crest for normal DRG formation.

Altered neural crest migration after perturbation of reck

Prior work has established that suppression of *reck* function leads to hypermigratory behavior in several cell lines (Chang et al., 2006; Liu et al., 2003; Morioka et al., 2009; Yoshida et al., 2008); conversely, forced expression of *reck* reduces migration (Hsu et al., 2006; Kang et al., 2007; Liu et al., 2003; Morioka et al., 2009; Silveira Corrêa et al., 2010; Yoshida et al., 2008). We hypothesized that *reck* loss-of-function might cause the neural crest to migrate excessively, causing the DRG deficit observed in *sdp*. We first measured the dorsoventral migration of neural crest streams at 24 hpf and found no significant difference in

neural crest migration distance (Figure 17), suggesting that the overall extent of migration is not perturbed.

We next used time-lapse microscopy to search for more subtle differences in neural crest behavior at two different stages of development. We first imaged *Tg(sox10:nls-eos)* embryos between 18s and 30 hpf; this interval encompasses initiation of neural crest migration (Figure 18A-F). Movies were analyzed as the first neural crest cell began to migrate ventrally. The position of each *sox10*$^{+}$ cell was manually tracked and its velocity in the dorsoventral axis was measured. We also followed cell count, proliferation, and apoptosis. During the initial migration of neural crest, we found cell velocity to be about 40% faster in *reck*-depleted neural crest cells (2.66 ± 0.25 μm/10 min, n=40 cells vs 1.88 ± 0.24 μm/10 min, n=54 cells; mean ±SEM, p=0.028). The overall number of cells, the rate of proliferation, and the rate of apoptosis were unchanged over this interval (Figure 18C-F).

To examine migratory behavior in differentiating neural crest cells, we imaged uninjected and *reck* MO-injected *Tg(sox10:nls-eos)/Tg(neurod:tagrfp)* embryos between 30 hpf and 60 hpf; this interval includes the overt expression of the first neuronal markers in DRG sensory neurons (Figure 18G-L). The position of each *sox10*$^{+}$ cell was manually tracked, and velocity (Figure 18J), cell count (Figure 18I), proliferation (Figure 18K), and apoptosis (Figure 18L) were measured as above. At this stage, we found cell velocity to be half that of *reck*-depleted neural crest cells (0.54±0.03 μm/10 min, n=72 cells vs. 1.14±0.14 μm/10 min, n=163 cells; mean ±SEM, p=0.005). The rate of proliferation and the overall number of cells were not statistically different following *reck* depletion. We observed a small but significantly greater apoptotic rate in *reck*-depleted neural crest cells compared to that in uninjected embryos, although still too infrequent to significantly change overall cell number.

To determine whether neural crest cells were capable of inhabiting the appropriate microenvironment for DRG formation following *reck* depletion, we

assessed the dorsoventral position each cell at each time point (Figure 18M). DRG precursors were previously noted to perform a dorsalward migration to the position of the future ganglion prior to differentiation (Raible and Eisen, 1994). This dorsal migration corresponds to the initiation of *neurog1* expression (McGraw et al., 2008). We found that by 55h, 68% of crest-derived *sox10*$^{+}$ cells observed in uninjected embryos were situated in this microenvironment, compared to only 20% in MO-injected embryos (Figure 18M). Therefore, in the absence of *reck*, neural crest cells exhibit aberrant migratory behavior and fail to inhabit the appropriate position to differentiate as DRG.

Discussion

The developmental phenotypes observed in our *reck* alleles reflect in part those seen in a previously published mouse knockout model (Oh et al., 2001). *Reck* is expressed in the zebrafish vasculature through 48 hpf (data not shown). We observe no overall gross deficit in trunk vasculogenesis; however the parachordal chain fails to form in *reck*-deficient embryos. Additionally, *reck* MO-injected embryos exhibit hypoperfusion and cerebral hemorrhage suggesting that vascular integrity is disrupted, concordant with the reported phenotypes in mouse. Zebrafish *reck* mutants may present a model for study of the role of this inhibitor in vascular development, and additional phenotypes will be described elsewhere. Recently, other investigators uncovered a developmental interplay between motor neurons and the formation of the parachordal chain (Lim et al., 2011); further study of the relationship between RECK function, vasculogenesis, and sensory neurogenesis may therefore be warranted. Nonetheless, expression and mosaic analysis suggest that *reck* acts within the neural crest population to regulate the formation of sensory neurons.

There are several possible explanations for what might happen in *sdp* mutants to the neural crest precursors normally fated to become DRG neurons. It is possible that cells fail to express *neurog1* and are respecified. We previously found that in *neurog1* mutants sensory neuron precursors instead became glia by

using the *neurog1:egfp* transgene to track their fates (McGraw et al., 2008). As *reck* acts upstream of the initiation of *neurog1* expression, we have no way of tracking these precursors in *reck* mutants. While it is possible to sample the fates of individual zebrafish neural crest cells by single cell injection, the cells that generate DRG neurons are only a small fraction of the trunk neural crest population. A possible change in fate would therefore be difficult to observe with statistical reliability. While it would be of interest to track *reck*-expressing neural crest cells *in vivo* using reporter constructs, we have been unable to identify genomic elements that direct *reck* expression due to the poor characterization of sequence surrounding its position at the end of chromosome 24.

An alternative possibility is that proliferation of DRG precursors is reduced following loss of *reck* function. Mouse embryonic fibroblasts have reduced proliferation following *reck* depletion (Kitajima et al., 2010). However, we observed no significant difference in proliferation in *reck*-depleted neural crest cells. A third mechanism that may contribute to the *sdp* phenotype involves the death of DRG progenitors. In our time-lapse experiments we observed a small increase in neural crest cell apoptosis during the interval of DRG neuron differentiation. However, apoptosis was undetectable in neural crest cells in either wildtype or mutant animals using histological techniques despite an abundance of nearby apoptotic cells, confirming that neural crest cell death is extremely rare (Figure 19, Table 4). Regardless, we do not view apoptosis of progenitors and inappropriate progenitor migration as being mutually exclusive mechanisms for DRG defects.

Reck was first identified in a large-scale screen for cDNAs capable of returning Ras-transformed cells to a flat morphology (Takahashi et al., 1998). Subsequent work has established RECK as a regulator of cell migration and invasion (Clark et al., 2007; Noda and Takahashi, 2007). Many cancers exhibit RECK downregulation via epigenetic modifications (Chang et al., 2006; Chang et al., 2007; Chang et al., 2004) transcriptional repression (Hsu et al., 2006; Liu et al., 2003; Sasahara et al., 1999), post-translational modifications (Simizu et al.,

2005), or endogenous microRNAs (Gabriely et al., 2008; Liu et al., 2010). In general, *reck* expression is negatively correlated with tumor aggressiveness (Clark et al., 2011; Gabriely et al., 2008; Li et al., 2007; Masui et al., 2003; Rabien et al., 2007; Song et al., 2006; Span et al., 2003; Takemoto et al., 2007; Takenaka et al., 2004; Takenaka et al., 2005; Takeuchi et al., 2004; van der Jagt et al., 2006; Xu et al., 2010); presumably in the absence of *reck*, metalloproteinase hyperactivity enables greater tumor cell migration and invasion.

Like cancer cells, neural crest cells migrate through the extracellular environment to reach their final targets. One possible explanation for the DRG phenotype caused by result of *reck* loss-of-function is that neurogenic neural crest migrates inappropriately. We observed broad *reck* expression in neural crest cells at 22 hpf followed by restriction to a subset of neural crest cells by 30 hpf, suggesting that winnowing of *reck* expression might confer DRG progenitor identity as development progresses. We found the requirement for *reck* to be cell-autonomous, a result that was somewhat surprising given the extensive expression of *reck* transcript in cells situated in the path of neural crest migration and the large increase in metalloproteinase activity in *sdp* embryos, suggesting that it is broadly active in tissues besides neural crest. RECK has been shown to inhibit metalloproteinases in *cis* (Muraguchi et al., 2007), suggesting that a potential metalloproteinase whose inhibition is critical for normal DRG development might be expressed within the neural crest itself, consistent with a cell-autonomous function. However we cannot rescue the *sdp* defect by treating with several broad-spectrum inhibitors of metalloproteinases (Figure 20), although the efficacy of these inhibitors against specific zebrafish metalloproteinases is unknown. Whether any of the over 50 zebrafish metalloproteinases may interact with RECK awaits further analysis.

When viewed by time-lapse microscopy, *reck*-depleted cells exhibit changes in migratory behavior. Initially, we observed neural crest to be hypermigratory in *reck* MO-injected embryos, showing a small but significant

increase in cell velocity. We note that we are unable to determine whether these differences reflect changes in behavior of all neural crest cells or only a subset. When viewed at later times, *reck*-depleted cells appear hypomigratory, in contrast to their earlier behavior. These results can be reconciled by a model in which *reck*-deficient cells initially show increased migration, as predicted from the cancer literature. In the absence of *reck* function DRG precursors would then be respecified (or die), leaving only slow-moving cells on the medial pathway destined to become Schwann glia. A subset of neural crest-derived *sox10*$^{+}$ cells are unambiguously mislocalized following *reck* depletion, failing to move dorsally. These include neuronal precursors and cells that will form satellite glia surrounding the DRG. However, dorsal migration occurs after initial expression of *neurog1*, and both the failure of dorsal movement to form DRG and subsequent accumulation of satellite cells may be caused indirectly by *neurog1* absence in *reck* mutants. Whether the lack of dorsal movement at this later stage is due to altered RECK function or whether it is the consequence of failed specification will await further study.

An alternative possibility for the function of *reck* in DRG specification is that altered activity of metalloproteinases could affect signaling required for neuron specification (Bai and Pfaff, 2011). In the mouse, RECK regulates cortical neurogenesis through Notch signaling (Muraguchi et al., 2007). When RECK is disrupted, hyperactive ADAM10 results in reduced Notch signaling and precocious neurogenesis with an ultimate decrease in neurons due to precursor depletion. Might a similar impairment be the mechanism by which *sdp* embryos fail to form DRG? Disruption in Notch signaling results in a decrease in DRG (Cornell and Eisen, 2000; Cornell and Eisen, 2002), but this phenotype is the result of prior depletion in all trunk neural crest with concomitant increase in Rohon-Béard sensory neurons. We observe no change in Rohon-Béard cells in mutant embryos (Figure 21) and normal crest formation and differentiation (Figure 7). Moreover, loss of zebrafish *notch1a* receptor causes an increase in DRG neurons (Gray et al., 2001), more consistent with a neurogenic phenotype expected with loss of Notch function. Does *sdp* instead behave as a mutation

resulting in Notch gain-of-function? We are unable to rescue DRG formation by treating *sdp* embryos with the Notch inhibitor DAPT (Geling et al., 2002) while seeing an increase in DRG neurons when treating wildtype animals (data not shown), consistent with the *notch1a* mutant phenotype. Alternatively, RECK might alter other metalloproteinases that affect signaling pathways needed for DRG differentiation.

A limited body of evidence provides clues as to how *reck* might fit into a genetic hierarchy controlling DRG development. *Erbb2* and *erbb3b* function have previously been shown to be essential to the formation of DRG neurons upstream of *neurog1* expression; migrating neural crest in these mutants becomes progressively disorganized and DRG precursors apparently fail to pause and differentiate (Honjo et al., 2008). ErbB2 is known to regulate RECK expression via ERK signaling (Hsu et al., 2006), and the loss of DRG observed in both *erbb2* and *reck* mutants suggests the two genes might act within a common signaling cascade to direct DRG formation. However, mutations affecting Erbb signaling also disrupt glial development (Lyons et al., 2005), suggesting this pathway may affect DRG development at an earlier step involving the neuroglial precursor.

Taken together, our results suggest that RECK cell-autonomously regulates the initial specification of DRG precursors upstream of *neurog1. Reck* expression is restricted to a subset of neural crest, suggesting that these cells might represent DRG precursors. DRG cell fate choice may therefore rely on regulation of *reck* expression. Understanding which metalloproteinases are inhibited by RECK during zebrafish neural crest development will be critical in resolving the mechanisms underlying how it regulates neural crest cell fate.

Figures

Figure 6. *sensory-deprived* (*sdp*) mutants exhibit a complete loss of DRG sensory neurons. (A) 3 dpf Tg(*neurog1:egfp)* embryos immunostained with Elavl1. **(A′)** DRG are absent in an *sdp*$^{w12/w12}$ mutant embryo. Scale bar: 500 μm. **(B, B′)** High-magnification image of (**A)**. Scale bar: 50 μm. **(C, C′)** *neurog1* expression at 48hpf. Box indicates position of high-magnification images in **(D)**. Scale bar: 250 μm. **(D, D′)** High-magnification image of **C**. Scale bar: 50 μm. **(E, E′)** 3 dpf *Tg(sox10:eos)* embryo immunostained for Elavl1. Although Schwann glia (empty arrowhead) are retained, satellite glia (filled arrowhead) are absent in *sdp*$^{w12/w12}$. Scale bar: 25 μm. **(F, F′)** Counts of *neurog1*$^{+}$ DRG at 3 dpf. Approximately 25% of embryos fail to form DRG, suggesting that *sdp*^{w12} is a fully penetrant recessive mutation. **(G)** Counts of *neurog1*$^{+}$ DRG followed over four days. DRG never appear in approximately 25% of the population, indicating that *sdp* does not delay in DRG development.

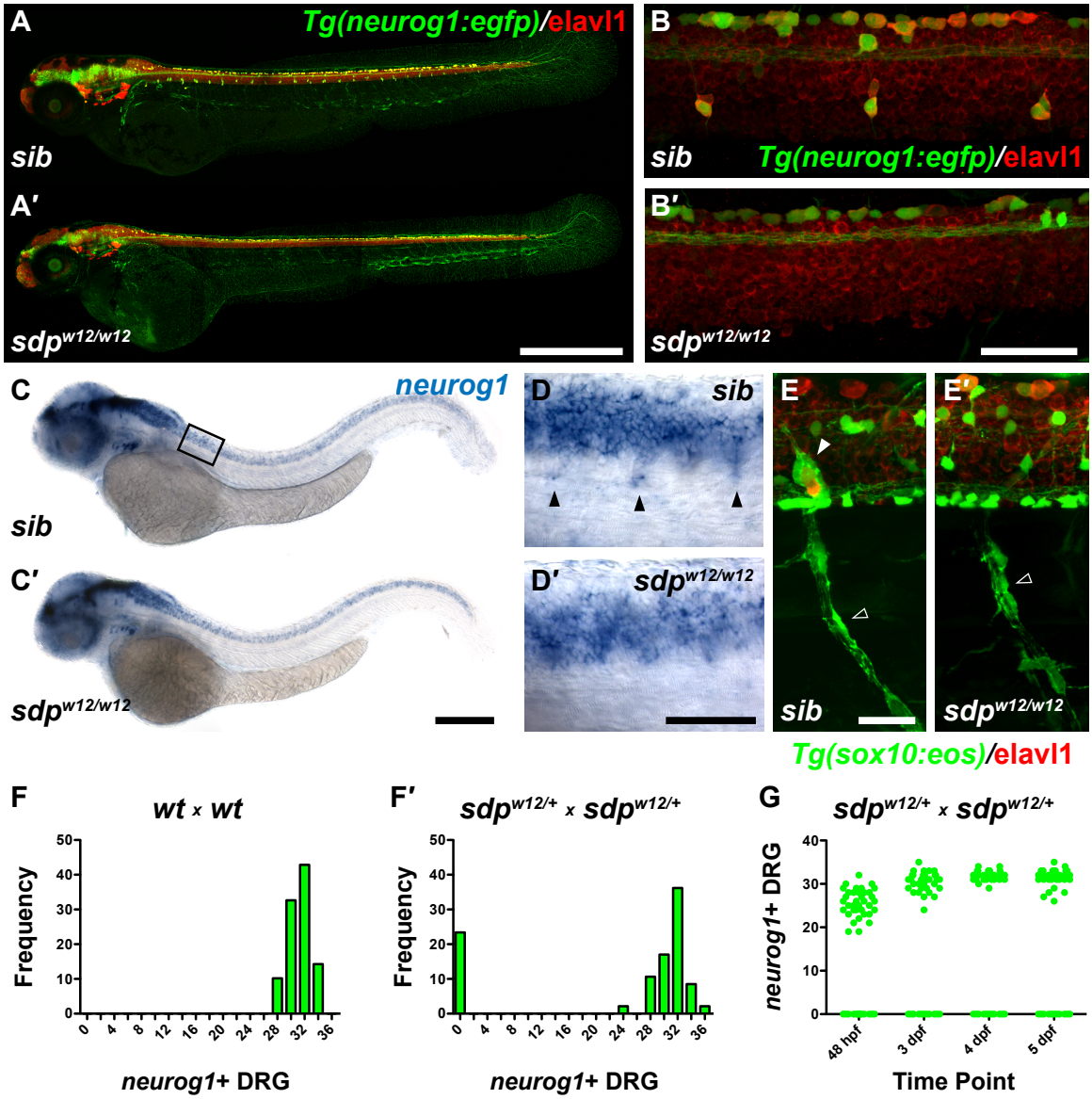
A
Tg(neurog1:egfp)/elavl1
sib
A′
sdpw12/w12
B
sib
Tg(neurog1:egfp)/elavl1
B′
sdpw12/w12
C
neurog1
sib
C′
sdpw12/w12
D
sib
D′
sdpw12/w12
E
sib
E′
sdpw12/w12
Tg(sox10:eos)/elavl1
F
wt x wt
Frequency
neurog1+ DRG
F′
sdpw12/+ x sdpw12/+
Frequency
neurog1+ DRG
G
sdpw12/+ x sdpw12/+
neurog1+ DRG
48 hpf
3 dpf
4 dpf
5 dpf
Time Point

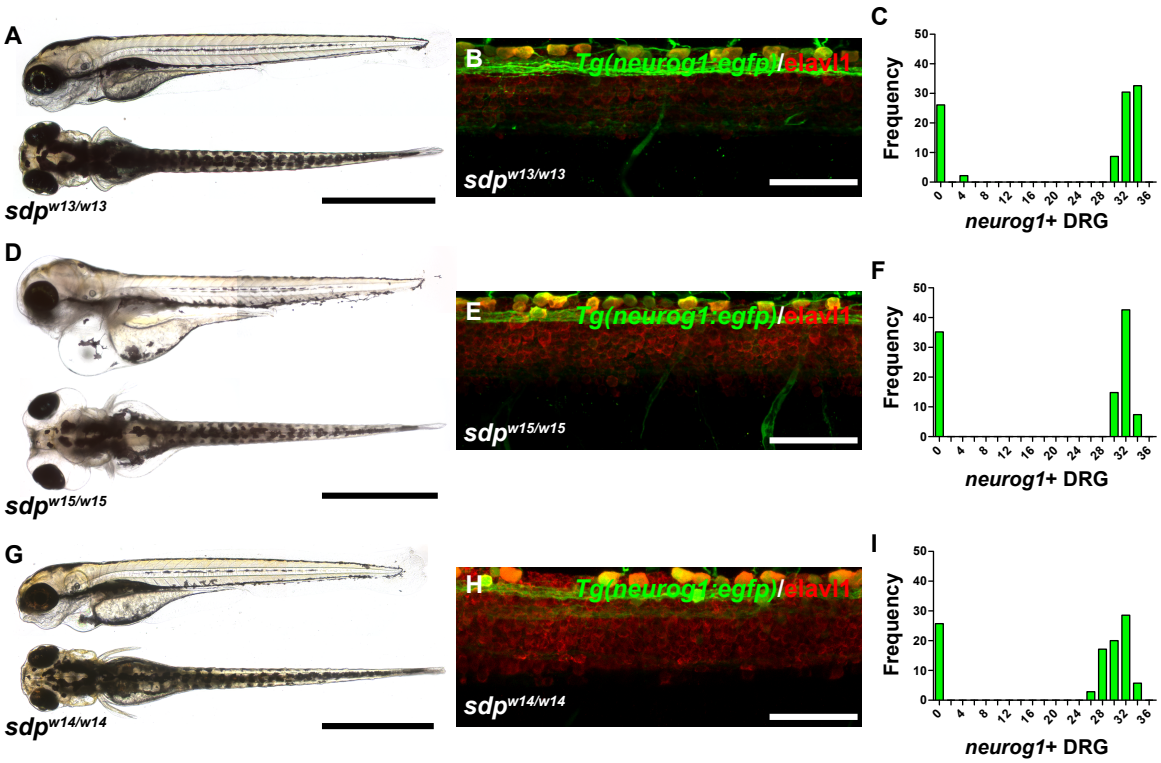

Figure 7. All alleles of *sdp* exhibit complete DRG loss. (A) *sdp*$^{w13/w13}$ exhibits normal morphology and pigmentation. Scale bar: 500 μm. **(B)** A high-magnification image of 3 dpf *Tg(neurog1:egfp)/sdp*$^{w13/w13}$ zebrafish immunostained with Elavl1 reveals no DRG neurons. Scale bar: 50 μm. **(C)** Approximately 25% of 3 dpf embryos from a cross between *sdp*$^{w13/+}$ parents fail to form *neurog1*+ DRG, indicating that *sdp*^{w13} is a fully penetrant recessive mutation. **(D)** *sdp*$^{w15/w15}$ exhibits normal pigmentation but acquires a progressively worsening edema around the eyes and heart beginning at 3 dpf. Scale bar: 500 μm. **(E)** A high-magnification image of 3 dpf *Tg(neurog1:egfp)/sdp*$^{w15/w15}$ zebrafish immunostained with Elavl1 reveals no DRG neurons. Scale bar: 50 μm. **(F)** Approximately 25% of 3 dpf embryos from a cross between *sdp*$^{w15/+}$ parents fail to form *neurog1*+ DRG, indicating that *sdp*^{w15} is a fully penetrant recessive mutation. **(G)** *sdp*$^{w14/w14}$ exhibits normal morphology and pigmentation. Scale bar: 500 μm. **(H)** A high-magnification image of 3 dpf *Tg(neurog1:egfp)/sdp*$^{w14/w14}$ zebrafish immunostained with Elavl1 reveals no DRG neurons. Scale bar: 50 μm. **(I)** Approximately 25% of 3 dpf embryos from a cross between *sdp*$^{w14/+}$ parents fail to form *neurog1*+ DRG, indicating that *sdp*^{w14} is a fully penetrant recessive mutation.

Figure 8. Derivatives of the neural crest other than DRG are largely unperturbed in *sdp* embryos. (A) Brightfield micrograph of a sibling 4 dpf zebrafish embryo. Scale bar: 500 μm. **(B)** Brightfield micrograph of a *sdp*$^{w12/w12}$ 4 dpf embryo. The *sdp*$^{w12/w12}$ jaw is retracted (arrowhead). **(C)** Cranial ganglia of a sibling 4 dpf embryo as identified by Elavl1 immunostaining. ad, anterodorsal lateral line ganglion; av, anteroventral lateral line ganglion; f, facial ganglion; g, glossopharyngeal ganglion; m, middle lateral line ganglion; o, octaval/statoacoustic ganglion; p, posterior lateral line ganglion; t, trigeminal ganglion; v, vagal ganglia. Scale bar: 100 μm. **(F)** All cranial ganglia are present in *sdp*$^{w12/w12}$ embryos. **(D)** Enteric nervous system of a sibling 5 dpf embryo as shown by Elavl1 immunostaining. Scale bar: 100 μm. **(G)** Enteric nervous system of a *sdp*$^{w12/w12}$ 5 dpf embryo. The enteric nervous system migrates the full extent of the gut. **(E)** Lateral line nerve of a sibling 4 dpf embryo stains positive for acetylated tubulin; myelinating glia are marked by the *sox10:eos* transgene. Scale bar: 50 μm. **(H)** Lateral line nerve and associated myelinating glia are present in *sdp*$^{w12/w12}$ embryos. **(I)** Sympathetic neurons (white arrowheads) in a sibling 5 dpf embryo immunostained for Elavl1. Scale bar: 150 μm. **(J)** Sympathetic neurons are also present in 5 dpf *sdp*$^{w12/w12}$ embryos. Scale bar: 150 μm. **(K)** Head cartilages of a sibling 4 dpf embryo. Note the position of the ceratohyal cartilage (arrowhead). ch, ceratohyal; hs, hyosymplectic; pq, palatoquadrate. Scale bar: 100 μm. **(K′)** Branchial arches of a sibling 4 dpf embryo. bh, basihyal; cb, ceratobranchial; ih, interhyal. Scale bar: 100 μm. **(L)** Head cartilages of a *sdp*$^{w12/w12}$ 4 dpf embryo. The ceratohyal cartilage is retracted (arrowhead). Scale bar: 100 μm. **(L′)** All branchial arches of the *sdp*$^{w12/w12}$ 4 dpf embryo are present. Scale bar: 100 μm.

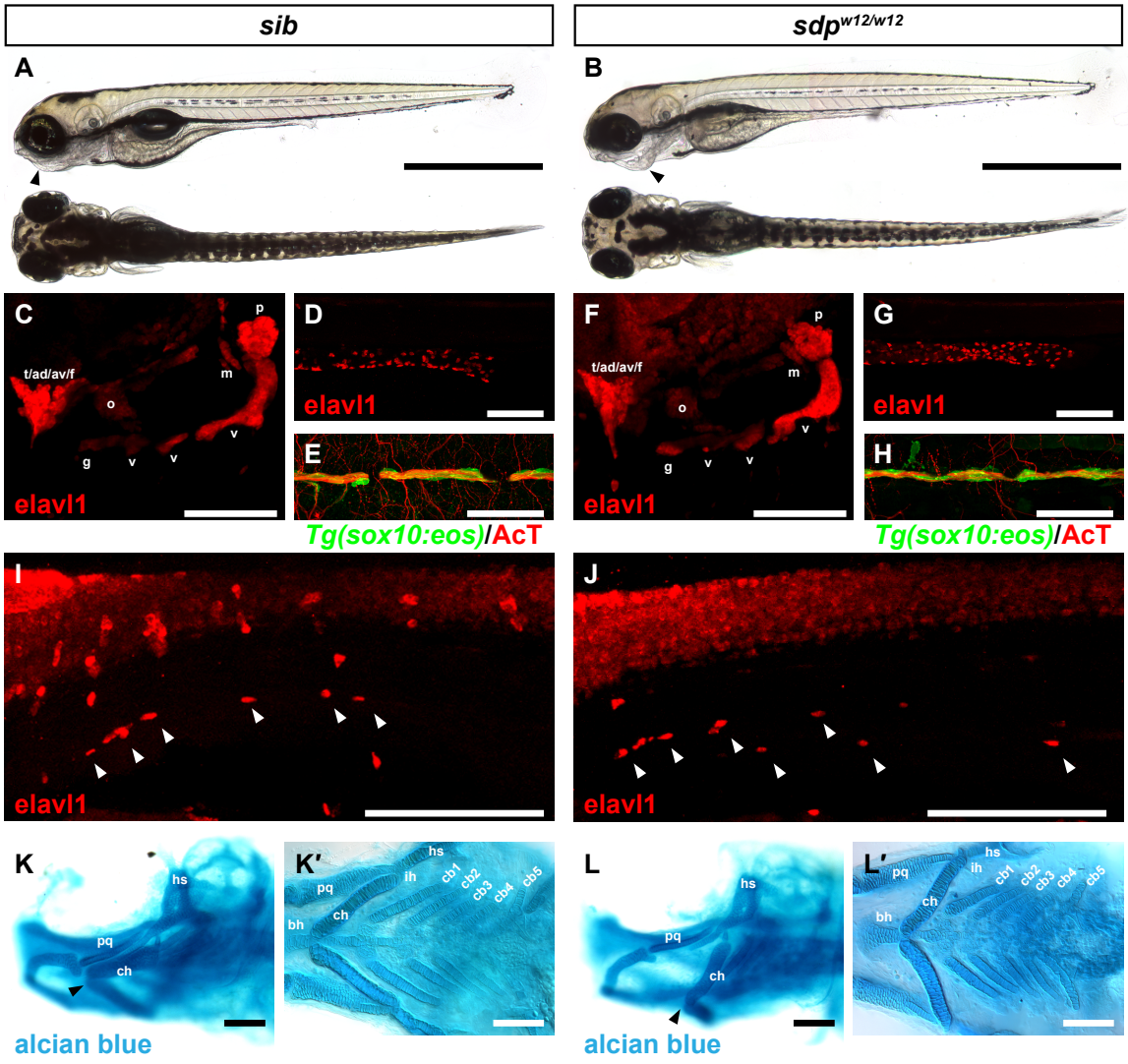
sib
sdp^w12/w12
A
B
C
D
E
F
G
H
I
J
K
K'
L
L'
p
t/ad/av/f
m
o
v
g
v
v
elavl1
Tg(sox10:eos)/AcT
hs
pq
ch
ih
bh
cb1
cb2
cb3
cb4
cb5
alcian blue

Figure 9. Cranial ganglia form normally in *sdp* embryos. (A) *Tg(sox10:eos)*/*sdp*$^{w12/+}$ embryo at 24 hpf immunostained for Elavl1. ad, anterodorsal lateral line ganglion; f, facial ganglion; o, octaval/statoacousic ganglion; t, trigeminal ganglia. Scale bar: 50 μm. **(B)** *Tg(sox10:eos)*/*sdp*$^{w12/+}$ embryo at 48 hpf immunostained for Elavl1. Scale bar: 50 μm. **(C)** *Tg(sox10:eos)*/*sdp*$^{w12/w12}$ embryo at 24 hpf immunostained for Elavl1. Scale bar: 50 μm. **(D)** *Tg(sox10:eos)*/*sdp*$^{w12/w12}$ embryo at 48 hpf immunostained for Elavl1. Scale bar: 50 μm. **(E)** Quantification of Elavl1+ cell counts per ganglion taken from *Tg(sox10:eos)*/*sdp*$^{w12/+}$ and *Tg(sox10:eos)*/*sdp*$^{w12/w12}$ embryos at 24 hpf. There is no significant difference in Elavl1+ cell count between genotypes in any ganglion counted. **(F)** Quantification of Elavl1+ cell counts in the trigeminal/facial ganglion taken from *Tg(sox10:eos)*/*sdp*$^{w12/+}$ and *Tg(sox10:eos)*/*sdp*$^{w12/w12}$ embryos at 48 hpf. There is no significant difference in Elavl1+ cell count between genotypes.

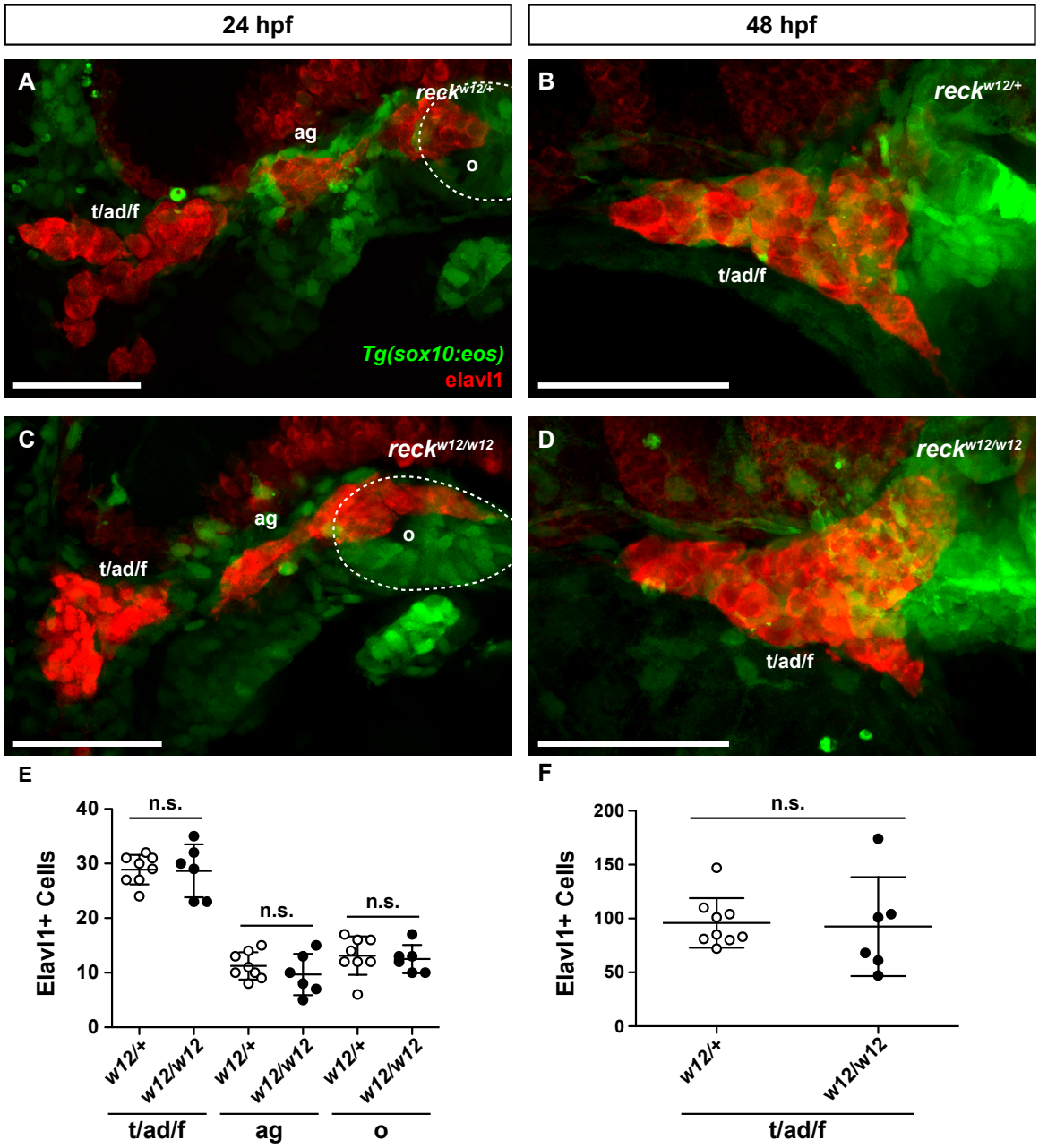
24 hpf
48 hpf
A
reckw12/+
ag
o
t/ad/f
Tg(sox10:eos)
elavl1
B
reckw12/+
t/ad/f
C
reckw12/w12
ag
o
t/ad/f
D
reckw12/w12
t/ad/f
E
Elavl1+ Cells
40
30
20
10
0
n.s.
n.s.
n.s.
w12/+
w12/w12
w12/+
w12/w12
w12/+
w12/w12
t/ad/f
ag
o
F
Elavl1+ Cells
200
150
100
50
0
n.s.
w12/+
w12/w12
t/ad/f

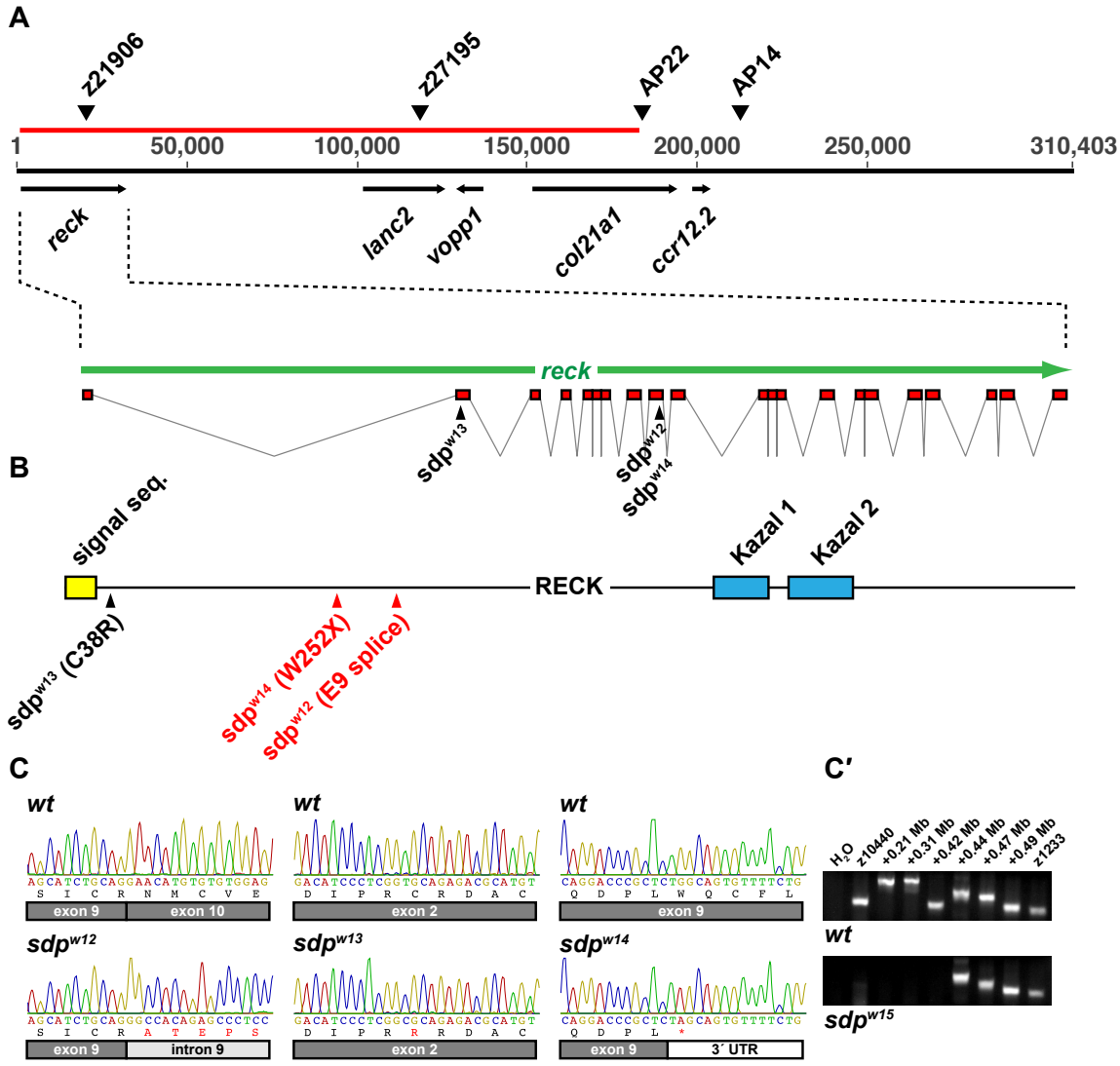

Figure 10. *sdp* alleles exhibit lesions in the *reck* coding sequence. (A) Physical map of the end of Chr24. *sdp* critical region (red line) contained at least four genes; SSLP markers used for mapping are shown, and locations of lesions indicated. **(B)** Predicted protein product zebrafish *reck* is 956 amino acids long, has an N-terminal signal sequence, and two Kazal motifs. **(C)** Electropherograms showing each of the *reck* single nucleotide polymorphisms (SNPs). *Sdp*^{w12} is a splice site mutation at the exon 9/intron 9 boundary, *sdp*^{w13} is a C38R substitution in exon 2, *sdp*^{w14} is a W252X substitution in exon 9. **(C′)** *Sdp*^{w15} is a large deletion of chromosome 24 encompassing at least 0.4 Mb and including the entire *sdp* critical region.

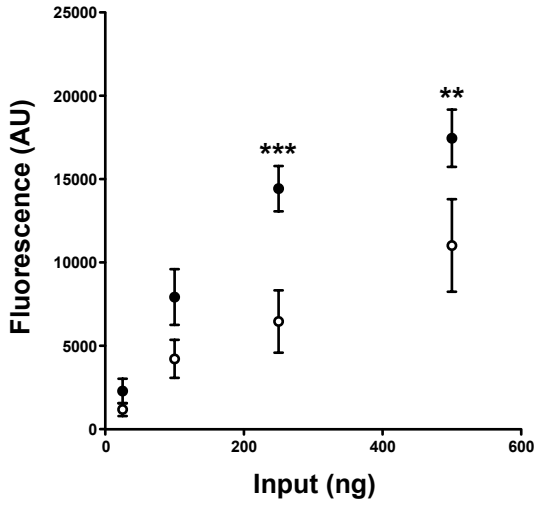

Figure 11. *sdp*$^{w12/w12}$ exhibits upregulation of metalloproteases. Whole protein isolate from both *sdp*$^{w12/w12}$ (black circles) and sibling embryos (white circles) was assayed for protease activity after a 4-hour incubation. Mean activity is indicated by circles; error bars are +/- standard error of the mean. A two-way analysis of variance showed that the genotype factor was significant, $F(1, 37) = 14.0447$, $p = 6E\text{-}4$. The Scheffé post-hoc criterion for significance (*: $\alpha = 0.05$, **: $\alpha = 0.01$, ***: $\alpha = 0.001$) revealed that protease activity was significantly elevated in *sdp*$^{w12/w12}$ protein isolate compared to siblings (100 ng *sdp*$^{w12/w12}$: $M = 9{,}114.8$, $SD = 4{,}084.2$; 100 ng sib: $M = 4{,}214.7$, $SD = 2{,}793.7$; 250 ng *sdp*$^{w12/w12}$: $M = 14{,}427.2$, $SD = 3{,}331.8$; 250 ng sib: $M = 6{,}463.0$, $SD = 4{,}579.0$; 500 ng *sdp*$^{w12/w12}$: $M = 18{,}886.0$, $SD = 3{,}587.3$; 500 ng sib: $M = 11{,}019.5$, $SD = 6{,}800.7$).

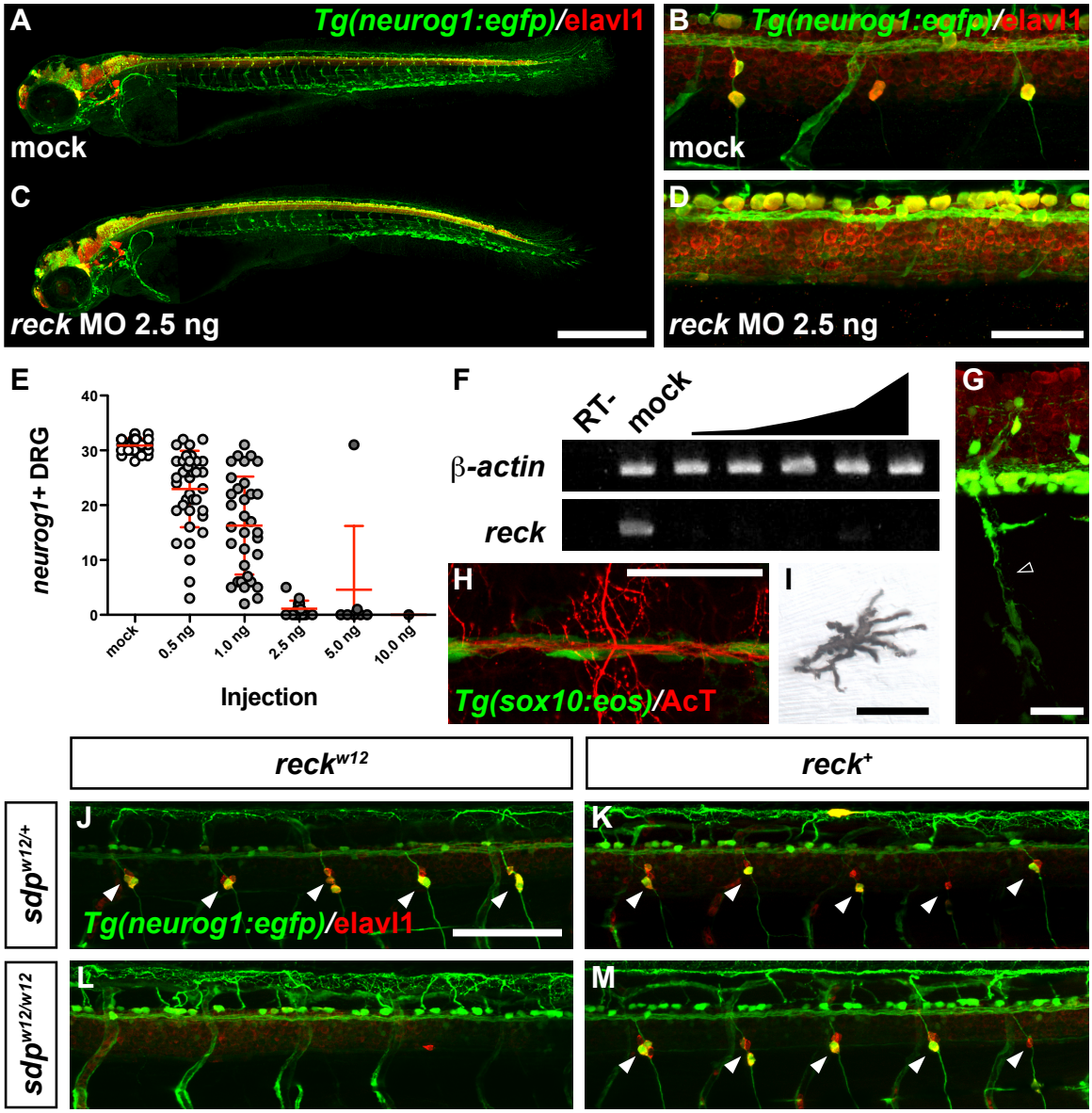

Figure 12. Phenocopy of *sdp* with *reck MO* and rescue by expression of *wt reck*. **(A, B)** Mock injected and **(C, D)** MO injected 3 dpf *Tg(neurog1:egfp)* embryo immunostained for Elavl1. Scale bar: 500 μm, **(A, C)**; 50 μm, **(B, D)**. **(E)** *neurog*1+ DRG at 3 dpf in embryos injected with indicated doses of *reck* MO. Error bars, SD. **(F)** Loss of correctly spliced *reck* transcript with *reck* MO. **(G-I)** 3 dpf *Tg(sox10:eos)* embryo injected with 1.5 ng *reck* MO and immunostained for Elavl1. **(G)** Crest-derived Schwann glia (empty arrowhead) are retained. Scale bar: 25 μm. **(H)** Crest-derived lateral line glia are retained. Scale bar: 50 μm. **(I)** Crest-derived pigment cells (melanophore shown) are retained. Scale bar: 25 μm. **(J)** Injection of 200 pg sdp^{w12} *reck* mRNA has no effect on $sdp^{w12/+}$ fish or **(L)** $sdp^{w12/w12}$ fish. **(K)** Injection of *wt reck* mRNA has no effect on $sdp^{w12/+}$ fish but **(M)** rescues DRG formation in $sdp^{w12/w12}$ fish. Scale bar: 100 μm.

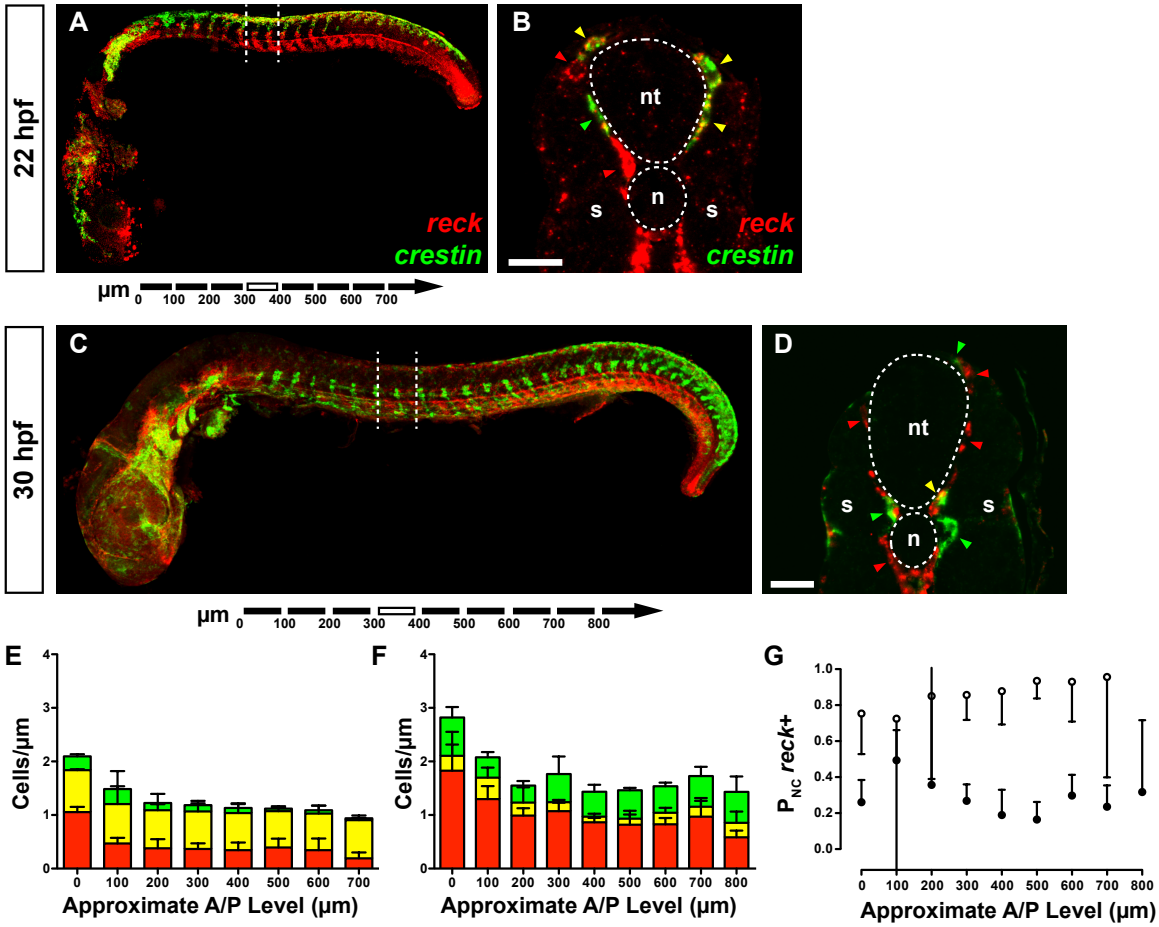

Figure 13. *reck* expression in neural crest cells. (A) 22 hpf embryo in wholemount. Dotted lines indicate the plane of section in **(B)**. **(B)** *reck*$^{+}$ cells (red arrowheads) are present in both the developing vasculature and presumptive neural crest. A small number of *crestin*$^{+}$ cells are also visible (green arrowheads). Most *crestin*$^{+}$ cells are also *reck*$^{+}$ (yellow arrowheads). Scale bar: 25 μm. **(C)** 30 hpf embryo in wholemount. Dotted lines indicate the plane of the section in **(D)**. **(D)** many *reck*$^{+}$ cells (red arrowheads) are present in the developing vasculature. Many *crestin*$^{+}$ cells (green arrowheads) are now apparent with few *crestin/reck*$^{+}$ cells (yellow arrowheads), suggesting the two markers have resolved into different populations. Scale bar: 25 μm. **(E)** Cell counts from serial sections of 22 hpf embryos. Error bars, SD. **(F)** Cell counts from serial sections of 30hpf embryos. **(G)** *crestin/reck*$^{+}$ cells as a proportion of all cells expressing *crestin* for 22 hpf (white circles) and 30 hpf (black circles) embryos. In most segments we observe significant segregation of *crestin* and *reck* expression. Error bars, 95% confidence interval.

Figure 14. *reck* is expressed in vasculature and other ventral tissues throughout early development. (A) *crestin* expression can be detected at shield stage. Scale bar: 200 μm. **(B)** *crestin* expression is faint and diffuse at bud stage. Scale bar: 200 μm. **(C)** *crestin* is strongly expressed in a dorsal domain corresponding to the premigratory neural crest (bracket). 9 somites, scale bar: 200 μm. **(D)** *crestin* expression is maintained in the neural crest as it begins migrating in dorsoventral streams (bracket). 18 somites, scale bar: 200 μm. **(E)** *reck* is not yet expressed at shield stage. Scale bar: 200 μm. **(F)** *reck* expression is initiated at bud stage in a bilateral patch flanking the midline (arrowhead). Scale bar: 200 μm. **(G)** *reck* expression expands to the somitic mesoderm (bracket). op, optic placode; ot, otic placode. 9 somites, scale bar: 200 μm. **(H)** reck expression remains restricted to the ventral somitic mesoderm (bracket). 18 somites, scale bar: 200 μm. **(I)** At 24 hpf, *crestin* expression is restricted to streams of neural crest migrating ventrally (arrowheads). Scale bar: 250 μm. **(I′)** High magnification image of the embryo in **(I)** showing streams of migrating neural crest (arrowheads). Scale bar: 100 μm. **(I″)** Section through the trunk of an embryo subjected to *crestin* in situ hybridization; anatomical references are overlaid. **(I‴)** In this cross-section, streams of neural crest migrating between the somite and the neural tube are defined by *crestin* expression (arrowheads); these ventromedially migrating cells give rise to DRG. Scale bar: 30 μm. **(J)** At 24 hpf, *reck* expression is strongest in the vasculature (white arrowheads), but a faint dorsal expression domain is also apparent (black arrowhead). Scale bar: 250 μm. **(J′)** High magnification image of the embryo in **(J)** showing *reck* expression in the ventrally-situated vasculature (white arrowheads) as well as the fainter dorsal expression domain (black arrowhead). Scale bar: 100 μm. **(J″)** Section through the trunk of an embryo subjected to *reck* in situ hybridization; anatomical references are overlaid. da, dorsal aorta; n, notochord; nt, neural tube; pcv, posterior cardinal vein; pn, pronephros; s, somite; ye, yolk extension. **(J‴)** In cross-section, *reck* expression is evident in both the developing vasculature (white arrowheads) and in a dorsolateral domain consistent with neural crest (black arrowheads). Scale bar: 30 μm.

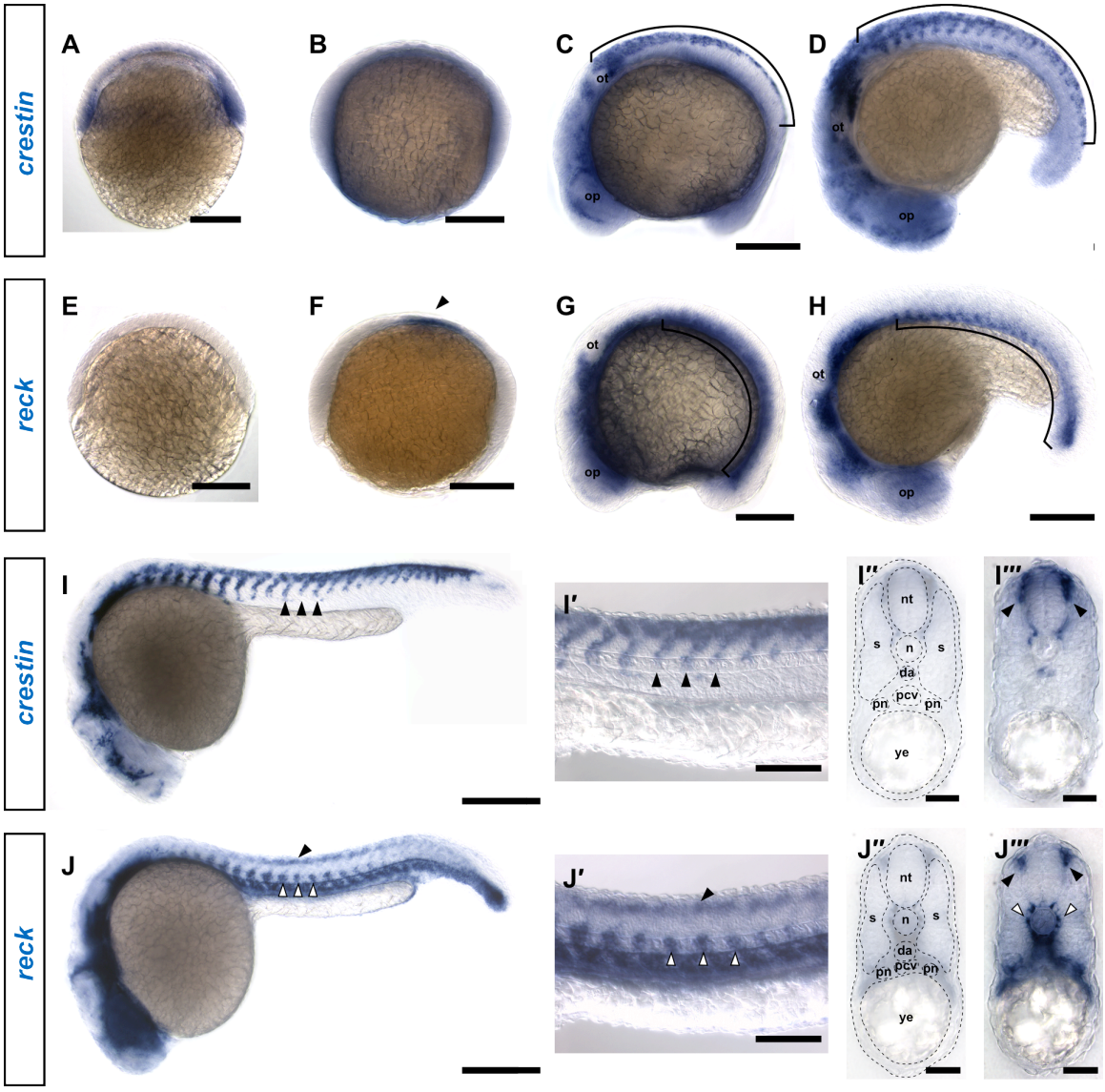
crestin
A
B
C
ot
op
D
ot
op
reck
E
F
G
ot
op
H
ot
op
crestin
I
I'
I''
nt
s
n
s
da
pcv
pn
pn
ye
I'''
reck
J
J'
J''
nt
s
n
s
da
pcv
pn
pn
ye
J'''

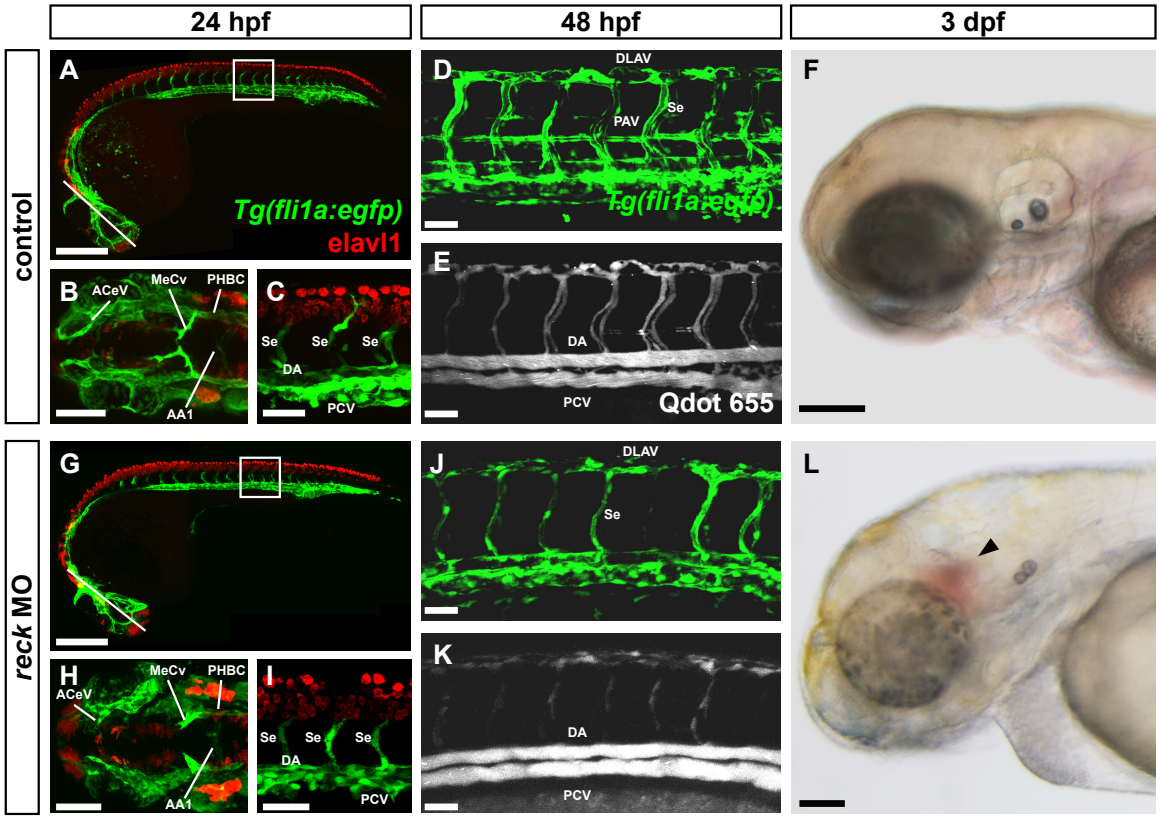

Figure 15. *reck*-deficient embryos exhibit defects in vascularization. (A-F) mock-injected; (**G-L**) *reck MO* injected. (**A, G**) 24hpf *Tg(fli1a:egfp)* embryo immunostained with Elavl1. Line indicates plane of image in **(B, H)**, box indicates plane of image in **(C, I)**. Scale bar: 250 μm. **(B, H)** cranial vasculature. AA1, mandibular arch; ACeV, anterior cerebral vein; MeCV, middle cerebral vein; PHBC, primordial hindbrain channel. Scale bar: 100 μm. **(C, I)** trunk vasculature. DA, dorsal aorta; PCV, posterior cardinal vein; Se, intersegmental vessel. Scale bar: 50 μm. All blood vessels form normally in MO-injected animals but are slightly delayed in their extension. **(D, J)** 48 hpf *Tg(fli1a:egfp)* embryo. DLAV, dorsal longitudinal anastomotic vessel; PAV, parachordal vessel. The PAV is reduced in size or fails to form entirely in MO-injected embryos. Scale bar: 50 μm. **(E, K)** Qdot angiogram of the embryo shown in **(D, J)**. Although blood flows through the DA and PCV after MO-injection, blood flow is somewhat reduced in the DLAV and intersegmental vessels. Scale bar: 50 μm. **(F, L)** Brightfield image of 3 dpf embryo. Cranial hemorrhage (arrowhead) is visible in a significant fraction of MO-injected embryos. Scale bar: 135 μm.

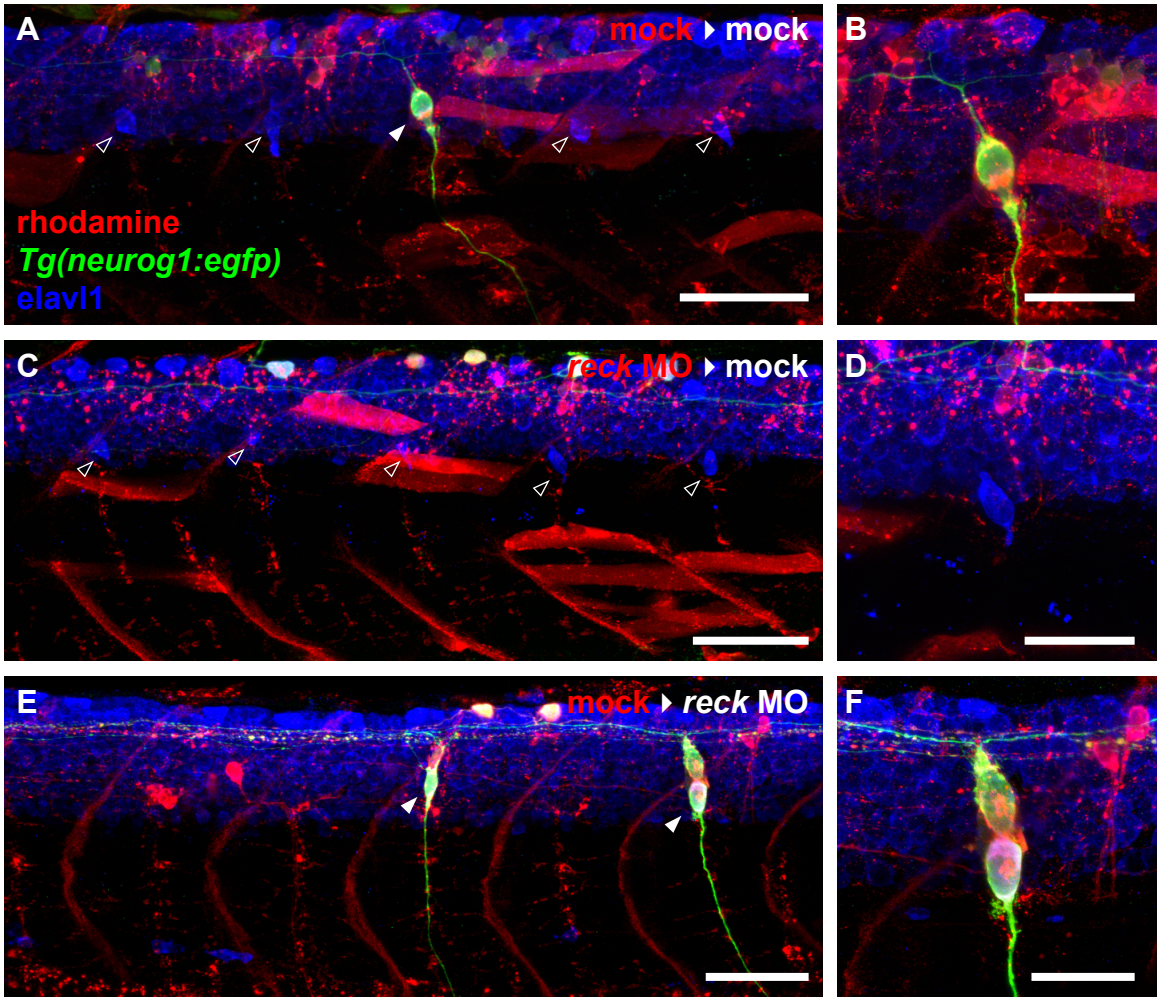

Figure 16. DRG defects from *reck* depletion are cell-autonomous. (A) 3 dpf mock-injected embryo implanted with mock-injected cells. Four host-derived DRG are visible (empty arrowheads) flanking one donor-derived DRG (filled arrowhead). Scale bar: 50 μm. **(B)** High-magnification image of the donor-derived DRG in **(A)**. Scale bar: 25 μm. **(C)** 3 dpf mock-injected embryo implanted with MO-injected cells. Five host-derived DRG are visible (empty arrowheads), but donor cells never give rise to DRG. Scale bar: 50 μm. **(D)** High-magnification image of one of the host-derived DRG in **(C)**. Scale bar: 25 μm. **(E)** 3 dpf MO-injected embryo implanted with mock-injected cells. Only donor-derived DRG (filled arrowheads) are present. Scale bar: 50 μm. **(F)** High-magnification image of one of the donor-derived DRG in **(E)**. Scale bar: 25 μm.

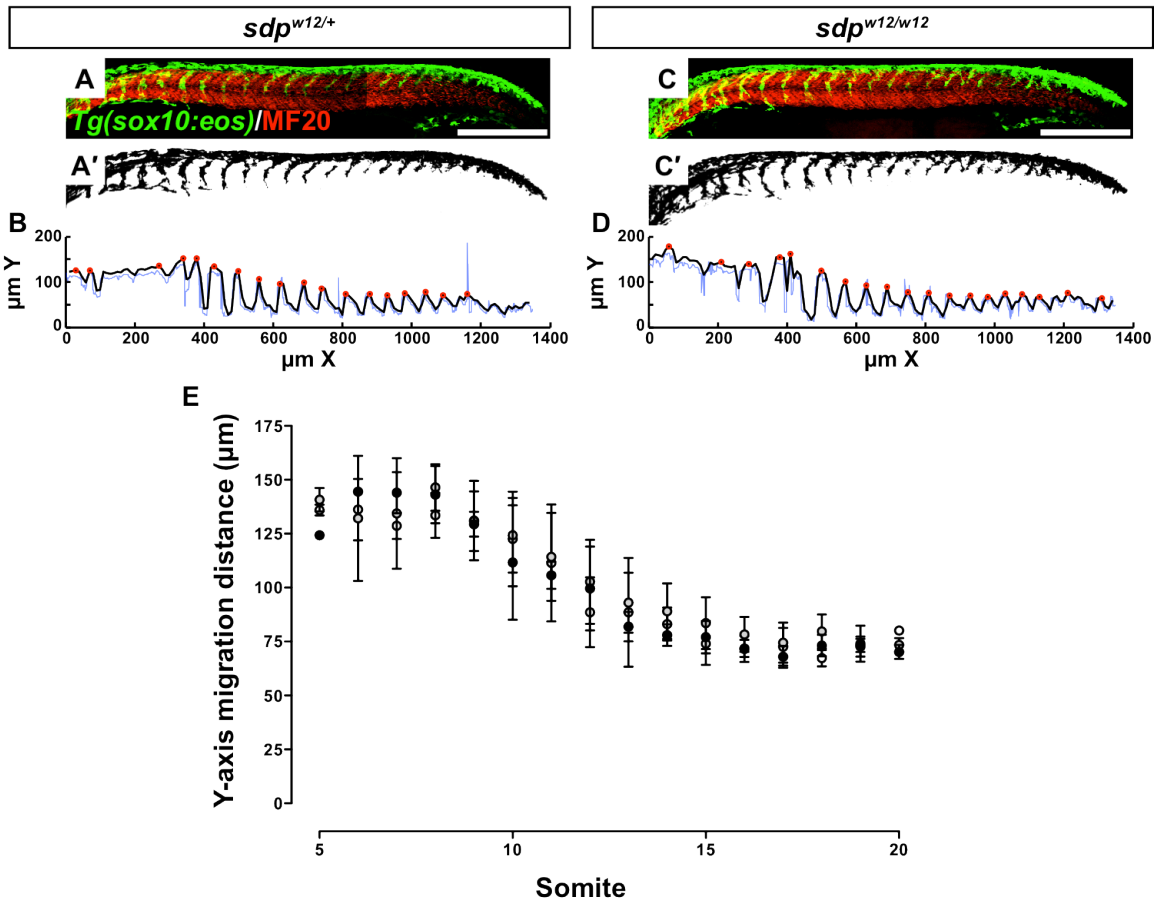

Figure 17. The neural crest of *sdp* embryos migrates to its normal extent. **(A)** Migrating streams of neural crest as seen in a 24 hpf *sox10:eos* transgenic background. Somites are immunostained for MF20. Scale bar: 250 µm. The neural crest signal (green) was thresholded **(A′)** and dorsoventral migration distance was measured across the rostrocaudal axis using a MatLab algorithm **(B)** (blue line). The raw migration data were smoothed by averaging (black line) and local maxima were detected by iterative point-to-point comparison (red circles). **(C, C′, D)** *sdp*$^{w12/w12}$ embryos exhibit neural crest that appears to migrate the appropriate distance. **(E)** Neural crest migration distance at 24 hpf is indistinguishable across all three *sdp*^{w12} genotypes. White circles: *sdp*$^{+/+}$, grey circles: *sdp*$^{w12/+}$, black circles: *sdp*$^{w12/w12}$, error bars are +/- standard deviation.

Figure 18. Alterations in migration after *reck* depletion. (A-F) Uninjected and MO-injected *Tg(sox10:nls-eos)* embryos were imaged from 18-40 hpf. **(A, B)** Migration of *reck* MO-injected neural crest is generally appropriate. Scale bar: 25 μm. **(C)** Number of cells is not altered after MO injection. **(D)** Average velocity in y-axis. MO-injected cells are hypermigratory compared to uninjected cells ($t(92) = 2.26$, $p = 2.84\text{E-}2$). **(E)** Division rate is not significantly altered following *reck* depletion. **(F)** Apoptosis s a rare event and was not observed in any MO-injected embryo time-lapses (preventing statistical analysis). **(G-L)** To examine cell behavior during overt DRG neuronal differentiation, uninjected and MO-injected *Tg(sox10:nls-eos)*/*Tg(neuroD:tagRFP)* embryos were imaged in time-lapse beginning at 30 hpf through 60 hpf. **(G)** In uninjected embryos, a subset of the cells in the migratory stream condense just ventral to the spinal cord (bin of ±10 μm is indicated by the bracket), forming the prospective DRG (empty arrowhead). These cells will become either the initial sensory neuron or its associated satellite glia. Note that *sox10*$^{+}$ oligodendrocytes (filled arrowheads) are visible in both conditions; they can be distinguished from neural crest by their position in the spinal cord, their spherical nuclei, and their late initiation of *sox10* expression. Scale bar: 25 μm. **(H)** Embryos injected with 1.5 ng *reck* MO fail to form the DRG neuroglial cluster. Other neural crest cells take up positions consistent with Schwann cells or migrate out of the field entirely. **(I)** Number of cells tracked per time-lapse is not different between uninjected and MO-injected embryos. **(J)** Average velocity in y-axis. MO-injected cells are hypomigratory compared to uninjected cells ($t(233) = 2.79$, $p = 5.6\text{E-}3$). **(K)** Division rate is not significantly altered following *reck* depletion. **(L)** MO-injected cells undergo apoptosis at a significantly greater rate than uninjected cells ($t(11) = 2.269$, $p = 4.44\text{E-}2$). **(M)** Proportion of cells inhabiting the ±10 μm bin flanking the ventralmost extent of the spinal cord at each point in time (bracket in G,H). LLX: time point at which the lateral line crosses the imaged segment. Uninjected embryos: (black), MO-injected embryos: (red). Error bars are ±95% confidence interval. Significantly fewer cells localize at the ventral aspect of the spinal cord. Simple linear regression of control and MO-injected data indicates that the proportion of uninjected cells inhabiting the prospective DRG microenvironment increases over time whereas the proportion of MO-injected cells inhabiting this region decreases ($F(1, 1858) = 647.832$, $p < 0.0001$; Control: $y = 2.76\times10^{-3}\,x + 0.178$; MO-injected: $y = -3.46\times10^{-4}\,x + 0.300$).

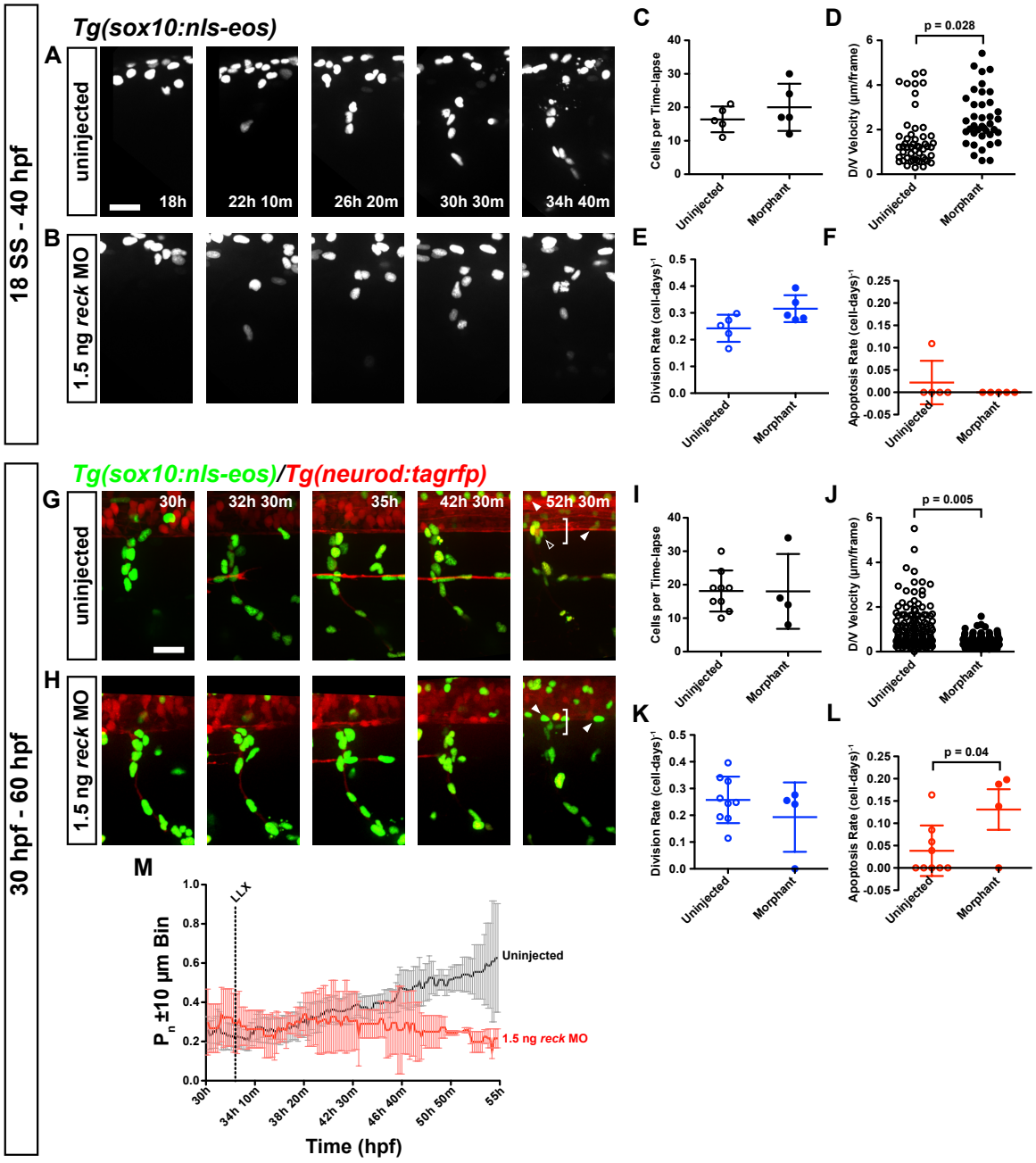
18 SS - 40 hpf
Tg(sox10:nls-eos)
A
uninjected
18h
22h 10m
26h 20m
30h 30m
34h 40m
B
1.5 ng reck MO
C
Cells per Time-lapse
Uninjected
Morphant
D
p = 0.028
D/V Velocity (μm/frame)
E
Division Rate (cell-days)-1
F
Apoptosis Rate (cell-days)-1
30 hpf - 60 hpf
Tg(sox10:nls-eos)/Tg(neurod:tagrfp)
G
30h
32h 30m
35h
42h 30m
52h 30m
H
I
J
p = 0.005
K
L
p = 0.04
M
LLX
Uninjected
1.5 ng reck MO
Pn ±10 μm Bin
Time (hpf)
30h
34h 10m
38h 20m
42h 30m
46h 40m
50h 50m
55h

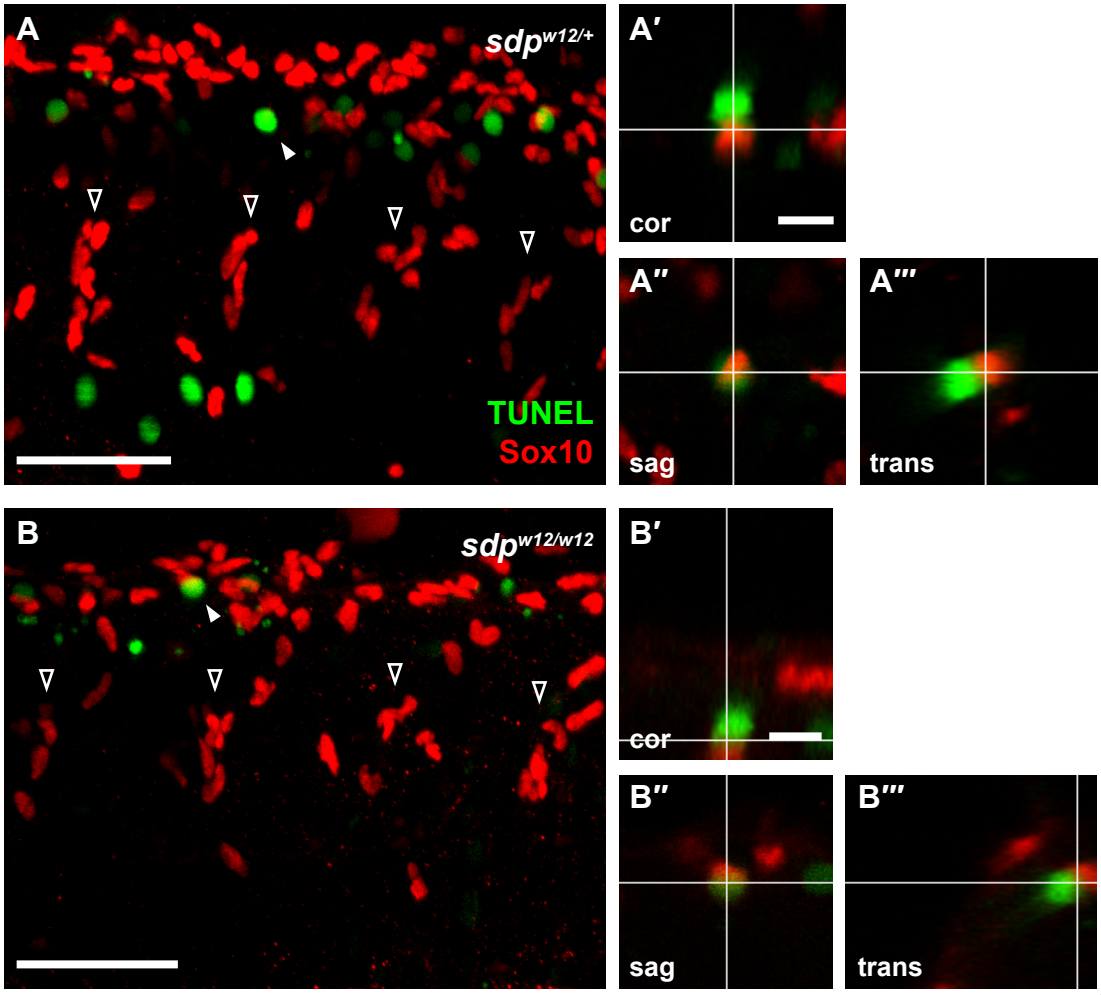

Figure 19. Increased apoptosis is not observed in *sdp* neural crest. *Sdp*$^{w12/+}$ fish were incrossed and the resulting embryos were subjected to Sox10 and TUNEL staining at 30 hpf. Four streams of neural crest cells (open arrowheads) are visible in each image. **(A)** Embryos heterozygous for *sdp*^{w12} exhibit numerous TUNEL^{+} cells, many of which are in close proximity to Sox10^{+} cells (filled arrowhead). Scale bar: 50 μm. Orthogonal projections of confocal stacks were generated to ascertain whether TUNEL and Sox10 staining is colocalized; as evident in the **(A′)** coronal, **(A″)** saggital, and **(A‴)** transverse projections, although TUNEL^{+} and Sox10^{+} cells are adjacent, the markers do not colocalize. Scale bar: 10 μm. **(B)** Embryos homozygous for *sdp*^{w12} exhibit a similar distribution of TUNEL^{+} and Sox10^{+} cells. Scale bar: 50 μm. Again in **(B′)** coronal, **(B″)** saggital, and **(B‴)** transverse projections, no colocalization of markers is observed. Scale bar: 10 μm.

Figure 20. Treatment of *sdp* embryos with MMP inhibitors fails to rescue DRG formation. *Tg(neurog1:egfp)*;*sdp*$^{w12/+}$ fish were incrossed and the resulting embryos were treated from 16 SS to 3 dpf in the following broad-spectrum MMP inhibitors. *neurog1*+ DRG neurons were subsequently counted. **(A)** Chemical structure of GM6001. **(B)** 100 μM GM6001 (black bars) fails to rescue the *sdp* DRG phenotype observed in vehicle-treated embryos (white bars). **(C)** Chemical structure of marimastat. **(D)** 100 μM marimastat (black bars) fails to rescue the *sdp* DRG phenotype observed in vehicle-treated embryos (white bars). **(E)** Chemical structure of batimastat. **(F)** 500 μM batimastat (black bars) fails to rescue the *sdp* DRG phenotype observed in vehicle-treated embryos (white bars).

A GM6001

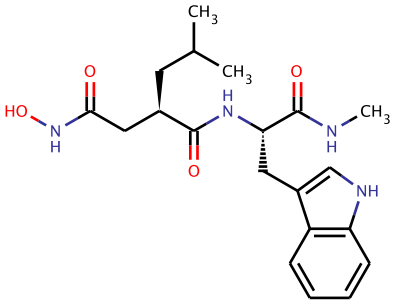

B

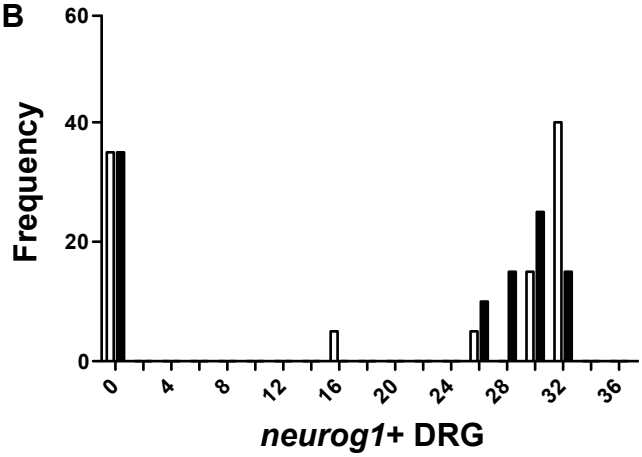

C Marimastat

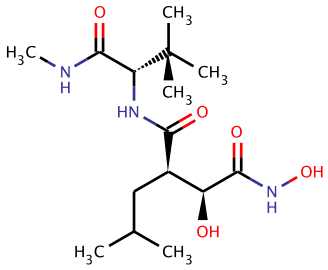

D

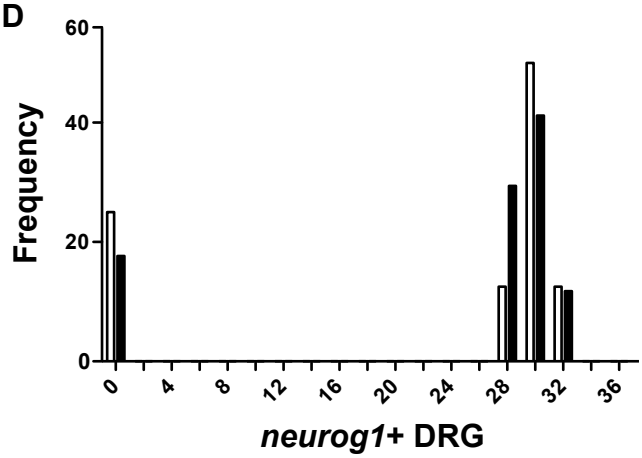

E Batimastat

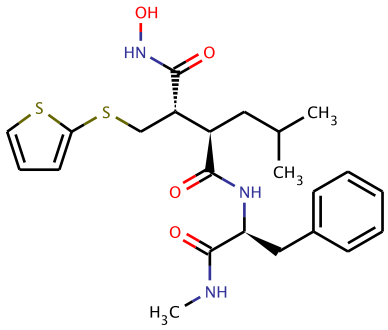

F

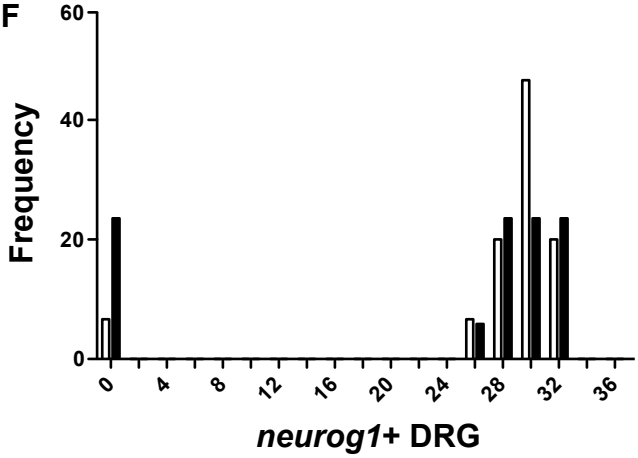

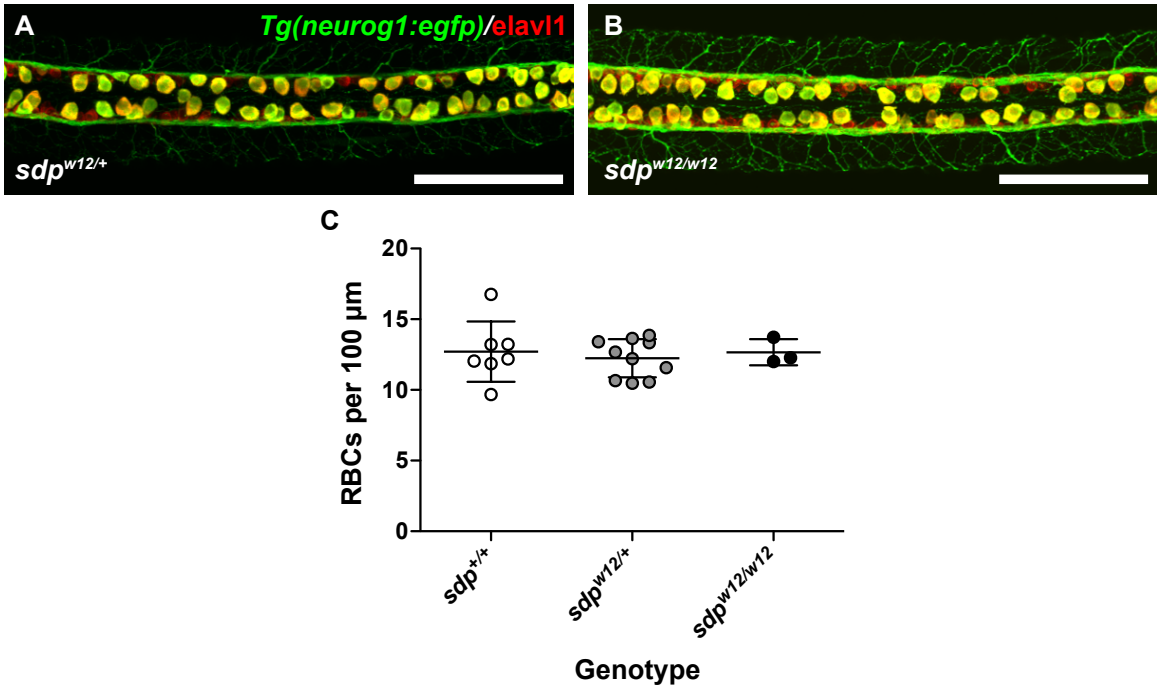

Figure 21. Abnormal Notch signaling does not appear to be the mechanism by which DRG fail to form in the *sdp* mutant. (A) Rohon-Béard cells in a 24 hpf *sdp*$^{w12/+}$ embryo carrying the *neurog1:egfp* transgene (green) and immunostained for Elavl1 (red). Scale bar: 100 µm. **(B)** Rohon-Béard cells are present in comparable density in *sdp*$^{w12/w12}$ embryos. Scale bar: 100 µm. **(C)** Counts of Rohon-Béard cells in all three *sdp* genotypes; Rohon-Béard cell count does not vary significantly across genotypes, $F(2, 17) = 0.1940$, $p = 0.8255$.

Tables

Genotype	Injection		Dorsal root ganglia			
			Mean	*(SD)*	n	*p*
+/+	Mock		29.6	*(1.6)*	8	-
	wt	100 pg	27.9	*(3.4)*	8	n.s.
		200 pg	29.8	*(2.6)*	4	n.s.
	sdp^{w12}	100 pg	31.1	*(1.4)*	9	n.s.
		200 pg	30.3	*(1.6)*	8	n.s.
+/w12	Mock		29.9	*(2.3)*	30	-
	wt	100 pg	27.7	*(3.0)*	19	n.s.
		200 pg	27.7	*(4.5)*	9	n.s.
	sdp^{w12}	100 pg	31.1	*(2.6)*	16	n.s.
		200 pg	30.2	*(2.0)*	22	n.s.
w12/w12	Mock		0.0	*(0.0)*	10	-
	wt	100 pg	15.4	*(8.8)*	10	< 0.001
		200 pg	23.4	*(2.9)*	5	< 0.001
	sdp^{w12}	100 pg	0.0	*(0.0)*	10	n.s.
		200 pg	0.0	*(0.0)*	2	n.s.

Table 1. Injection of *reck* mRNA rescues *sdp$^{w12/w12}$* in a dose-dependent fashion. DRG counts of mRNA-injected embryos at 4 dpf are displayed with standard deviation for each genotype/injection permutation. A two-way analysis of variance showed that the injection factor was significant, $F(4,155) = 19.77$, $p = 3.61E\text{-}13$. The Scheffé post-hoc criterion for significance revealed that only the injection of *wt reck* into *sdp$^{w12/w12}$* embryos had a significant effect on DRG counts relative to mock-injected embryos of the same genotype (100 pg: $M = 15.4$, $SD = 8.8$; 200 pg: $M = 23.4$, $SD = 2.9$).

Donor	Host	*n*	Donor contribution		*Hit rate*
			Neural crest	Dorsal root ganglia	
Mock	Mock	32	14	4	28.6%
Morphant	Mock	119	18	0	0.0%
Mock	Morphant	15	9	5	55.6%

Table 2. Mock-injected cells can form DRG in *reck* morphant embryos, but *reck* morphant cells cannot form DRG in mock-injected embryos. Transplant conditions are presented along with the number of instances neural crest was targeted and the number of instances DRG were targeted. The hit rate is derived by dividing the latter number by the former. A Fisher's exact test showed that DRG formation by donor cells was not equivalent across all conditions, $p = 0.003$, Fisher's exact test. Post-hoc analysis using Fisher's exact test and adjusted α for repeated statistical tests ($\alpha_{adj} = 0.0475$) revealed that the mock into mock condition exhibited more DRG targeting than the morphant into mock condition, the morphant into mock condition exhibited less DRG targeting than the mock into morphant condition, but the degree of DRG targeting in the mock into mock condition was not significantly different from that observed in the mock into morphant condition (mock>mock vs. MO>mock: $p = 0.037$, Fisher's exact test; MO>mock vs. mock>MO: $p = 0.002$, Fisher's exact test; mock>mock vs. mock>MO: $p = 0.383$, Fisher's exact test).

Injection	n	DLAV (32 hpf)			Axial circulation (48 hpf)		
		Present	Absent	*p*	Normal	Impaired	*p*
Control MO	34	34	0	<1.00E-4	34	0	<0.01
3 ng *reck* MO	45	5	40		34	11	

Injection	n	Parachordal chain (72 hpf)			Intracranial hemorrhage (72 hpf)		
		Present	Absent	*p*	Present	Absent	*p*
Control MO	34	34	0	<1.00E-4	34	0	<1.00E-3
3 ng *reck* MO	45	5	40		33	12	

Table 3. *Reck* morphants exhibit defective vasculature. *Tg(fli1a:egfp)* embryos were injected with control MO or 3 ng *reck* MO and scored for the following phenotypes: dorsal longitudinal anastomotic vessel (DLAV) formation at 32 hpf, axial circulation at 48 hpf, parachordal chain (PAV) formation at 72 hpf, and intracranial hemorrhage at 72 hpf. All data were analyzed using Fisher's exact test. *Reck* morphants exhibited significantly impaired DLAV formation (p < 1.00E-4), significantly impaired axial circulation (p < 0.01), significantly impaired PAV formation (p < 1.00E-4) and significantly increased incidence of intracranial hemorrhage (p < 1.00E-3).

Genotype	Cells per hemisegment		n	
	TUNEL+	Sox10/TUNEL+	Embryos	TUNEL+
+/+	4.16	0	7	167
+/w12	2.64	0	23	365
w12/w12	3.57	0	5	107

Table 4. Apoptotic markers do not colocalize with neural crest markers. $TUNEL^+$ cells per hemisegment are presented for each genotype. In 639 $TUNEL^+$ cells counted across 35 embryos, we observed no $Sox10^+/TUNEL^+$ cells.

Chapter III: Attempts to identify metalloproteinases subject to Reck inhibition and observation of putative perdurant adult DRG stem cells

Chapter abstract

Neurogenin1 (Neurog1) is the first proneural gene expressed in nascent DRG neurons as they differentiate from neural crest. How a subset of the neural crest initiates Neurog1 remains mysterious. Previously, we performed a mutant screen for phenotypes lacking Neurog1 expression in DRG in an attempt to identify upstream factors controlling its expression. We identified one such factor: Reck, an inhibitor of metalloproteinases. The discovery of Reck has only generated additional questions, as it is unclear how metalloproteinase signalling might interact with expression of Neurog1. To address these questions, I performed a FACS-based screen of MMPs expressed in neural crest. I also generated fusion proteins to facilitate coimmunoprecipitation of Reck-interacting MMPs.

Introduction

Metalloproteinases are a large family of zinc-dependent proteases. These are frequently subcategorized; two of the most commonly studied divisions of the metalloproteases are the a-disintegrin and metalloproteinases (ADAMs) and the matrix metalloproteinases (MMPs). Although perhaps traditionally conceived of as factors responsible for remodeling extracellular matrix (ECM) (an extensive list of ECM proteins and the metalloproteinases that degrade them can be found in (Edwards et al., 2008; Sternlicht and Werb, 2001)), the digestion of ECM has consequences beyond the mere reorganization of the cellular substrata. An example of this is the digestion of the ECM component decorin which acts as a depot for TGFβ; following metalloprotease digestion, free TGFβ is released (Imai et al., 1997). MMPs also catalyze the generation of active signaling ligands from

proproteins, as is observed in chemokine (English et al., 2000; Van den Steen et al., 2003) or neurotrophic (Hwang et al., 2005; Lee et al., 2001) signaling.

Metalloproteinases also participate in signaling pathways in more complex ways. ADAMs are capable of acting as pathway-activating “sheddases” in EGFR (Sahin, 2004), Delta/Notch (Lieber et al., 2002; Muraguchi et al., 2007), Slit/Robo (Coleman et al., 2010; Fambrough et al., 1996; Schimmelpfeng et al., 2001), Eph/Ephrin (Hattori et al., 2000; Janes et al., 2005), and Netrin/DCC (Galko and Tessier-Lavigne, 2000) signaling systems. The nature of this signaling is complex, with ADAMs often being involved on both sides of these bipartite signaling systems. ADAMs also may regulate cell/cell contacts directly through interaction with integrins (reviewed in (White, 2003)).

Dorsal root ganglia (DRG) are derived from the neural crest—a transient, migratory cell population that generates elements of the peripheral nervous system, pigment cells, secretory cells, and facial cartilages. Recently, I determined that a zebrafish phenotype lacking DRG, *sensory-deprived* (*sdp*), is caused by loss of function of the metalloproteinase inhibitor Reck (reversion-inducing, cysteine-rich protein containing Kazal motifs). I also showed that gelatinase activity is increased in *sdp* embryos, suggesting that metalloproteinase dysregulation is related to the DRG phenotype. However, achieving a mechanistic explanation of this phenotype is complicated by the fact that there are many metalloproteinases expressed in the vertebrate organism (at least 37 ADAMs and 21 MMPs in mouse (Puente and López-Otín, 2004) and perhaps more in zebrafish due to gene duplication), and each of these may have diverse functions. Although Reck is known to bind and inhibit Mmp2, Mmp9, Mmp14, and Adam10, a comprehensive study of its regulatory activity has not been performed. To better understand the role metalloproteinase activity might play in peripheral nervous system neurogenesis, I attempted to use several screening methods to identify potential targets of Reck inhibition.

Materials and methods

Fluorescence activated cell sorting

24 hpf *AB and *Tg(sox10:eos)* embryos (approximately 400/genotype) were dechorionated and dissociated into a single cell suspension by incubating embryos in 2 mL of a solution consisting of 1X PBS, 1mM EDTA, 0.25% trypsin (Sigma), and 2U DNAseI (Fermentas) at 28.5 º C (Covassin et al., 2006). Dissociation was encouraged by frequent trituration and monitored under a dissecting microscope. The digest was killed by adding 0.5 mL 5mM $CaCl_2$ and 50% FCS (Gibco/Invitrogen) in 1X PBS.

Cells were pelleted by centrifugation at 3000 rpm for 3 minutes, rinsed in 1X PBS, pelleted again, and resuspended in L-15 (Gibco/Invitrogen) media supplemented with 1% FCS, 0.8 mM $CaCl_2$, 50U/mL penicillin (Gibco/Invitrogen), and 0.05 mg/mL streptomycin (Gibco/Invitrogen). Cells were sorted using a BD Biosciences FACS Canto flow cytometer and either plated for tissue culture or processed for RNA. This procedure routinely yielded ~1.5×10^6 cells/run.

Zebrafish embryo extract

200 3dpf *AB embryos were rinsed in chilled 0.5% bleach for 2 minutes and then in Ca^{2+}-free Ringer's for 2 minutes. Embryos were syringe-homogenized and resuspended in 1 mL L-15 media supplemented with 0.3 mg/mL glutamine, 0.8 mM $CaCl_2$, 50U/mL penicillin, and 0.05 mg/mL streptomycin.

Cell culture

Sorted cells were plated at low density 2.63×10^3 cells/cm^2 on poly-D-lysine-coated coverslips (BD Biosciences) in L-15 media supplemented with 0.8 mM $CaCl_2$, 10% FCS, 10% zebrafish embryo extract, 50U/mL penicillin, and 0.05 mg/mL streptomycin.

Immunohistochemistry

Embryos were stained with rabbit α-GFP (Invitrogen) at 1:1000, rabbit α-RFP (Invitrogen) at 1:200, and mouse α-Elavl1 (Invitrogen) at 1:500 as previously described (Westerfield). Cultured cells on coverslips were stained by the same method using rabbit α-Sox10 (generous gift of Sarah Kucenas, University of Virginia) at 1:500 and counterstained with DAPI (Invitrogen).

Quantitative real-time PCR

RNA was isolated from FAC sorted cells by homogenization in Trizol (Invitrogen) followed by column purification (Qiagen). RNA was treated with DNAseI to remove contaminating genomic DNA and reverse transcribed (Invitrogen). Zebrafish MMP transcripts were identified in the NCBI database; these were often predicted transcripts. qPCR primers were designed preferentially against regions that aligned to zebrafish ESTs. Quantitative RT-PCR was executed using an MJ Research Opticon light cycler and data were analyzed using the $\log 2^{-\Delta\Delta C(t)}$ method with normalization to β-actin.

Morpholino knockdown of metalloproteinase transcripts

Previously verified antisense morpholio oligonucleotides were obtained for *mmp2* (5′-GTGGCGAACAGCCCTTTCAGACGTG-3′) (Coyle et al., 2008), *mmp9* (5′-GAGTCGCAAATATAAAAGTAAATTC-3′) (Coyle et al., 2008), *mmp14a* (5′-GACGGTACTCAAGTCGGGACACAAA-3′) (Coyle et al., 2008), and *mmp17b* (5′-TGAGAACTGTTGAGACACATTTTGA -3′) (Leigh et al.) (GeneTools). These were injected at varying concentrations in 0.2% phenol red, 0.1M KCl as previously described (Westerfield).

In situ hybridization

Digoxigenin-labeled probes for *mmp2*, *mmp9*, and *mmp14a* were generated from linearized plasmid (*mmp2*: EcoRI, *mmp9*: PstI, *mmp14a*: EcoRI) (NEB) followed by *in vitro* transcription (*mmp2*: T7, *mmp9*: T7, *mmp14a*: T7)

(Roche). *In situ* hybridization was performed as previously described (Thisse and Thisse, 2008).

Generation of Reck fusion proteins

Site-tagged primers were designed against tagRFP such that BglII, NcoI, and XmaI sites were inserted 5′ to the fluorophore and an XbaI site was inserted 3′. Similar primers were designed for the wild type Reck sequence such that BglII, NcoI, and XmaI sites were inserted 3′ to Reck. TagRFP was amplified from pME-tagRFP (Arminda Suli, unpublished) and Reck was amplified from pCS2+Reck(AB) (Prendergast et al., 2012). The two fragments were inserted into pCS2+ using a three-fragment, T4 ligase-catalyzed ligation (NEB) to generate the C-terminal pCS2+Reck+tagRFP fusion construct.

To generate the N-terminal fusion, site-directed mutagenesis was employed to insert a single NcoI site between the putative Reck signal sequence (after 69 NT of the wild type sequence). TagRFP was then flanked with NcoI sites using site-tagged primers and ligated into the novel NcoI site as above.

The ΔN+tagRFP+Reck fusion protein was generated by amplifying all Reck sequence downstream of the putative signal sequence from pCS2+tagRFP+Reck with site-tagged primers to add a 5′ XhoI site. This cassette was ligated into pCS2+ as above.

mRNA injection

pCS2 expression constructs were linearized with NotI (NEB) and transcribed *in vitro* with SP6 polymerase (Ambion) to generate capped, polyadenylated mRNA. 200 pg RNA/embryo was injected in 0.2% phenol red, 0.1M KCl as previously described (Westerfield).

Photoconversion and lineage tracing

Tg(sox10:nls-eos) and *Tg(neurod:nls-eos)* embryos were mounted in 1.2% low-melt agarose/E2 media on chambered coverglass (Nunc). Small cell

clones in 48 hpf embryos were photoconverted using the 405 nm laser line on a Olympus FluoView FV-1000 scanning confocal microscope. Embryos were then freed from the agarose, allowed to develop to 96 hpf, and processed for immunohistochemistry as described.

Results

Generation of photoconvertible transgenic embryos for the study of neural crest and examination of cell lineage in DRG

Photoactivateable fluorescent proteins (PAFPs) are fluorophores that undergo irreversible (Ando et al., 2002; Gurskaya et al., 2006; Patterson and Lippincott-Schwartz, 2004; Tsutsui et al., 2005; Wiedenmann et al., 2004) or reversible (Adam et al., 2008; Chudakov et al., 2003; Habuchi et al., 2005) (but see also (Lukyanov et al., 2005) for some review of the involved chemistry) changes in their emission spectra following light-catalyzed reactions. The use of these proteins has become fairly extensive in zebrafish, with PAFPs being used to trace neuronal projections (Sato et al., 2006), perform cell birthdating and analyze proliferation (Caron et al., 2008), and in studies of cell lineage and differentiation (Curran et al., 2010). To exploit these tools in studying the neural crest and dorsal root ganglia, I generated transgenic lines in which the PAFP Eos either with or without a fused SV40 nuclear localization sequence (nls-Eos) under the control of a 4.9 Kb fragment of the Sox10 promoter (Figure 23A, D) (Carney et al., 2006) or a 5.0 Kb fragment of the NeuroD promoter (Figure 23G, J) (from Teresa Nicolson, unpublished).

Stable F2 *sox10* transgenics exhibited faithful expression in neural crest which was verified by double fluorescent in situ hybridization (Figure 23B, C, E, F, M-O). Reporter expression driven by the NeuroD promoter was much more extensive than endogenous *neuroD* expression (Figure 23P, Q); this transgenic appears to be essentially pan-neuronal. However, it is expressed in DRG, and this pan-neuronal expression proves to be an asset in the studies that follow.

Consistent with prior reports, Eos photoconverted efficiently when subjected to light pulses generated by a 405 nm laser (Figure 23F, L).

Neural crest cells are efficiently isolated from Tg(sox10:eos) embryos using fluorescence activated cell sorting

24 hpf *Tg(sox10:eos)*embryos were easily dissociated and the resulting cell suspension was sorted for fluorescence (Figure 24A, B) to segregate neural crest and non-neural crest. Culturing dissociated, sorted neural crest cells revealed many Eos+ cells that also expressed Sox10 protein (Figure 24C-C‴). To additionally verify that sorted cells were neural crest, I isolated cDNA pools from sorted neural crest and non-neural crest cells and performed quantitative RT-PCR to examine the relative quantities of neural crest-specific transcripts between the two pools. *sox10* (Dutton et al., 2001), *crestin* (Rubinstein et al., 2000), *foxd3* (Kelsh et al., 2000), and *snai1b* (Thisse et al., 1995) expression were upregulated about 2- to 6-fold in neural crest compared to non-neural crest. The MMP inhibitor *reck* was notably expressed approximately 10-fold less in neural crest compared to non-neural crest, despite the fact that I have shown *reck* to be essential for the normal development of neural crest-derived tissues (Prendergast et al., 2012). This is probably owing to the fact that *reck* is more strongly expressed in vascular tissues than in neural crest.

Comparative quantative RT-PCR identifies metalloproteinases that may be of high relevance to neural crest development

Since some genes essential to neural crest development exhibit enhanced expression in neural crest in this comparative FACS/RT-PCR assay, I reasoned that MMPs upregulated in neural crest relative to non-neural crest might also be essential to its development. Furthermore, these MMPs would be excellent candidate targets of Reck inhibition. A large (but not comprehensive) panel of MMP qPCR markers was developed based on available zebrafish ESTs and full-length cDNAs (see Materials and methods). This panel was then employed against isolated cDNA pools from neural crest and non-neural crest.

I observed relative upregulation of only 11 of 30 MMPs (Figure 25). Of these, only 6 exhibited more than a 2-fold increase in expression relative to the non-neural crest cDNA pool. Of the 11 upregulated MMPs, 4 (Mmp2, Mmp9, Mmp14a, and Adam10b) are homologues of previously identified regulatory targets of Reck (Muraguchi et al., 2007; Oh et al., 2001; Takahashi et al., 1998). Of the highly-enriched set of 6, all candidates are membrane associated, either via transmembrane domains (Mmp16a, Adam10b) or GPI linkages (Mmp25a/b, Mmp17a/b) (reviewed in (Ethell and Ethell, 2007). Notably, Reck is itself a GPI-linked protein, and some investigators have hypothesized that GPI-linked proteins may localize to common cellular microdomains such as lipid rafts (Glebov and Nichols, 2004; Sharom and Lehto, 2002). Therefore, the fact that this approach identifies the only known GPI-linked MMPs identified in the zebrafish as potential candidate molecules is of some interest.

Morpholino oligonucleotide knockdown of individual candidate MMPs does not rescue sdp

If MMP hyperactivity pursuant to Reck loss-of-function is responsible for the defect observed in *sdp*, it may be possible to rescue this defect by inhibiting the function of the Reck-related MMP. Such a result has been observed in a Reck mouse null allele; vascular defects that occur as a consequence of Reck loss-of-function are partially rescued by crossing into an *mmp2*$^{-/-}$ background (Oh et al., 2001). I knocked down the expression of several candidate MMPs using previously verified morpholinos (see Materials and methods, Figure 26), but did not observe any rescue of the *sdp* phenotype.

Reck fusion proteins are fully functional and suggest that zebrafish Reck is a GPI-linked protein

Reck has previously been established as a GPI-linked, membrane-associated protein. To verify whether this is also true in zebrafish, I generated constructs in which tagRFP is fused in frame to the Reck coding sequence. Injecting mRNA coding for EGFP, a fluorophore of approximately the same size

as tagRFP, reveals that small proteins are free to diffuse throughout the cyoplasm and are not excluded from the nucleus (Figure 27A). Reck possesses a putative N-terminal signal sequence that theoretically directs its packaging into the endoplasmic reticulum prior to extracellular secretion. Insertion of the fluorophore tagRFP between this signal sequence and the Reck coding sequence reveals that Reck exhibits a strong association with the cell membrane (Figure 27 B′).

Reck also possesses a putative GPI signal sequence. During translation, this sequence is cleaved, and a glycosylphosphatidylinositol moiety is added (reviewed in (Udenfriend and Kodukula, 1995)); the modified protein is inserted into the cell membrane. Injection of a C-terminal fusion protein in which tagRFP is fused after the GPI signal sequence reveals a very different pattern of subcellular localization. The fluorophore in the C-terminal fusion exhibits a diffuse cytoplasmic localization, but is excluded from the nucleus (Figure 27 C′). This is consistent either with a cyotsolic fusion protein too large to pass through nuclear pores freely (Goldberg and Allen, 1993; Peters, 1986) or a protein that is maintained in the endoplasmic reticulum (ER). Deleting the N-terminal signal sequence from the N-terminal fusion should ensure that the resulting protein is retained in the cytoplasm and is retained in the cytosol; however, the resulting protein should be too large to enter the nucleus without directed transport. Indeed, ΔN-tagRFP-Reck exhibits just such a subcellular distribution (Figure 27D′).

I have previously shown that injection of functional *reck* mRNAs is capable of rescuing the DRG phenotype observed in *sdp* (Prendergast et al., 2012). Injection of *reck* mRNA carrying the *w12* mutation is not capable of rescuing *sdp* (Figure 27E). However, injection of either the N-terminal or the C-terminal fusion protein is fully capable of rescuing *sdp*, despite their vastly different subcellular localizations. Notably, ΔN-tagRFP-Reck exhibits a similar subcellular localization as the C-terminal Reck fusion, yet it is wholly incapable of rescuing *sdp* (Figure 27D′, E). These results suggest that when the C-terminal Reck fusion is injected,

the fluorophore is cleaved during processing and retained in the endoplasmic reticulum, leaving Reck itself to be transported to the membrane and act as it normally does. Since tagRFP alone is small enough to diffuse freely in and out of the nucleus were its distribution strictly cytosolic, it is probably retained in the ER. It does remain possible that Reck exerts its *sdp*-rescuing effects within the ER itself (since both the N-terminal and C-terminal fusions pass through that compartment but the ΔN fusion does not), but this remains fairly strong evidence that Reck's localization to the secretory pathway and beyond is essential for its appropriate function.

A latent sox10+/neuroD- stem cell exists in the DRG and contributes to later DRG growth

The majority of neuronal addition to DRG in mammalian and avian embryos is compressed into a very short interval—a few days at most (see Figure 1). Zebrafish are notable in comparison to these other models in that they initally form DRG containing only one or two neurons; however, over the course of development, each ganglion must expand to contain perhaps a hundred neurons and their associated glia (An et al., 2002; McGraw et al., 2008; McGraw et al., 2012).

To determine if local progenitors generate neurons throughout development, I attempted to photoconvert single *sox10*+ cells (actually, 1-4 cells were converted per experiment) in the DRG of 48 hpf embryos (Figure 28A). Two days later, the labeled cells were assessed to determine how many labeled cells were present and for the expression of the neuronal marker Elavl1 (Figure 28B-E). Almost all *sox10*+ cells proliferate, and many give rise to neurons (Figure 28F, but see (McGraw et al., 2012) for a more thorough analysis of the differentiation of these cells). Since no cells from the neural crest migrate into the DRG chain beyond 36 hpf, all progeny must be derived from local progenitors (Figure 28G). Conversely, differentiated neurons, identified using the

Tg(neurod:nls-eos), never divided following photoconversion and instead simply went on to express Elavl1 (Figure 28H-M).

Discussion

In work described in this chapter, I attempt to identify MMPs that influence DRG development in conjunction with Reck. Previously, I showed that loss of Reck function imparts a hypermigratory phenotype on neural crest, and that neural crest deficient in Reck fails to form sensory neurons in the dorsal root ganglia (Prendergast et al., 2012). I developed a simple model wherein a critical MMP subject to Reck regulation might promote the migration of non-neurogenic neural crest; disinhibition of this MMP might therefore cause all neural crest to migrate excessively and consequently impair neuronal differentiation. I anticipated that inhibition of this MMP using morpholino oligonucleotides would rescue the DRG defect observed when Reck is lost. Other Reck loss-of-function phenotypes have previously been rescued in response to this sort of manipulation (Oh et al., 2001).

Identifying a cognate MMP was complicated by the immense number of MMPs present in the vertebrate genome. To narrow this pool of potential targets, I performed a differential expression screen comparing sorted neural crest cells to non-neural crest. This approach yielded a handful of MMPs expressed more highly in neural crest than in other tissues; this candidate pool consisted almost entirely of known targets of Reck inhibition and membrane-associated MMPs, potentially validating this approach. I reasoned the higher expression might reflect a greater relevance to the development of the neural crest. Although I have not yet exhausted the candidate pool derived from this screen, it would appear that knocking down single MMPs is not sufficient to rescue the effects of Reck loss-of-function observed in *sdp*. Since MMPs are clearly expressed in overlapping domains and often share targets, it may be necessary to knock down a whole set of complementary MMPs in order to rescue *sdp*.

In a parallel set of experiments, I generated a series of fusion constructs in which the fluorophore tagRFP (Merzlyak et al., 2007) was fused to the coding sequence of Reck. These fusion proteins assumed subcellular localizations consistent with prior reports (Takahashi et al., 1998), with Reck translocating to the membrane except following the removal of its signal sequence. Fusing tagRFP to the GPI signal sequence, which is cleaved during protein processing and transport, resulted in a diffuse localization consistent with fluorophore retention in the ER. Taken together, these results suggest zebrafish Reck, like its mammalian counterpart, is a GPI-linked, membrane-attached protein.

The N-terminal tagRFP-Reck fusion protein is fully functional and exhibits appropriate subcellular localization. It therefore represents a powerful tool for further studies of Reck signaling. Immunoprecipitation of tagRFP-Reck should co-precipitate MMPs and other factors essential to its function in neurogenic signaling. Because it is genetically encoded, this protein can be expressed specifically under the control of the Sox10 promoter (Carney et al., 2006) and pulled down specifically from neural crest, thereby partially avoiding binding partners irrelevant to DRG development.

In this chapter I also present evidence to suggest the expansion of DRG throughout later larval development is mediated by the expansion and neuronal differentiation of a local, Sox10+ progenitor cell (see also (McGraw et al., 2012) for extension of these results). Sox10 is known to be essential for maintenance of a progenitor state in cultured neural crest stem cells (Kim et al., 2003) and is downregulated upon neuronal differentiation (Cheng et al., 2000; Kim et al., 2003; Paratore et al., 2001). It remains to be seen whether Sox10 acts similarly in the context of the zebrafish DRG. This result is consistent with recent results in chicken embryos suggesting that a Sox10+ population at the periphery of the DRG is mitotically active and contributes to DRG growth (George et al., 2010); it should be noted that other reports relying on immunohistochemistry suggest neurons themselves divide in zebrafish DRG (An et al., 2002; Carney et al., 2006).

Figures

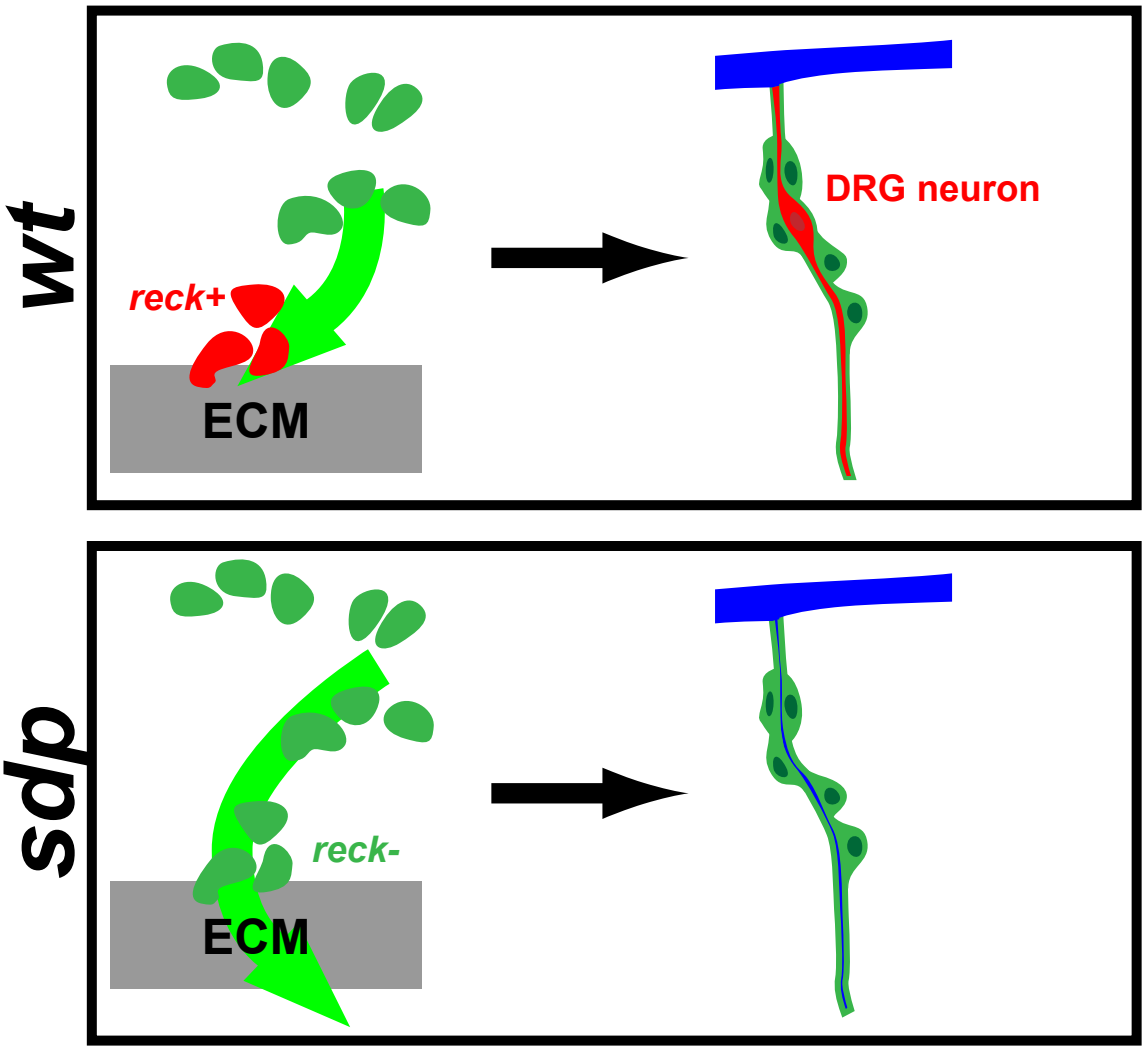

Figure 22. Tentative model explaining Reck's role in neural crest migration and DRG differentiation. (Top) In wild type embryos, Reck becomes restricted to a subset of migrating cells. In these cells, Reck might inhibit a critical MMP capable of digeseting extracellular matrix barriers, and consequently, Reck-expressing cells would arrest and differentiate as sensory neurons. (Bottom) In *sdp* embryos, MMPs would be unrestricted in all migrating neural crest. Consequently, all cells would migrate past this hypothetical extracellular matrix signal, and no sensory neurons would form as a result.

Figure 23. Generation of transgenics using Tol2. (A) A Tol2 vector was constructed containing 4.9 Kb of the Sox10 promoter region (Carney et al., 2006) upstream of the photoconvertible protein Eos (Wiedenmann et al., 2004). **(B)** Isolation of stable transgenics incorporating this construct yields embryos with faithful expression of Eos in neural crest at 24 hpf. **(C)** Close up of neural crest migratory streams. **(D)** A similar construct was generated with the SV40 nuclear localization sequence fused to Eos. **(E)** Stable transgenics are comparable to cytosolic versions, except **(F)** the fluorophore is nuclear localized, making isolation of individual cells easy. The central stream has been photoconverted. **(G)** Eos was also driven using a 5.0 Kb fragment of the NeuroD promoter. **(H, I)** Stable transgenics exhibit pan-neuronal expression of Eos. **(J)** The NeuroD promoter was also used to drive nuclear-localized Eos. **(K)** Stable transgenics are similar to cytosolic versions except the fluorophore is nuclear localized. Several segments of spinal cord have been photoconverted in **(L)**. **(M)** A 24 hpf *Tg(sox10:eos)* embryo immunostained for Eos was also subjected to fluorescent *in situ* hybridization for *sox10* transcript **(N)**; **(O)** colocalization is essentially perfect. **(P)** *In situ* hybridization for *neuroD* in a 48 hpf embryo. Only the head is pictured, but staining can be observed in the layers of the retina (r), the cranial ganglia (cg), and the pancreas (p). **(Q)** A 48 hpf *Tg(neurod:eos)* embryo. Note the extensive staining in the brain and spinal cord that is completely absent from the endogenous expression pattern.

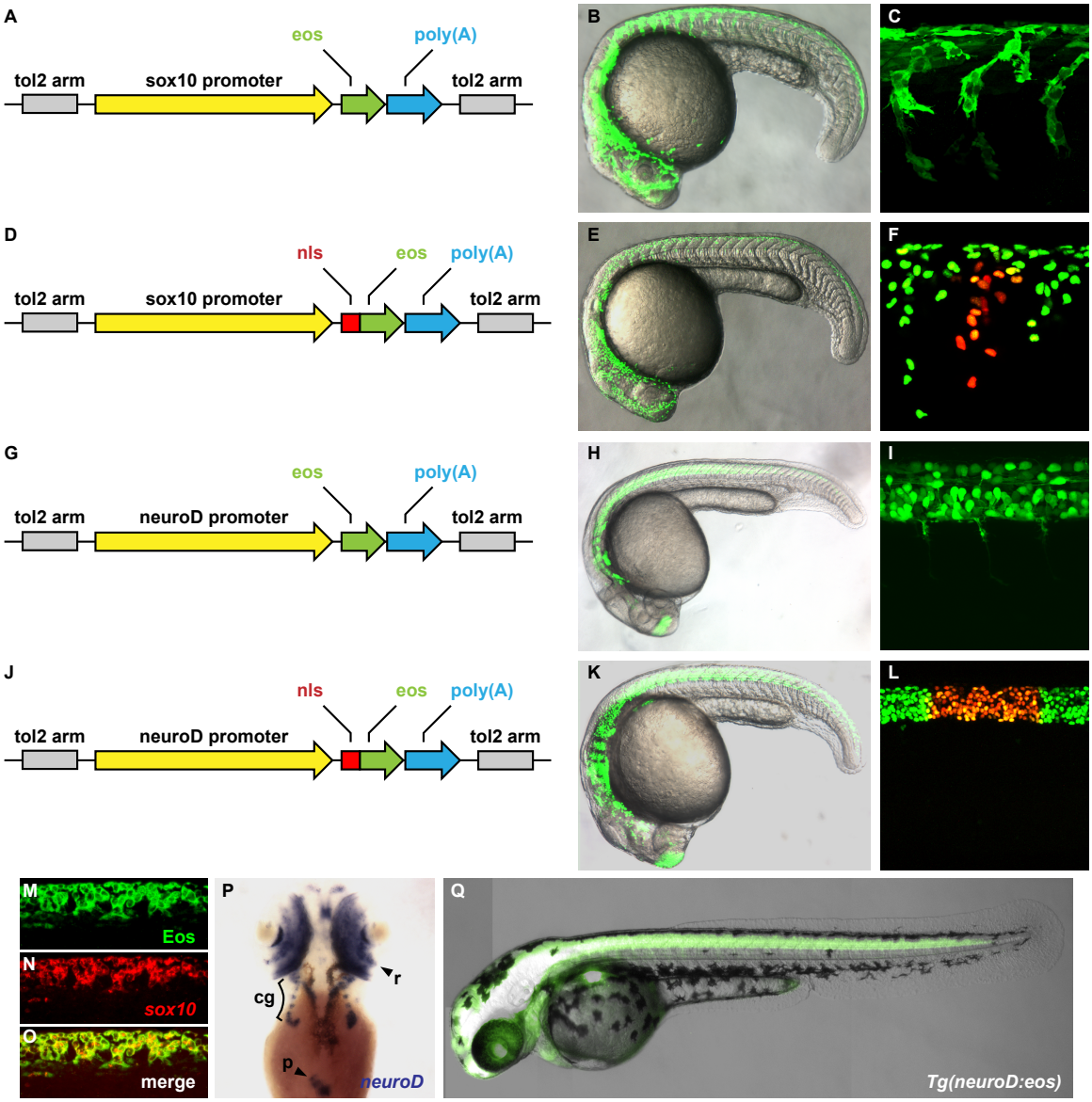
A
eos
poly(A)
tol2 arm
sox10 promoter
tol2 arm
B
C
D
nls
eos
poly(A)
tol2 arm
sox10 promoter
tol2 arm
E
F
G
eos
poly(A)
tol2 arm
neuroD promoter
tol2 arm
H
I
J
nls
eos
poly(A)
tol2 arm
neuroD promoter
tol2 arm
K
L
M
Eos
N
sox10
O
merge
P
cg
r
p
neuroD
Q
Tg(neuroD:eos)

Figure 24. Fluorescence activated cell sorting of neural crest. (A) Example FACS run plotting side-scatter (SSC-A) against fluorescence at 488 nm (FITC). Cells from wild type embryos are depicted by black points, cells from *Tg(sox10:eos)* embryos are depicted by green points. Note that many cells from transgenic embryos are green-shifted. **(B)** Same FACS run with phycoerythrin (PE-A)/broad spectrum fluorescence plotted against fluorescence at 488 nm (FITC). Polygons indicate gating parameters for Eos+ and Eos- cells. Sorted Eos+ cells were plated at low density and imaged for DAPI **(C)** Eos **(C′)** and Sox10 **(C″)**. Merged images are displayed in **(C‴)**; note that plated transgenic cells express Eos and endogenous Sox10. **(D)** Differential quantitative real-time PCR of several neural crest-specific transcripts comparing expression levels between neural crest and non-neural crest cells. Values indicate fold change in Eos+ cells relative to Eos- cells; positive deflections therefore denote relative upregulation and negative deflections denote relative downregulation. Error bars indicate standard deviations from four biological replicates. The crest-specific transcripts *sox10*, *crestin*, *foxd3*, and *snai1b* are all upregulated in Eos+ cells; *reck* is relatively underexpressed in neural crest compared to its high expression in many other parts of the embryo.

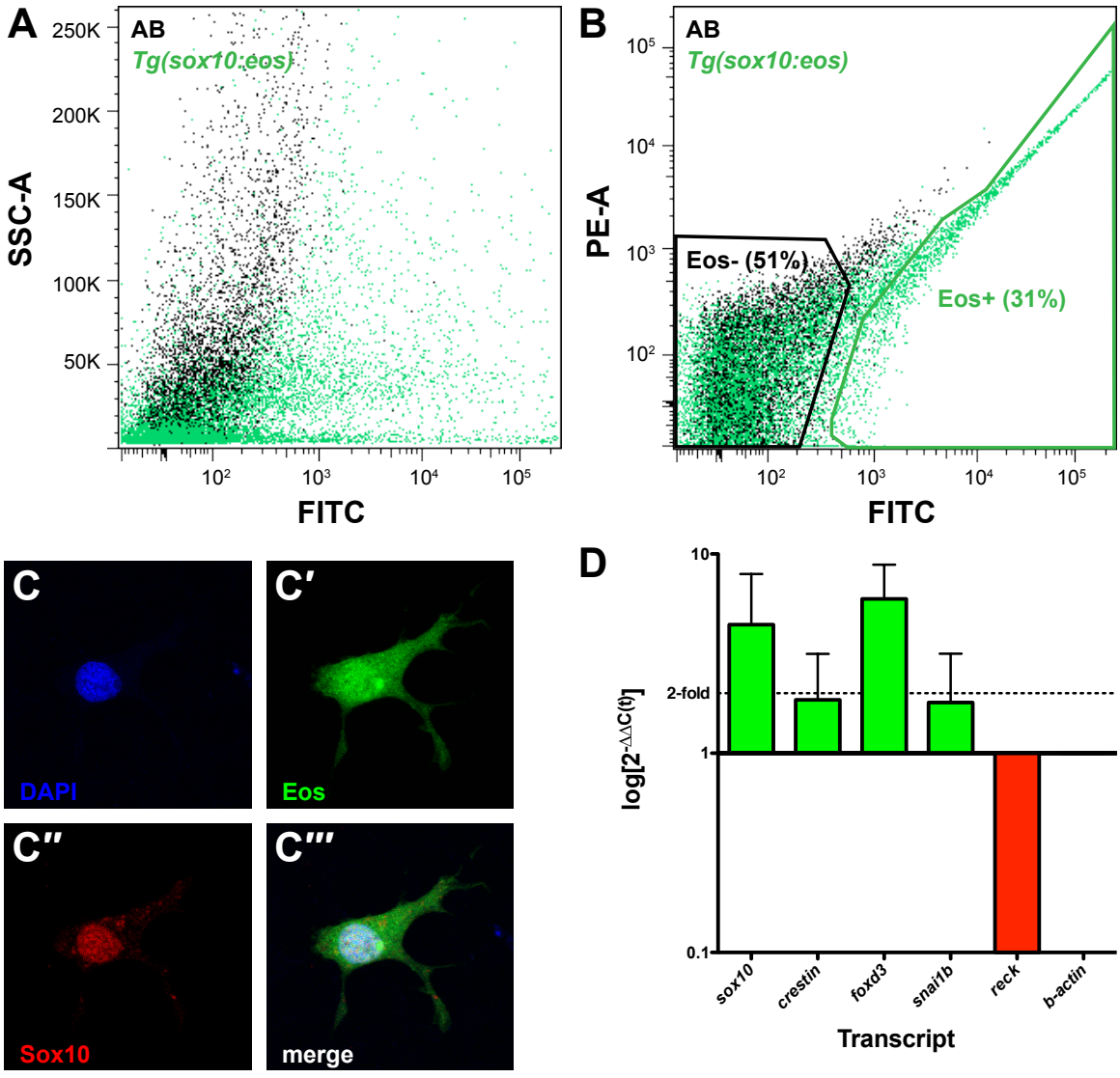
A
AB
Tg(sox10:eos)
250K
200K
150K
100K
50K
SSC-A
10^2
10^3
10^4
10^5
FITC
B
AB
Tg(sox10:eos)
10^5
10^4
10^3
10^2
PE-A
Eos- (51%)
Eos+ (31%)
FITC
C
DAPI
C′
Eos
C″
Sox10
C‴
merge
D
log[$2^{-\Delta\Delta C(t)}$]
10
2-fold
1
0.1
sox10
crestin
foxd3
snail1b
reck
b-actin
Transcript

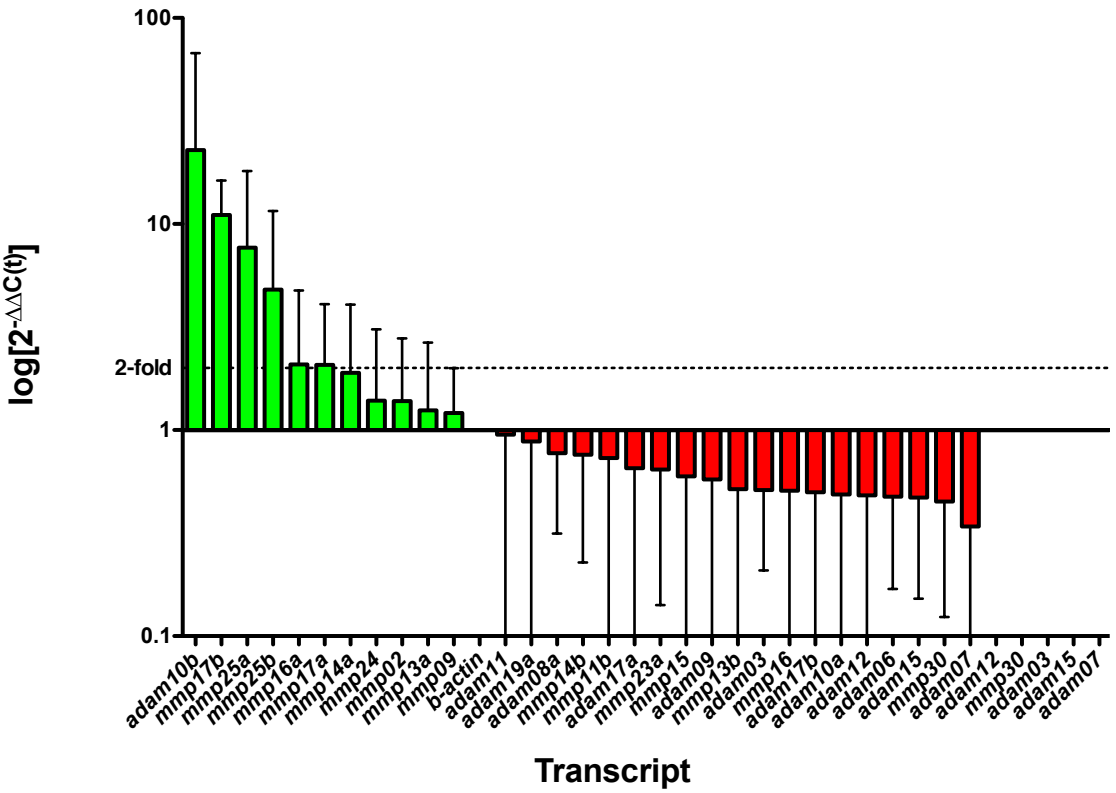

Figure 25. Differential quantitative real-time PCR of metalloproteinases comparing expression between neural crest and non-neural crest cells. Values indicate fold change in Eos+ cells relative to Eos- cells, and values are ranked from most upregulated transcripts to most downregulated transcripts. Error bars indicate standard deviations from four biological replicates. *adam12, mmp30, adam3, adam15,* and *adam7* could not be reliably detected and so are not presented with a fold change value.

Figure 26. Attempts to rescue *sdp* using antisense morpholinos to knock down individual metalloproteinases. Candidate MMPs were selected if they were previously established as a regulatory target of Reck or if they were upregulated in neural crest relative to non-neural crest. *mmp2*, *mmp9*, and *mmp14a* fulfill both criteria ; *mmp17b* fulfills only the latter. **(A)** Unsorted embryos from an *sdp*$^{w12/+}$ incross were injected with varying quantities of *mmp2* MO and *neurog1:egfp*+ DRG were counted at 4 dpf. No rescue is observed at any MO dosage (note the mutant population at the bottom of the plot). **(B)** *In situ* hybridization for *mmp2* in a 24 hpf embryo. The *mmp2* expression pattern is similar to that of *reck* (see Figure 13A and 14J for comparison). **(C)** DRG counts from an *sdp*$^{w12/+}$ incross injected with varying quantities of *mmp9* MO. No rescue is observed. **(D)** *In situ* hybridization for *mmp9* in a 24 hpf embryo. The expression pattern is diffuse and nonspecific. **(E)** DRG counts from an *sdp*$^{w12/+}$ incross injected with varying quantities of *mmp14a* MO. No rescue is observed. **(F)** *In situ* hybridization for *mmp14a* in a 24 hpf embryo. Expression is not particularly specific, although some enrichment is observed in the developing vasculature and in the mesodermal progenitor in the tail. **(G)** DRG counts from an *sdp*$^{w12/+}$ incross injected with varying quantities of *mmp17b* MO. No rescue is observed. *In situ* hybridization has not yet been performed for this transcript.

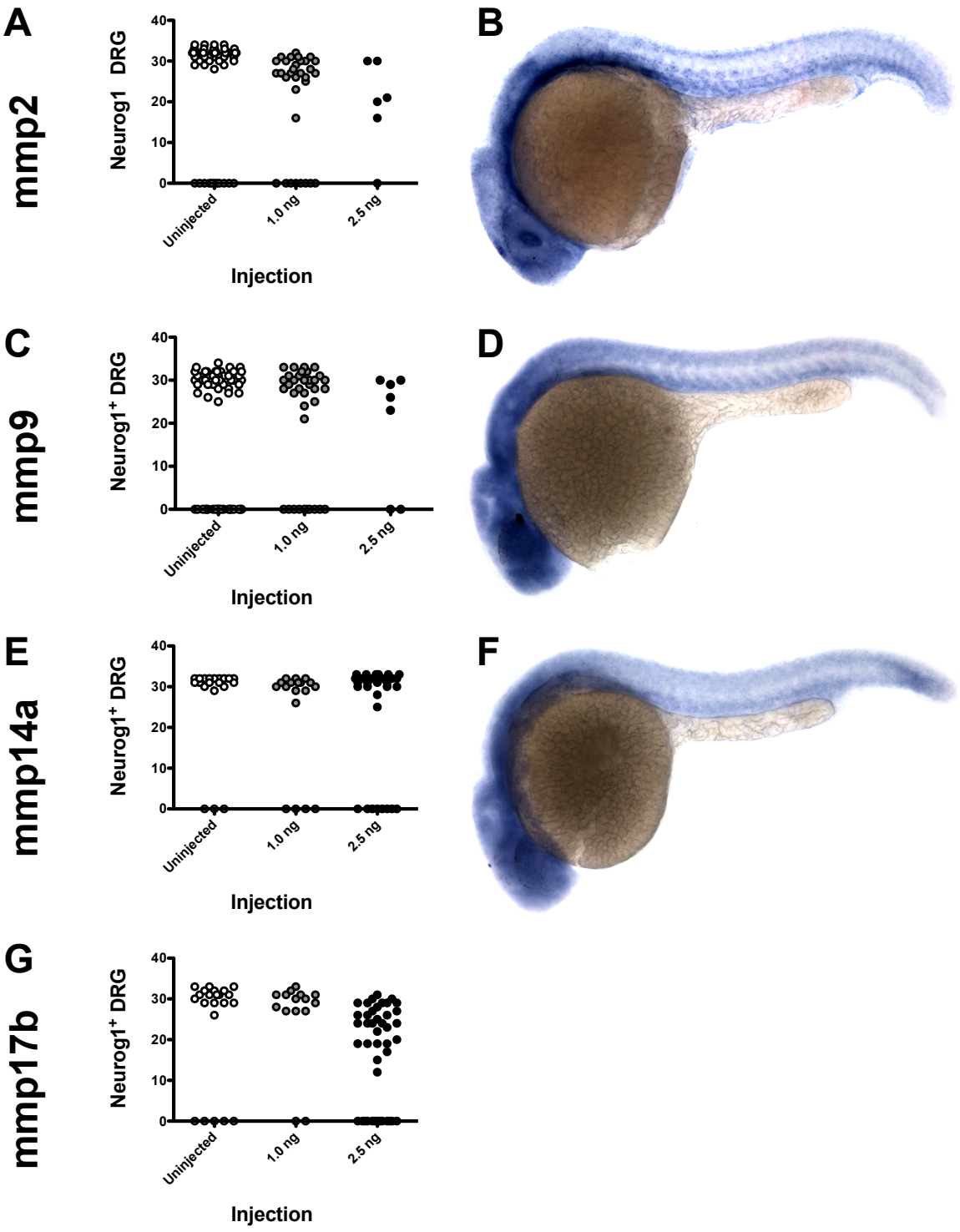
A
mmp2
Neurog1 DRG
40
30
20
10
0
Uninjected
1.0 ng
2.5 ng
Injection
B
C
mmp9
Neurog1+ DRG
40
30
20
10
0
Uninjected
1.0 ng
2.5 ng
Injection
D
E
mmp14a
Neurog1+ DRG
40
30
20
10
0
Uninjected
1.0 ng
2.5 ng
Injection
F
G
mmp17b
Neurog1+ DRG
40
30
20
10
0
Uninjected
1.0 ng
2.5 ng
Injection

Figure 27. The subcellular distribution of Reck fusion proteins establish suggest that it is a GPI-linked, membrane-associated protein. Five Reck fusion proteins were generated (see Materials and methods), injected as mRNA, and their subcellular localization was assessed at 24 hpf in somitic tissue. **(A)** *egfp*-injected embryo imaged in the 488 nm (green) channel and **(A′)** the 568 nm (red) channel. Note that the fluorophore is cytoplasmic and not excluded from the nucleus. **(B)** *tagrfp+reck*-injected embryo imaged in green and **(B′)** red. The N-terminal fusion protein exhibits strong membrane localization. **(C)** *reck+tagrfp*-injected embryo imaged in green and **(C′)** red. The C-terminal fusion protein exhibits an apparent cytosolic distribution but is excluded from the nucleus. **(D)** ∆*N+tagRFP-reck*-injected embryo imaged in green and **(D′)** red. Deletion of the N-terminal signal sequence causes the fusion protein to adopt a cytosolic distribution with nuclear exclusion. **(E)** $sdp^{w12/w12}$ (columns 1-3) or $sdp^{w13/w13}$ (column 4) embryos were injected with fusion mRNAs and *neurog1:egfp*+ DRG were counted at 4 dpf. Injection of sdp^{w12} mRNA does not rescue *sdp*. Both *tagrfp+reck* (N-terminal fusion) and *reck+tagrfp* (C-terminal fusion) rescue *sdp* despite the differing localizations of their fluorophores. However, injection of ∆*N+tagRFP+reck*, which is identical to *tagrfp+reck* except for a deleted N-terminal signal sequence that directs packaging for extracellular secretion, fails to rescue *sdp*.

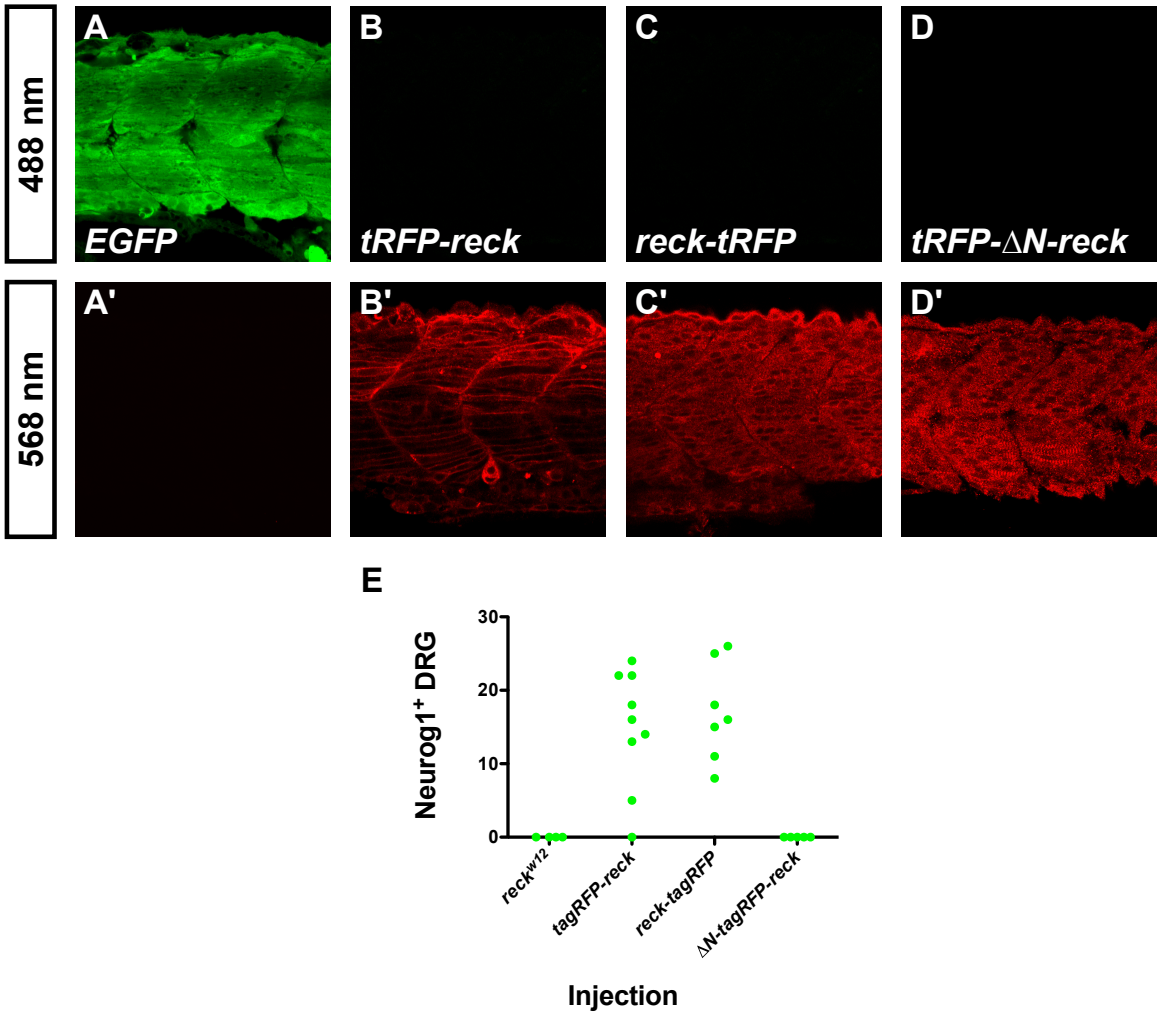
488 nm
568 nm
A
EGFP
B
tRFP-reck
C
reck-tRFP
D
tRFP-ΔN-reck
A'
B'
C'
D'
E
Neurog1+ DRG
30
20
10
0
reckw12
tagRFP-reck
reck-tagRFP
ΔN-tagRFP-reck
Injection

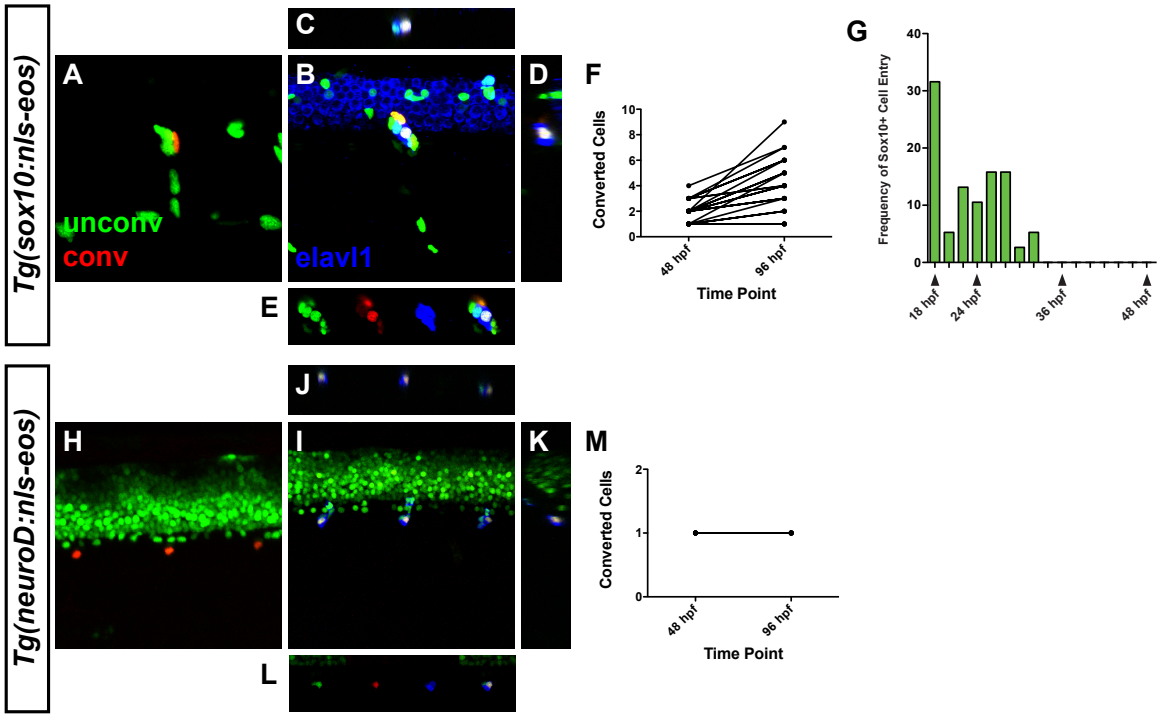

Figure 28. Sox10+ cells act as stem cells in the dorsal root ganglia, but nascent neurons cannot. (A) Small clone photoconversions (1-4 cells, n = 28 conversions) were carried out in *Tg(sox10:nls-eos)* embryos at 48 hpf. **(B)** Photoconversions were immunostained for Elavl1 at 96 hpf. Orthogonal projections **(C, D)** and single optical sections **(E)** were studied to verify colocalization. Note that Sox10+ cells at 48 hpf divide to give rise to both neurons and non-neuronal cells. **(F)** Quantification of the clonal expansion of each photoconversion. Most Sox10+ clones expand over the course of this interval. **(G)** Time lapse analysis of *Tg(sox10:nls-eos)* embryos from 18SS to 48 hpf showing the frequency of neural crest cell entry into the DRG chain. No cells enter later than 36 hpf; therefore any cell addition is due to local proliferation. **(H)** Single cell photoconversions (n = 7 conversions) were carried out in *Tg(neurod:nls-eos)* embryos at 48 hpf. **(I)** Photoconversions were immunostained for Elavl1 at 96 hpf. Orthoganal projections **(J, K)** and single optical sections **(L)** were again studied to verify colocalization. Here, three cells have been labeled, none of which divide. **(M)** Quantification of the clonal expansion of each photoconversion. NeuroD+ clones never expand.

Chapter IV: Summary and future directions

Chapter abstract

In the course of this work, I have identified the metalloproteinase inhibitor Reck as an apparent fate determinant of sensory neurons in the dorsal root ganglia. Furthermore, I have provided evidence to suggest interaction with one or more membrane-associated metalloproteinases may be critical to this determination. Here, I further experiments that may serve to further elucidate the mechanism of Reck-mediated fate choice.

Future experiments to address the Reck signaling mechanism

In reviewing the development of the dorsal root ganglia from neural crest and comparing that process to the development of the sympathetic ganglia, it becomes clear that although an initial proneural induction signal has been characterized for sympathetic ganglia—the emission of BMP from the dorsal aorta—a comparable signal has not been identified for dorsal root ganglia neurons. The discovery of the Neurogenin transcription factors represented a major breakthrough in understanding the specification of these neurons. At the time of their discovery, the field was presented with the problem of a morphologically and molecularly homogenous population—the trunk neural crest—that nonetheless exhibited clear biases for the adoption of different fates.

This is a problem that is often merely renewed every time an earlier step in a signaling hierarchy is revealed. We know now that Neurogenins are capable of inducing sensory fates, and that their expression identifies prospective sensory neurons just before they adopt obvious morphological characteristics. But the mechanism by which Neurogenin expression is initiated in a subset of neural crest is still entirely unclear.

It was this problem I sought to address in mapping, cloning, and further characterizing the *sensory deprived* mutant—the process of which I described in

the second chapter of this volume. *Sdp* is a singular mutation in that neural crest migration and differentiation are generally unfazed—with the exception of a minor cartilage defect, all neural crest derivatives save the DRG develop normally. The implication of these results is that Reck, the gene disrupted in *sdp*, is in some way an essential fate determinant for the sensory neurons of the dorsal root ganglia.

We consequently hypothesized that Reck, a membrane-tethered inhibitor of metalloproteases, might compel neural crest to differentiate as neurons by halting their dorsoventral migration and forcing their exposure to neurogenic factors emanating from the spinal cord (I review some of the evidence for these signals in the first chapter of this volume). Reck is known to be dowregulated in many primary cancers and transformed cell lines, and cells become hypermigratory following Reck inactivation. Conversely, forced expression of Reck has been observed to rescue hypermigratory behavior in these contexts. I observed moderately increased migration in Reck-deficient cells, consistent with these reports.

However, the simple model we have proposed (Figure 22) is clearly inadequate to explain the *sdp* phenotype. For example, why does overexpression of Reck never lead to massive neuronal differentiation when the tools used to do so are so reliable at rescuing the defect observed in *sdp*? It could be that a second set of factors overlaps with Reck expression—this overlap could occur either broadly, for an inhibitor of Reck action, or sparsely, for a Reck effector. Reck becomes restricted to a small subset of neural crest towards the end of its migration, and this may be evidence of some sort of inhibitory mechanism that is not overcome by Reck overexpression.

This two-factor model is somewhat cumbersome, however. An alternative explanation is that Reck participates in some signaling mechanism that inevitably terminates in the activation of a single cell or a very small group of cells—that is, a laterally inhibitory mechanism. The Delta/Notch pathway is one such pathway,

and there is ample evidence that it is implicated in several fate choice events in the course of DRG development. Furthermore, Reck has already been shown to influence Delta/Notch signaling in embryonic mouse cortex via inhibition of ADAM10, which acts as a Delta "sheddase." Therefore, in this context, Reck inhibits Notch signaling by preventing a requisite cleavage in the Delta ligand. Since we are unable to rescue *sdp* by treating embryos with the Notch inhibitor DAPT, I feel this mechanism is unlikely to be involved in the phenotype we observe.

Since we are unable to rescue *sdp* with nonspecific pharmacological inhibitors of metalloproteases, another contingency remains: Reck may exert some effects wholly independent of metalloproteases. This would represent a completely novel function for Reck, and one that I have no positive evidence in favor of. Until the metalloprotease-inhibiting activity of Reck can be tied directly to the *sdp* phenotype however, it must remain a possibility.

Given these ambiguities, I favor using some kind of screening approach to identify additional signaling partners for Reck, some of which I have already attempted. Inhibition of a molecule that acts with Reck in specifying DRG should rescue the phenotype observed in *sdp*—this could be carried out pharmacologically or using antisense morpholino oligonucleotides, and would confirm the signaling interaction. The first of these attempts to screen for interacting molecules, discussed in Chapter III, was a FACS/qPCR experiment in which sorted neural crest cells were probed for MMPs that were differentially expressed more highly in neural crest than in other cells in the embryo. Though this approach yielded interesting candidates and was internally consistent, it did not lead to a single molecule whose inhibition was capable of rescuing *sdp*. A second approach, currently incomplete, would be to immunoprecipitate a Reck fusion protein from neural crest cells, then use mass spectroscopy to sequence any binding partners. A third approach would be to perform a genetic screen in the *sdp* background for suppressing mutations.

Future experiments to address migratory behavior in neural crest

Neural crest clearly exhibits fate restriction long before the expression of any fate-specific markers, and this represents a persistent problem in studies of neural crest. Sox10 reliably marks all essentially all neural crest throughout its migration (data not shown), and we are in possession of genetic tools to follow its expression throughout this period. However, like all known neural crest markers, it does not exhibit any selectivity for derivative cell types until overt morphological differentiation, when it becomes restricted to glial progeny of the neural crest.

Study of neural crest in time-lapse presents a possible solution to this problem. Cells exhibit highly variable migratory behavior—even a coarse study of neural crest migration reveals a number of continuous and binary variables that might correlate in some fashion with fate identity: velocity, order of pathway entry, proliferative capacity, local cohesion, number of migratory inflections, etc. Surprisingly, few analyses of neural crest migration of any kind have been performed using 4-dimensional microscopy. It is therefore possible that migratory "markers" of cell fate may yet be discovered using detailed cell tracking and a more sophisticated statistical analysis.

Future experiments to address persistent stem cell function in DRG

The ability of certain glial subpopulations to self-renew and give rise to neurons is well-described. Radial glia (reviewed in (Kriegstein and Alvarez-Buylla, 2009)), astrocytes (reviewed in (Kriegstein and Alvarez-Buylla, 2009)), and Müller glia (reviewed in (Wohl et al., 2012)) have all been identified as progenitor populations capable of giving rise to neurons and glia via partially restricted intermediaries. It is perhaps little surprise then that glia in the DRG appear to retain similar potency.

These stem cells remain mysterious, however. Recent work has established that these stem cells are regulated by Delta/Notch signaling (McGraw et al., 2012), but no other regulatory mechanisms or obligate transcription factors have

been identified. Sox10 is necessary for maintaining the progenitor state in cultured neural crest stem cells (Kim et al., 2003) and may serve a similar function in DRG progenitors. Development of systems where Sox10 can be selectively activated or repressed *in vivo* would help to answer this question. Enhancer trap or gene trap screening to identify more restricted markers of glial cells/progenitors in the neural crest would also be of great utility in this endeavor.

References

Adam, V., Lelimousin, M., Boehme, S., Desfonds, G., Nienhaus, K., Field, M. J., Wiedenmann, J., McSweeney, S., Nienhaus, G. U. and Bourgeois, D. (2008). Structural characterization of IrisFP, an optical highlighter undergoing multiple photo-induced transformations. *Proc Natl Acad Sci USA* **105**, 18343–18348.

An, M., Luo, R. and Henion, P. D. (2002). Differentiation and maturation of zebrafish dorsal root and sympathetic ganglion neurons. *J Comp Neurol* **446**, 267–275.

Andermann, P., Ungos, J. and Raible, D. W. (2002). Neurogenin1 defines zebrafish cranial sensory ganglia precursors. *Dev Biol* **251**, 45–58.

Ando, R., Hama, H., Yamamoto-Hino, M., Mizuno, H. and Miyawaki, A. (2002). An optical marker based on the UV-induced green-to-red photoconversion of a fluorescent protein. *Proc Natl Acad Sci USA* **99**, 12651–12656.

Averill, S., McMahon, S. B., Clary, D. O., Reichardt, L. F. and Priestley, J. V. (1995). Immunocytochemical localization of trkA receptors in chemically identified subgroups of adult rat sensory neurons. *Eur. J. Neurosci.* **7**, 1484–1494.

Bahary, N., Davidson, A., Ransom, D., Shepard, J., Stern, H., Trede, N., Zhou, Y., Barut, B. and Zon, L. I. (2004). The Zon laboratory guide to positional cloning in zebrafish. *Methods Cell Biol* **77**, 305–329.

Bai, G. and Pfaff, S. L. (2011). Protease Regulation: The Yin and Yang of Neural Development and Disease. *Neuron* **72**, 9–21.

Baker, C. V., Bronner-Fraser, M., Le Douarin, N. M. and Teillet, M. A. (1997). Early- and late-migrating cranial neural crest cell populations have equivalent developmental potential in vivo. *Development* **124**, 3077–3087.

Banerjee, S., Gordon, L., Donn, T. M., Berti, C., Moens, C. B., Burden, S. J. and Granato, M. (2011). A novel role for MuSK and non-canonical Wnt signaling during segmental neural crest cell migration. *Development* **138**, 3287–3296.

Barde, Y. A. (1989). Trophic factors and neuronal survival. *Neuron* **2**, 1525–1534.

Baroffio, A., Dupin, E. and Le Douarin, N. M. (1988). Clone-forming ability and differentiation potential of migratory neural crest cells. *Proc Natl Acad Sci USA* **85**, 5325–5329.

Birren, S. J., Lo, L. and Anderson, D. J. (1993). Sympathetic neuroblasts undergo a developmental switch in trophic dependence. *Development* **119**, 597–610.

Blader, P., Fischer, N., Gradwohl, G., Guillemot, F. and Strähle, U. (1997). The activity of neurogenin1 is controlled by local cues in the zebrafish embryo. *Development* **124**, 4557–4569.

Britsch, S., Goerich, D. E., Riethmacher, D., Peirano, R. I., Rossner, M., Nave, K. A., Birchmeier, C. and Wegner, M. (2001). The transcription factor Sox10 is a key regulator of peripheral glial development. *Genes Dev* **15**, 66–78.

Britsch, S., Li, L., Kirchhoff, S., Theuring, F., Brinkmann, V., Birchmeier, C. and Riethmacher, D. (1998). The ErbB2 and ErbB3 receptors and their ligand, neuregulin-1, are essential for development of the sympathetic nervous system. *Genes Dev* **12**, 1825–1836.

Bronner-Fraser, M. (1986a). Analysis of the early stages of trunk neural crest migration in avian embryos using monoclonal antibody HNK-1. *Dev Biol* **115**, 44–55.

Bronner-Fraser, M. (1986b). An antibody to a receptor for fibronectin and laminin perturbs cranial neural crest development in vivo. *Dev Biol* **117**, 528–536.

Bronner-Fraser, M. and Fraser, S. E. (1988). Cell lineage analysis reveals multipotency of some avian neural crest cells. *Nature* **335**, 161–164.

Bronner-Fraser, M., Sieber-Blum, M. and Cohen, A. M. (1980). Clonal analysis of the avian neural crest: migration and maturation of mixed neural crest clones injected into host chicken embryos. *J Comp Neurol* **193**, 423–434.

Burstyn-Cohen, T., Stanleigh, J., Sela-Donenfeld, D. and Kalcheim, C. (2004). Canonical Wnt activity regulates trunk neural crest delamination linking BMP/noggin signaling with G1/S transition. *Development* **131**, 5327–5339.

Busfield, S. J., Michnick, D. A., Chickering, T. W., Revett, T. L., Ma, J., Woolf, E. A., Comrack, C. A., Dussault, B. J., Woolf, J. and Goodearl, A. D. (1997). Characterization of a neuregulin-related gene, Don-1, that is highly expressed in restricted regions of the cerebellum and hippocampus. *Molecular and Cellular Biology* **17**, 4007–4014.

Carney, T. J., Dutton, K. A., Greenhill, E., Delfino-Machín, M., Dufourcq, P., Blader, P. and Kelsh, R. N. (2006). A direct role for Sox10 in specification of neural crest-derived sensory neurons. *Development* **133**, 4619–4630.

Caron, S. J. C., Prober, D., Choy, M. and Schier, A. F. (2008). In vivo birthdating by BAPTISM reveals that trigeminal sensory neuron diversity depends on early neurogenesis. *Development* **135**, 3259–3269.

Carr, V. M. and Simpson, S. B. (1978). Proliferative and degenerative events in the early development of chick dorsal root ganglia. II. Responses to altered peripheral fields. *J Comp Neurol* **182**, 741–755.

Carroll, S. L., Silos-Santiago, I., Frese, S. E., Ruit, K. G., Milbrandt, J. and Snider, W. D. (1992). Dorsal root ganglion neurons expressing trk are selectively sensitive to NGF deprivation in utero. *Neuron* **9**, 779–788.

Castro, D. S., Martynoga, B., Parras, C., Ramesh, V., Pacary, E., Johnston, C., Drechsel, D., Lebel-Potter, M., Garcia, L. G., Hunt, C., et al. (2011). A novel function of the proneural factor Ascl1 in progenitor proliferation identified by genome-wide characterization of its targets. *Genes Dev* **25**, 930–945.

Chalazonitis, A., Rothman, T. P., Chen, J., Lamballe, F., Barbacid, M. and Gershon, M. D. (1994). Neurotrophin-3 induces neural crest-derived cells from fetal rat gut to develop in vitro as neurons or glia. *J Neurosci* **14**, 6571–6584.

Chalpe, A. J., Prasad, M., Henke, A. J. and Paulson, A. (2010). Regulation of cadherin expression in the chicken neural crest by the Wnt/ β-catenin signaling pathway. *celladhesion* **4**, 431–438.

Chang, C. and Hemmati-Brivanlou, A. (1998). Neural crest induction by Xwnt7B in Xenopus. *Dev Biol* **194**, 129–134.

Chang, H.-C., Cho, C.-Y. and Hung, W.-C. (2007). Downregulation of RECK by promoter methylation correlates with lymph node metastasis in non-small cell lung cancer. *Cancer Sci* **98**, 169–173.

Chang, H.-C., Cho, C.-Y. and Hung, W.-C. (2006). Silencing of the metastasis suppressor RECK by RAS oncogene is mediated by DNA methyltransferase 3b-induced promoter methylation. *Cancer Res* **66**, 8413–8420.

Chang, H.-C., Liu, L.-T. and Hung, W.-C. (2004). Involvement of histone deacetylation in ras-induced down-regulation of the metastasis suppressor RECK. *Cell Signal* **16**, 675–679.

Chen, A. I., de Nooij, J. C. and Jessell, T. M. (2006a). Graded Activity of Transcription Factor Runx3 Specifies the Laminar Termination Pattern of Sensory Axons in the Developing Spinal Cord. *Neuron* **49**, 395–408.

Chen, C.-L., Broom, D. C., Liu, Y., de Nooij, J. C., Li, Z., Cen, C., Samad, O. A., Jessell, T. M., Woolf, C. J. and Ma, Q. (2006b). Runx1 Determines Nociceptive Sensory Neuron Phenotype and Is Required for Thermal and Neuropathic Pain. *Neuron* **49**, 365–377.

Cheng, Y., Cheung, M., Abu-Elmagd, M. M., Orme, A. and Scotting, P. J. (2000). Chick sox10, a transcription factor expressed in both early neural crest cells and central nervous system. *Brain Res Dev Brain Res* **121**, 233–241.

Chudakov, D. M., Belousov, V. V., Zaraisky, A. G., Novoselov, V. V., Staroverov, D. B., Zorov, D. B., Lukyanov, S. and Lukyanov, K. A. (2003). Kindling fluorescent proteins for precise in vivo photolabeling. *Nat Biotechnol* **21**, 191–194.

Citri, A. and Yarden, Y. (2006). EGF–ERBB signalling: towards the systems level. *Nat Rev Mol Cell Biol* **7**, 505–516.

Clark, J. C. M., Akiyama, T., Thomas, D. M., Labrinidis, A., Evdokiou, A., Galloway, S. J., Kim, H.-S., Dass, C. R. and Choong, P. F. M. (2011). RECK in osteosarcoma. *Cancer* **117**, 3517–3528.

Clark, J. C. M., Thomas, D. M., Choong, P. F. M. and Dass, C. R. (2007). RECK--a newly discovered inhibitor of metastasis with prognostic significance in multiple forms of cancer. *Cancer Metastasis Rev* **26**, 675–683.

Coleman, H. A., Labrador, J. P., Chance, R. K. and Bashaw, G. J. (2010). The Adam family metalloprotease Kuzbanian regulates the cleavage of the roundabout receptor to control axon repulsion at the midline. *Development* **137**, 2417–2426.

Cornell, R. A. and Eisen, J. S. (2000). Delta signaling mediates segregation of neural crest and spinal sensory neurons from zebrafish lateral neural plate. *Development* **127**, 2873–2882.

Cornell, R. A. and Eisen, J. S. (2002). Delta/Notch signaling promotes formation of zebrafish neural crest by repressing Neurogenin 1 function. *Development* **129**, 2639–2648.

Covassin, L., Amigo, J. D., Suzuki, K., Teplyuk, V., Straubhaar, J. and Lawson, N. D. (2006). Global analysis of hematopoietic and vascular endothelial gene expression by tissue specific microarray profiling in zebrafish. *Dev Biol* **299**, 551–562.

Coyle, R. C., Latimer, A. and Jessen, J. R. (2008). Membrane-type 1 matrix metalloproteinase regulates cell migration during zebrafish gastrulation: evidence for an interaction with non-canonical Wnt signaling. *Exp Cell Res* **314**, 2150–2162.

Crowley, C., Spencer, S. D., Nishimura, M. C., Chen, K. S., Pitts-Meek, S., Armanini, M. P., Ling, L. H., McMahon, S. B., Shelton, D. L. and Levinson, A. D. (1994). Mice lacking nerve growth factor display perinatal loss of sensory and sympathetic neurons yet develop basal forebrain cholinergic neurons. *Cell* **76**, 1001–1011.

Cserjesi, P., Brown, D., Lyons, G. E. and Olson, E. N. (1995). Expression of the novel basic helix-loop-helix gene eHAND in neural crest derivatives and extraembryonic membranes during mouse development. *Dev Biol* **170**, 664–678.

Curran, K., Lister, J. A., Kunkel, G. R., Prendergast, A., Parichy, D. M. and Raible, D. W. (2010). Interplay between Foxd3 and Mitf regulates cell fate plasticity in the zebrafish neural crest. *Dev Biol* **344**, 107–118.

De Calisto, J., Araya, C., Marchant, L., Riaz, C. F. and Mayor, R. (2005). Essential role of non-canonical Wnt signalling in neural crest migration. *Development* **132**, 2587–2597.

Dencker, L., Annerwall, E., Busch, C. and Eriksson, U. (1990). Localization of specific retinoid-binding sites and expression of cellular retinoic-acid-binding protein (CRABP) in the early mouse embryo. *Development* **110**, 343–352.

DiCicco-Bloom, E., Friedman, W. J. and Black, I. B. (1993). NT-3 stimulates sympathetic neuroblast proliferation by promoting precursor survival. *Neuron* **11**, 1101–1111.

Dorsky, R. I., Moon, R. T. and Raible, D. W. (1998). Control of neural crest cell fate by the Wnt signalling pathway. *Nature* **396**, 370–373.

Downs, K. M. and Davies, T. (1993). Staging of gastrulating mouse embryos by morphological landmarks in the dissecting microscope. *Development* **118**, 1255–1266.

Dupin, E., Baroffio, A., Dulac, C., Cameron-Curry, P. and Le Douarin, N. M. (1990). Schwann-cell differentiation in clonal cultures of the neural crest, as evidenced by the anti-Schwann cell myelin protein monoclonal antibody. *Proc Natl Acad Sci USA* **87**, 1119–1123.

Dutton, K. A., Pauliny, A., Lopes, S. S., Elworthy, S., Carney, T. J., Rauch, J., Geisler, R., Haffter, P. and Kelsh, R. N. (2001). Zebrafish colourless encodes sox10 and specifies non-ectomesenchymal neural crest fates. *Development* **128**, 4113–4125.

Dykes, I. M., Tempest, L., Lee, S. I. and Turner, E. E. (2011). Brn3a and Islet1 Act Epistatically to Regulate the Gene Expression Program of Sensory Differentiation. *J Neurosci* **31**, 9789–9799.

Edwards, D. R., Handsley, M. M. and Pennington, C. J. (2008). The ADAM metalloproteinases. *Molecular Aspects of Medicine* **29**, 258–289.

Eisen, J. S. and Weston, J. A. (1993). Development of the neural crest in the zebrafish. *Dev Biol* **159**, 50–59.

ElShamy, W. M. and Ernfors, P. (1996). A local action of neurotrophin-3 prevents the death of proliferating sensory neuron precursor cells. *Neuron* **16**, 963–972.

ElShamy, W. M., Linnarsson, S., Lee, K. F., Jaenisch, R. and Ernfors, P. (1996). Prenatal and postnatal requirements of NT-3 for sympathetic neuroblast survival and innervation of specific targets. *Development* **122**, 491–500.

Embryonic expression and cloning of the murine GATA-3 gene (1994). Embryonic expression and cloning of the murine GATA-3 gene. **120**, 2673–2686.

Eng, S. R., Dykes, I. M., Lanier, J., Fedtsova, N. and Turner, E. E. (2007). POU-domain factor Brn3a regulates both distinct and common programs of gene expression in the spinal and trigeminal sensory ganglia. *Neural development* **2**, 3.

Eng, S. R., Gratwick, K., Rhee, J. M., Fedtsova, N., Gan, L. and Turner, E. E. (2001). Defects in sensory axon growth precede neuronal death in Brn3a-deficient mice. *J Neurosci* **21**, 541–549.

English, W. R., Puente, X. S., Freije, J. M., Knauper, V., Amour, A., Merryweather, A., Lopez-Otin, C. and Murphy, G. (2000). Membrane type 4 matrix metalloproteinase (MMP17) has tumor necrosis factor-alpha convertase activity but does not activate pro-MMP2. *J Biol Chem* **275**, 14046–14055.

Ernfors, P., Lee, K. F. and Jaenisch, R. (1994a). Mice lacking brain-derived neurotrophic factor develop with sensory deficits. *Nature* **368**, 147–150.

Ernfors, P., Lee, K. F., Kucera, J. and Jaenisch, R. (1994b). Lack of neurotrophin-3 leads to deficiencies in the peripheral nervous system and loss of limb proprioceptive afferents. *Cell* **77**, 503–512.

Ernsberger, U., Patzke, H., Tissier-Seta, J. P., Reh, T., Goridis, C. and Rohrer, H. (1995). The expression of tyrosine hydroxylase and the transcription factors cPhox-2 and Cash-1: evidence for distinct inductive steps in the differentiation of chick sympathetic precursor cells. *Mech Dev* **52**, 125–136.

Ernsberger, U., Reissmann, E., Mason, I. and Rohrer, H. (2000). The expression of dopamine beta-hydroxylase, tyrosine hydroxylase, and Phox2 transcription factors in sympathetic neurons: evidence for common regulation during noradrenergic induction and diverging regulation later in development. *Mech Dev* **92**, 169–177.

Ethell, I. M. and Ethell, D. W. (2007). Matrix metalloproteinases in brain development and remodeling: Synaptic functions and targets. *J Neurosci Res* **85**, 2813–2823.

Fambrough, D., Pan, D., Rubin, G. M. and Goodman, C. S. (1996). The cell surface metalloprotease/disintegrin Kuzbanian is required for axonal extension in Drosophila. *Proc Natl Acad Sci USA* **93**, 13233–13238.

Fariñas, I., Jones, K. R., Backus, C., Wang, X. Y. and Reichardt, L. F. (1994). Severe sensory and sympathetic deficits in mice lacking neurotrophin-3. *Nature* **369**, 658–661.

Fariñas, I., Wilkinson, G. A., Backus, C., Reichardt, L. F. and Patapoutian, A. (1998). Characterization of neurotrophin and Trk receptor functions in developing sensory ganglia: direct NT-3 activation of TrkB neurons in vivo. *Neuron* **21**, 325–334.

Fariñas, I., Yoshida, C. K., Backus, C. and Reichardt, L. F. (1996). Lack of neurotrophin-3 results in death of spinal sensory neurons and premature differentiation of their precursors. *Neuron* **17**, 1065–1078.

Fedtsova, N. G. and Turner, E. E. (1995). Brn-3.0 expression identifies early post-mitotic CNS neurons and sensory neural precursors. *Mech Dev* **53**, 291–304.

Fisher, S., Grice, E. A., Vinton, R. M., Bessling, S. L., Urasaki, A., Kawakami, K. and McCallion, A. S. (2006). Evaluating the biological relevance of putative enhancers using Tol2 transposon-mediated transgenesis in zebrafish. *UNKNOWN* **1**, 1297–1305.

Frank, E. and Sanes, J. R. (1991). Lineage of neurons and glia in chick dorsal root ganglia: analysis in vivo with a recombinant retrovirus. *Development* **111**, 895–908.

Gabriely, G., Wurdinger, T., Kesari, S., Esau, C. C., Burchard, J., Linsley, P. S. and Krichevsky, A. M. (2008). MicroRNA 21 promotes glioma invasion by targeting matrix metalloproteinase regulators. *Molecular and Cellular Biology* **28**, 5369–5380.

Galko, M. J. and Tessier-Lavigne, M. (2000). Function of an axonal chemoattractant modulated by metalloprotease activity. *Science* **289**, 1365–1367.

Gans, C. and Northcutt, R. G. (1983). Neural crest and the origin of vertebrates: a new head. *Science* **220**, 268–273.

García-Castro, M. I., Marcelle, C. and Bronner-Fraser, M. (2002). Ectodermal Wnt function as a neural crest inducer. *Science* **297**, 848–851.

Gassmann, M., Casagranda, F., Orioli, D., Simon, H., Lai, C., Klein, R. and Lemke, G. (1995). Aberrant neural and cardiac development in mice lacking the ErbB4 neuregulin receptor. *Nature* **378**, 390–394.

Geling, A., Steiner, H., Willem, M., Bally-Cuif, L. and Haass, C. (2002). A gamma-secretase inhibitor blocks Notch signaling in vivo and causes a severe neurogenic phenotype in zebrafish. *EMBO Rep* **3**, 688–694.

George, L., Chaverra, M., Todd, V., Lansford, R. and Lefcort, F. (2007). Nociceptive sensory neurons derive from contralaterally migrating, fate-restricted neural crest cells. *Nat Neurosci* **10**, 1287–1293.

George, L., Kasemeier-Kulesa, J., Nelson, B. R., Koyano-Nakagawa, N. and Lefcort, F. (2010). Patterned assembly and neurogenesis in the chick dorsal root ganglion. *J Comp Neurol* **518**, 405–422.

Glebov, O. O. and Nichols, B. J. (2004). Distribution of lipid raft markers in live cells. *Biochem. Soc. Trans.* **32**, 673–675.

Goedert, M., Otten, U., Hunt, S. P., Bond, A., Chapman, D., Schlumpf, M. and Lichtensteiger, W. (1984). Biochemical and anatomical effects of antibodies against nerve growth factor on developing rat sensory ganglia. *Proc Natl Acad Sci USA* **81**, 1580–1584.

Goldberg, M. W. and Allen, T. D. (1993). The nuclear pore complex: three-dimensional surface structure revealed by field emission, in-lens scanning electron microscopy, with underlying structure uncovered by proteolysis. *J Cell Sci* **106 (Pt 1)**, 261–274.

Goldstein, B. (2001). Anatomy of the peripheral nervous system. *Phys Med Rehabil Clin N Am* **12**, 207–236.

Gomes, W. A. and Kessler, J. A. (2001). Msx-2 and p21 Mediate the Pro-Apoptotic but Not the Anti-Proliferative Effects of BMP4 on Cultured Sympathetic Neuroblasts. *Dev Biol* **237**, 212–221.

Gray, M., Moens, C. B., Amacher, S. L., Eisen, J. S. and Beattie, C. E. (2001). Zebrafish deadly seven functions in neurogenesis. *Dev Biol* **237**, 306–323.

Greenwood, A. L., Turner, E. E. and Anderson, D. J. (1999). Identification of dividing, determined sensory neuron precursors in the mammalian neural crest. *Development* **126**, 3545–3559.

Groves, A. K., George, K. M., Tissier-Seta, J. P., Engel, J. D., Brunet, J. F. and Anderson, D. J. (1995). Differential regulation of transcription factor gene expression and phenotypic markers in developing sympathetic neurons. *Development* **121**, 887–901.

Guillemot, F., Lo, L. C., Johnson, J. E., Auerbach, A., Anderson, D. J. and Joyner, A. L. (1993). Mammalian achaete-scute homolog 1 is required for the early development of olfactory and autonomic neurons. *Cell* **75**, 463–476.

Gurskaya, N. G., Verkhusha, V. V., Shcheglov, A. S., Staroverov, D. B., Chepurnykh, T. V., Fradkov, A. F., Lukyanov, S. and Lukyanov, K. A. (2006). Engineering of a monomeric green-to-red photoactivatable fluorescent protein induced by blue light. *Nat Biotechnol* **24**, 461–465.

Habuchi, S., Ando, R., Dedecker, P., Verheijen, W., Mizuno, H., Miyawaki, A. and Hofkens, J. (2005). Reversible single-molecule photoswitching in the GFP-like fluorescent protein Dronpa. *Proc Natl Acad Sci USA* **102**, 9511–9516.

Haldin, C. E. and Labonne, C. (2010). SoxE factors as multifunctional neural crest regulatory factors. *The International Journal of Biochemistry & Cell Biology* **42**, 441–444.

Hamburger, V. and Hamilton, H. L. (1992). A series of normal stages in the development of the chick embryo. 1951. *Dev Dyn* **195**, 231–272.

Hamburger, V., Brunso-Bechtold, J. K. and Yip, J. W. (1981). Neuronal death in the spinal ganglia of the chick embryo and its reduction by nerve growth factor. *J Neurosci* **1**, 60–71.

Harari, D., Tzahar, E., Romano, J., Shelly, M., Pierce, J. H., Andrews, G. C. and Yarden, Y. (1999). Neuregulin-4: a novel growth factor that acts through the ErbB-4 receptor tyrosine kinase. *Oncogene* **18**, 2681–2689.

Hari, L., Brault, V., Kléber, M., Lee, H.-Y., Ille, F., Leimeroth, R., Paratore, C., Suter, U., Kemler, R. and Sommer, L. (2002). Lineage-specific requirements of beta-catenin in neural crest development. *J Cell Biol* **159**, 867–880.

Hari, L., Miescher, I., Shakhova, O., Suter, U., Chin, L., Taketo, M., Richardson, W. D., Kessaris, N. and Sommer, L. (2012). Temporal control of neural crest lineage generation by Wnt/ -catenin signaling. *Development* **139**, 2107–2117.

Hattori, M., Osterfield, M. and Flanagan, J. G. (2000). Regulated cleavage of a contact-mediated axon repellent. *Science* **289**, 1360–1365.

Hempstead, B. L., Martin-Zanca, D., Kaplan, D. R., Parada, L. F. and Chao, M. V. (1991). High-affinity NGF binding requires coexpression of the trk proto-oncogene and the low-affinity NGF receptor. *Nature* **350**, 678–683.

Hendershot, T. J., Liu, H., Clouthier, D. E., Shepherd, I. T., Coppola, E., Studer, M., Firulli, A. B., Pittman, D. L. and Howard, M. J. (2008). Conditional deletion of Hand2 reveals critical functions in neurogenesis and cell type-specific gene expression for development of neural crest-derived noradrenergic sympathetic ganglion neurons. *Dev Biol* **319**, 179–191.

Henion, P. D. and Weston, J. A. (1994). Retinoic acid selectively promotes the survival and proliferation of neurogenic precursors in cultured neural crest cell populations. *Dev Biol* **161**, 243–250.

Henion, P. D. and Weston, J. A. (1997). Timing and pattern of cell fate restrictions in the neural crest lineage. *Development* **124**, 4351–4359.

Henion, P. D., Garner, A. S., Large, T. H. and Weston, J. A. (1995). trkC-mediated NT-3 signaling is required for the early development of a subpopulation of neurogenic neural crest cells. *Dev Biol* **172**, 602–613.

Henion, P. D., Raible, D. W., Beattie, C. E., Stoesser, K. L., Weston, J. A. and Eisen, J. S. (1996). Screen for mutations affecting development of Zebrafish neural crest. *Dev Genet* **18**, 11–17.

Herbarth, B., Pingault, V., Bondurand, N., Kuhlbrodt, K., Hermans-Borgmeyer, I., Puliti, A., Lemort, N., Goossens, M. and Wegner, M. (1998). Mutation of the Sry-related Sox10 gene in Dominant megacolon, a mouse model for human Hirschsprung disease. *Proc Natl Acad Sci USA* **95**, 5161–5165.

Higashiyama, S., Horikawa, M., Yamada, K., Ichino, N., Nakano, N., Nakagawa, T., Miyagawa, J., Matsushita, N., Nagatsu, T. and Taniguchi, N. (1997). A novel brain-derived member of the epidermal growth factor family that interacts with ErbB3 and ErbB4. *Journal of biochemistry* **122**, 675–680.

Hirsch, M. R., Tiveron, M. C., Guillemot, F., Brunet, J. F. and Goridis, C. (1998). Control of noradrenergic differentiation and Phox2a expression by MASH1 in the central and peripheral nervous system. *Development* **125**, 599–608.

Honjo, Y., Kniss, J. and Eisen, J. S. (2008). Neuregulin-mediated ErbB3 signaling is required for formation of zebrafish dorsal root ganglion neurons. *Development* **135**, 2615–2625.

Honoré, S. M., Aybar, M. J. and Mayor, R. (2003). Sox10 is required for the early development of the prospective neural crest in Xenopus embryos. *Dev Biol* **260**, 79–96.

Hosang, M. and Shooter, E. M. (1985). Molecular characteristics of nerve growth factor receptors on PC12 cells. *J Biol Chem* **260**, 655–662.

Howard, M. J., Stanke, M., Schneider, C., Wu, X. and Rohrer, H. (2000). The transcription factor dHAND is a downstream effector of BMPs in sympathetic neuron specification. *Development* **127**, 4073–4081.

Howard, M., Foster, D. N. and Cserjesi, P. (1999). Expression of HAND gene products may be sufficient for the differentiation of avian neural crest-derived cells into catecholaminergic neurons in culture. *Dev Biol* **215**, 62–77.

Hsu, M.-C., Chang, H.-C. and Hung, W.-C. (2006). HER-2/neu represses the metastasis suppressor RECK via ERK and Sp transcription factors to promote cell invasion. *J Biol Chem* **281**, 4718–4725.

Hwang, J. J., Park, M.-H., Choi, S.-Y. and Koh, J.-Y. (2005). Activation of the Trk signaling pathway by extracellular zinc. Role of metalloproteinases. *J Biol Chem* **280**, 11995–12001.

Imai, K., Hiramatsu, A., Fukushima, D., Pierschbacher, M. D. and Okada, Y. (1997). Degradation of decorin by matrix metalloproteinases: identification of the cleavage sites, kinetic analyses and transforming growth factor-beta1 release. *Biochem. J.* **322 (Pt 3)**, 809–814.

Inoue, K.-I., Ito, K., Osato, M., Lee, B., Bae, S.-C. and Ito, Y. (2007). The transcription factor Runx3 represses the neurotrophin receptor TrkB during lineage commitment of dorsal root ganglion neurons. *J Biol Chem* **282**, 24175–24184.

Ito, K. and Morita, T. (1995). Role of retinoic acid in mouse neural crest cell development in vitro. *Dev Dyn* **204**, 211–218.

Ito, K. and Sieber-Blum, M. (1993). Pluripotent and developmentally restricted neural-crest-derived cells in posterior visceral arches. *Dev Biol* **156**, 191–200.

Janes, P. W., Saha, N., Barton, W. A., Kolev, M. V., Wimmer-Kleikamp, S. H., Nievergall, E., Blobel, C. P., Himanen, J.-P., Lackmann, M. and Nikolov, D. B. (2005). Adam Meets Eph: An ADAM Substrate Recognition Module Acts as a Molecular Switch for Ephrin Cleavage In trans. *Cell* **123**, 291–304.

Jin, E.-J., Erickson, C. A., Takada, S. and Burrus, L. W. (2001). Wnt and BMP Signaling Govern Lineage Segregation of Melanocytes in the Avian Embryo. *Dev Biol* **233**, 22–37.

Johnson, E. M., Gorin, P. D., Brandeis, L. D. and Pearson, J. (1980). Dorsal root ganglion neurons are destroyed by exposure in utero to maternal antibody to nerve growth factor. *Science* **210**, 916–918.

Johnson, J. E., Birren, S. J. and Anderson, D. J. (1990). Two rat homologues of Drosophila achaete-scute specifically expressed in neuronal precursors. *Nature* **346**, 858–861.

Jones, K. R., Fariñas, I., Backus, C. and Reichardt, L. F. (1994). Targeted disruption of the BDNF gene perturbs brain and sensory neuron development but not motor neuron development. *Cell* **76**, 989–999.

Kahane, N. and Kalcheim, C. (1994). Expression of trkC receptor mRNA during development of the avian nervous system. *J Neurobiol* **25**, 571–584.

Kalcheim, C., Carmeli, C. and Rosenthal, A. (2004). Neurotrophin 3 is a mitogen for cultured neural crest cells. *Proc Natl Acad Sci USA* **89**, 1661–1665.

Kamei, M., Isogai, S., Pan, W. and Weinstein, B. M. (2010). Imaging blood vessels in the zebrafish. *Methods Cell Biol* **100**, 27–54.

Kang, H.-G., Kim, H.-S., Kim, K.-J., Oh, J. H., Lee, M.-R., Seol, S. M. and Han, I. (2007). RECK expression in osteosarcoma: correlation with matrix metalloproteinases activation and tumor invasiveness. *J Orthop Res* **25**, 696–702.

Kaplan, D. R., Hempstead, B. L., Martin-Zanca, D., Chao, M. V. and Parada, L. F. (1991a). The trk proto-oncogene product: a signal transducing receptor for nerve growth factor. *Science* **252**, 554–558.

Kaplan, D. R., Martin-Zanca, D. and Parada, L. F. (1991b). Tyrosine phosphorylation and tyrosine kinase activity of the trk proto-oncogene product induced by NGF. *Nature* **350**, 158–160.

Kashiba, H., Noguchi, K., Ueda, Y. and Senba, E. (2003). Coexpression of trk family members and low-affinity neurotrophin receptors in rat dorsal root ganglion neurons. *Brain Res. Mol. Brain Res.* **30**, 158–164.

Kashiba, H., Ueda, Y. and Senba, E. (1996). Coexpression of preprotachykinin-A, alpha-calcitonin gene-related peptide, somatostatin, and neurotrophin receptor family messenger RNAs in rat dorsal root ganglion neurons. *Neuroscience* **70**, 179–189.

Kelsh, R. N. and Eisen, J. S. (2000). The zebrafish colourless gene regulates development of non-ectomesenchymal neural crest derivatives. *Development* **127**, 515–525.

Kelsh, R. N., Dutton, K., Medlin, J. and Eisen, J. S. (2000). Expression of zebrafish fkd6 in neural crest-derived glia. *Mech Dev* **93**, 161–164.

Kim, H. S., Seo, H., Yang, C., Brunet, J. F. and Kim, K. S. (1998). Noradrenergic-specific transcription of the dopamine beta-hydroxylase gene requires synergy of multiple cis-acting elements including at least two Phox2a-binding sites. *J Neurosci* **18**, 8247–8260.

Kim, J., Lo, L., Dormand, E. and Anderson, D. J. (2003). SOX10 maintains multipotency and inhibits neuronal differentiation of neural crest stem cells. *Neuron* **38**, 17–31.

Kimmel, C. B., Ballard, W. W., Kimmel, S. R., Ullmann, B. and Schilling, T. F. (1995). Stages of embryonic development of the zebrafish. *Dev Dyn* **203**, 253–310.

Kitajima, S., Miki, T., Takegami, Y., Kido, Y., Noda, M., Hara, E., Shamma, A. and Takahashi, C. (2010). Reversion-inducing cysteine-rich protein with Kazal motifs interferes with epidermal growth factor receptor signaling. *Oncogene*.

Klein, R., Parada, L. F., Coulier, F. and Barbacid, M. (1989). trkB, a novel tyrosine protein kinase receptor expressed during mouse neural development. *EMBO J* **8**, 3701–3709.

Klein, R., Silos-Santiago, I., Smeyne, R. J., Lira, S. A., Brambilla, R., Bryant, S., Zhang, L., Snider, W. D. and Barbacid, M. (1994). Disruption of the neurotrophin-3 receptor gene trkC eliminates la muscle afferents and results in abnormal movements. *Nature* **368**, 249–251.

Klein, R., Smeyne, R. J., Wurst, W., Long, L. K., Auerbach, B. A., Joyner, A. L. and Barbacid, M. (1993). Targeted disruption of the trkB neurotrophin receptor gene results in nervous system lesions and neonatal death. *Cell* **75**, 113–122.

Klymkowsky, M., Cortez Rossi, C. and Artinger, K. B. (2010). Mechanisms driving neural crest induction and migration in the zebrafish and Xenopus laevis. *celladhesion* **4**, 595–608.

Knecht, A. K. and Bronner-Fraser, M. (2002). Induction of the neural crest: a multigene process. *Nat Rev Genet* **3**, 453–461.

Kobayashi, A., Senzaki, K., Ozaki, S., Yoshikawa, M. and Shiga, T. (2012). Runx1 promotes neuronal differentiation in dorsal root ganglion. *Mol Cell Neurosci* **49**, 23–31.

Kobayashi, K., Fukuoka, T., Obata, K., Yamanaka, H., Dai, Y., Tokunaga, A. and Noguchi, K. (2005). Distinct expression of TRPM8, TRPA1, and TRPV1 mRNAs in rat primary afferent neurons with aδ/c-fibers and colocalization with trk receptors. *J Comp Neurol* **493**, 596–606.

Kobayashi, M., Fujii, M., Kurihara, K. and Matsuoka, I. (1998). Bone morphogenetic protein-2 and retinoic acid induce neurotrophin-3 responsiveness in developing rat sympathetic neurons. *Brain Res. Mol. Brain Res.* **53**, 206–217.

Korzh, V., Sleptsova, I., Liao, J., He, J. and Gong, Z. (1998). Expression of zebrafish bHLH genes ngn1 and nrd defines distinct stages of neural differentiation. *Dev Dyn* **213**, 92–104.

Kramer, I., Sigrist, M., de Nooij, J. C., Taniuchi, I., Jessell, T. M. and Arber, S. (2006). A Role for Runx Transcription Factor Signaling in Dorsal Root Ganglion Sensory Neuron Diversification. *Neuron* **49**, 379–393.

Kramer, R., Bucay, N., Kane, D. J., Martin, L. E., Tarpley, J. E. and Theill, L. E. (1996). Neuregulins with an Ig-like domain are essential for mouse myocardial and neuronal development. *Proc Natl Acad Sci USA* **93**, 4833–4838.

Kriegstein, A. and Alvarez-Buylla, A. (2009). The Glial Nature of Embryonic and Adult Neural Stem Cells. *Annu Rev Neurosci* **32**, 149–184.

Krispin, S., Nitzan, E., Kassem, Y. and Kalcheim, C. (2010). Evidence for a dynamic spatiotemporal fate map and early fate restrictions of premigratory avian neural crest. *Development* **137**, 585–595.

Kucera, J., Fan, G., Jaenisch, R., Linnarsson, S. and Ernfors, P. (1995). Dependence of developing group Ia afferents on neurotrophin-3. *J Comp Neurol* **363**, 307–320.

Kuhlbrodt, K., Herbarth, B., Sock, E., Hermans-Borgmeyer, I. and Wegner, M. (1998a). Sox10, a novel transcriptional modulator in glial cells. *J Neurosci* **18**, 237–250.

Kuhlbrodt, K., Schmidt, C., Sock, E., Pingault, V., Bondurand, N., Goossens, M. and Wegner, M. (1998b). Functional analysis of Sox10 mutations found in human Waardenburg-Hirschsprung patients. *J Biol Chem* **273**, 23033–23038.

Kwan, K. M., Fujimoto, E., Grabher, C., Mangum, B. D., Hardy, M. E., Campbell, D. S., Parant, J. M., Yost, H. J., Kanki, J. P. and Chien, C.-B. (2007). The Tol2kit: a multisite gateway-based construction kit for Tol2 transposon transgenesis constructs. *Dev Dyn* **236**, 3088–3099.

LaBonne, C. and Bronner-Fraser, M. (1998). Neural crest induction in Xenopus: evidence for a two-signal model. *Development* **125**, 2403–2414.

Lamballe, F., Klein, R. and Barbacid, M. (1991). trkC, a new member of the trk family of tyrosine protein kinases, is a receptor for neurotrophin-3. *Cell* **66**, 967–979.

Lamers, C. H., Rombout, J. W. and Timmermans, L. P. (1981). An experimental study on neural crest migration in Barbus conchonius (Cyprinidae, Teleostei), with special reference to the origin of the enteroendocrine cells. *J Embryol Exp Morphol* **62**, 309–323.

Lawson, N. D. and Weinstein, B. M. (2002). In Vivo Imaging of Embryonic Vascular Development Using Transgenic Zebrafish. *Dev Biol* **248**, 307–318.

Lawson, S. N. and Biscoe, T. J. (1979). Development of mouse dorsal root ganglia: an autoradiographic and quantitative study. *J Neurocytol* **8**, 265–274.

Le Douarin, N. M. *The neural crest*. Cambridge.

Le Lievre, C. S., Schweizer, G. G., Ziller, C. M. and Le Douarin, N. M. (1980). Restrictions of developmental capabilities in neural crest cell derivatives as tested by in vivo transplantation experiments. *Dev Biol* **77**, 362–378.

Lee, H.-Y., Kléber, M., Hari, L., Brault, V., Suter, U., Taketo, M. M., Kemler, R. and Sommer, L. (2004). Instructive role of Wnt/beta-catenin in sensory fate specification in neural crest stem cells. *Science* **303**, 1020–1023.

Lee, K. E., Nam, S., Cho, E.-A., Seong, I., Limb, J.-K., Lee, S. and Kim, J. (2008). Identification of direct regulatory targets of the transcription factor Sox10 based on function and conservation. *BMC Genomics* **9**, 408.

Lee, K. F., Simon, H., Chen, H., Bates, B., Hung, M. C. and Hauser, C. (1995). Requirement for neuregulin receptor erbB2 in neural and cardiac development.

Lee, R., Kermani, P., Teng, K. K. and Hempstead, B. L. (2001). Regulation of cell survival by secreted proneurotrophins. *Science* **294**, 1945–1948.

Lefcort, F., Clary, D. O., Rusoff, A. C. and Reichardt, L. F. (1996). Inhibition of the NT-3 receptor TrkC, early in chick embryogenesis, results in severe reductions in multiple neuronal subpopulations in the dorsal root ganglia. *J Neurosci* **16**, 3704–3713.

Leigh, N., Schupp, M.-O., Li, K., Padmanabhan, V., Gastonguay, A., Wang, L., Chung, C. Z. and Ramchandran, R. Mmp17 and its putative substrate Reck is essential for neural crest migration *in vivo*.

Levanon, D., Bettoun, D., Harris-Cerruti, C., Woolf, E., Negreanu, V., Eilam, R., Bernstein, Y., Goldenberg, D., Xiao, C., Fliegauf, M., et al. (2002). The Runx3 transcription factor regulates development and survival of TrkC dorsal root ganglia neurons. *EMBO J* **21**, 3454–3463.

Levi-Montalcini, R. (1987). The nerve growth factor 35 years later. *Science* **237**, 1154–1162.

Lewis, J. L. (2004). Reiterated Wnt signaling during zebrafish neural crest development. *Development* **131**, 1299–1308.

Li, S.-L., Gao, D.-L., Zhao, Z.-H., Liu, Z.-W., Zhao, Q.-M., Yu, J.-X., Chen, K.-S. and Zhang, Y.-H. (2007). Correlation of matrix metalloproteinase suppressor genes RECK, VEGF, and CD105 with angiogenesis and biological behavior in esophageal squamous cell carcinoma. *World J Gastroenterol* **13**, 6076–6081.

Lieber, T., Kidd, S. and Young, M. W. (2002). kuzbanian-mediated cleavage of Drosophila Notch. *Genes Dev* **16**, 209–221.

Liebl, D. J., Tessarollo, L., Palko, M. E. and Parada, L. F. (1997). Absence of sensory neurons before target innervation in brain-derived neurotrophic factor-, neurotrophin 3-, and TrkC-deficient embryonic mice. *J Neurosci* **17**, 9113–9121.

Lim, A. H., Suli, A., Yaniv, K., Weinstein, B., Li, D. Y. and Chien, C. B. (2011). Motoneurons are essential for vascular pathfinding. *Development* **138**, 4813–4813.

Lim, K. C., Lakshmanan, G., Crawford, S. E., Gu, Y., Grosveld, F. and Engel, J. D. (2000). Gata3 loss leads to embryonic lethality due to noradrenaline deficiency of the sympathetic nervous system. *Nat Genet* **25**, 209–212.

Lister, J. A., Robertson, C. P., Lepage, T., Johnson, S. L. and Raible, D. W. (1999). nacre encodes a zebrafish microphthalmia-related protein that regulates neural-crest-derived pigment cell fate. *Development* **126**, 3757–3767.

Liu, C., Yu, J., Yu, S., Lavker, R. M., Cai, L., Liu, W., Yang, K., He, X. and Chen, S. (2010). MicroRNA-21 acts as an oncomir through multiple targets in human hepatocellular carcinoma. *Journal of Hepatology* **53**, 98–107.

Liu, H., Margiotta, J. F. and Howard, M. J. (2005). BMP4 supports noradrenergic differentiation by a PKA-dependent mechanism. *Dev Biol* **286**, 521–536.

Liu, L.-T., Peng, J.-P., Chang, H.-C. and Hung, W.-C. (2003). RECK is a target of Epstein-Barr virus latent membrane protein 1. *Oncogene* **22**, 8263–8270.

Lo, L. C., Johnson, J. E., Wuenschell, C. W., Saito, T. and Anderson, D. J. (1991). Mammalian achaete-scute homolog 1 is transiently expressed by spatially restricted subsets of early neuroepithelial and neural crest cells. *Genes Dev* **5**, 1524–1537.

Lo, L., Morin, X., Brunet, J. F. and Anderson, D. J. (1999). Specification of neurotransmitter identity by Phox2 proteins in neural crest stem cells. *Neuron* **22**, 693–705.

Lo, L., Sommer, L. and Anderson, D. J. (1997). MASH1 maintains competence for BMP2-induced neuronal differentiation in post-migratory neural crest cells. *Curr Biol* **7**, 440–450.

Lo, L., Tiveron, M. C. and Anderson, D. J. (1998). MASH1 activates expression of the paired homeodomain transcription factor Phox2a, and couples pan-neuronal and subtype-specific components of autonomic neuronal identity. *Development* **125**, 609–620.

Lucas, M. E., Müller, F., Rüdiger, R., Henion, P. D. and Rohrer, H. (2006). The bHLH transcription factor hand2 is essential for noradrenergic differentiation of sympathetic neurons. *Development* **133**, 4015–4024.

Lukyanov, K. A., Chudakov, D. M., Lukyanov, S. and Verkhusha, V. V. (2005). Innovation: Photoactivatable fluorescent proteins. *Nat Rev Mol Cell Biol* **6**, 885–891.

Lyons, D. A., Pogoda, H.-M., Voas, M. G., Woods, I. G., Diamond, B., Nix, R., Arana, N., Jacobs, J. and Talbot, W. S. (2005). erbb3 and erbb2 are essential for schwann cell migration and myelination in zebrafish. *Curr Biol* **15**, 513–524.

Lyons, K. M., Hogan, B. L. and Robertson, E. J. (1995). Colocalization of BMP 7 and BMP 2 RNAs suggests that these factors cooperatively mediate tissue interactions during murine development. *Mech Dev* **50**, 71–83.

Ma, Q., Fode, C., Guillemot, F. and Anderson, D. J. (1999). Neurogenin1 and neurogenin2 control two distinct waves of neurogenesis in developing dorsal root ganglia. *Genes Dev* **13**, 1717–1728.

Ma, Q., Kintner, C. and Anderson, D. J. (1996). Identification of neurogenin, a vertebrate neuronal determination gene. *Cell* **87**, 43–52.

Maden, M., Hunt, P., Eriksson, U., Kuroiwa, A., Krumlauf, R. and Summerbell, D. (1991). Retinoic acid-binding protein, rhombomeres and the neural crest. *Development* **111**, 35–43.

Maden, M., Ong, D. E. and Chytil, F. (1990). Retinoid-binding protein distribution in the developing mammalian nervous system. *Development* **109**, 75–80.

Maden, M., Ong, D. E., Summerbell, D., Chytil, F. and Hirst, E. A. (1989). Cellular retinoic acid-binding protein and the role of retinoic acid in the development of the chick embryo. *Dev Biol* **135**, 124–132.

Marchionni, M. A., Goodearl, A. D., Chen, M. S., Bermingham-McDonogh, O., Kirk, C., Hendricks, M., Danehy, F., Misumi, D., Sudhalter, J. and Kobayashi, K. (1993). Glial growth factors are alternatively spliced erbB2 ligands expressed in the nervous system. *Nature* **362**, 312–318.

Marmigère, F. and Ernfors, P. (2007). Specification and connectivity of neuronal subtypes in the sensory lineage. *Nat Rev Neurosci* **8**, 114–127.

Maro, G. S., Vermeren, M., Voiculescu, O., Melton, L., Cohen, J., Charnay, P. and Topilko, P. (2004). Neural crest boundary cap cells constitute a source of neuronal and glial cells of the PNS. *Nat Neurosci* **7**, 930–938.

Martinsen, B. J. (2005). Reference guide to the stages of chick heart embryology. *Dev Dyn* **233**, 1217–1237.

Marusich, M. F., Furneaux, H. M., Henion, P. D. and Weston, J. A. (1994). Hu neuronal proteins are expressed in proliferating neurogenic cells. *J Neurobiol* **25**, 143–155.

Masui, T., Doi, R., Koshiba, T., Fujimoto, K., Tsuji, S., Nakajima, S., Koizumi, M., Toyoda, E., Tulachan, S., Ito, D., et al. (2003). RECK expression in pancreatic cancer: its correlation with lower invasiveness and better prognosis. *Clin Cancer Res* **9**, 1779–1784.

Matthews, H. K., Marchant, L., Carmona-Fontaine, C., Kuriyama, S., Larraín, J., Holt, M. R., Parsons, M. and Mayor, R. (2008). Directional migration of neural crest cells in vivo is regulated by Syndecan-4/Rac1 and non-canonical Wnt signaling/RhoA. *Development* **135**, 1771–1780.

McEvilly, R. J., Erkman, L., Luo, L., Sawchenko, P. E., Ryan, A. F. and Rosenfeld, M. G. (1996). Requirement for Brn-3.0 in differentiation and survival of sensory and motor neurons. *Nature* **384**, 574–577.

McGraw, H. F., Nechiporuk, A. and Raible, D. W. (2008). Zebrafish dorsal root ganglia neural precursor cells adopt a glial fate in the absence of neurogenin1. *J Neurosci* **28**, 12558–12569.

McGraw, H. F., Snelson, C. D., Prendergast, A., Suli, A. and Raible, D. W. (2012). Postembryonic neuronal addition in zebrafish dorsal root ganglia is regulated by Notch signaling. *Neural development* **7**, 23.

McKeown, S. J., Lee, V. M., Bronner-Fraser, M., Newgreen, D. F. and Farlie, P. G. (2005). Sox10 overexpression induces neural crest-like cells from all dorsoventral levels of the neural tube but inhibits differentiation. *Dev Dyn* **233**, 430–444.

McMahon, S. B., Armanini, M. P., Ling, L. H. and Phillips, H. S. (1994). Expression and coexpression of Trk receptors in subpopulations of adult primary sensory neurons projecting to identified peripheral targets. *Neuron* **12**, 1161–1171.

McPherson, C. E., Varley, J. E. and Maxwell, G. D. (2000). Expression and Regulation of Type I BMP Receptors during Early Avian Sympathetic Ganglion Development. *Dev Biol* **221**, 220–232.

Memberg, S. P. and Hall, A. K. (1995). Proliferation, differentiation, and survival of rat sensory neuron precursors in vitro require specific trophic factors. *Mol Cell Neurosci* **6**, 323–335.

Merzlyak, E. M., Goedhart, J., Shcherbo, D., Bulina, M. E., Shcheglov, A. S., Fradkov, A. F., Gaintzeva, A., Lukyanov, K. A., Lukyanov, S., Gadella, T. W. J., et al. (2007). Bright monomeric red fluorescent protein with an extended fluorescence lifetime. *Nat Meth* **4**, 555–557.

Meyer, D. and Birchmeier, C. (1995). Multiple essential functions of neuregulin in development. *Nature* **378**, 386–390.

Meyer, D., Yamaai, T., Garratt, A., Riethmacher-Sonnenberg, E., Kane, D., Theill, L. E. and Birchmeier, C. (1997). Isoform-specific expression and function of neuregulin. *Development* **124**, 3575–3586.

Milet, C. and Monsoro-Burq, A. H. (2012). Neural crest induction at the neural plate border in vertebrates. *Dev Biol* **366**, 22–33.

Minichiello, L., Piehl, F., Vazquez, E., Schimmang, T., Hökfelt, T., Represa, J. and Klein, R. (1995). Differential effects of combined trk receptor mutations on dorsal root ganglion and inner ear sensory neurons. *Development* **121**, 4067–4075.

Moriguchi, T. (2006). Gata3 participates in a complex transcriptional feedback network to regulate sympathoadrenal differentiation. *Development* **133**, 3871–3881.

Morikawa, Y., D'Autréaux, F., Gershon, M. D. and Cserjesi, P. (2007). Hand2 determines the noradrenergic phenotype in the mouse sympathetic nervous system. *Dev Biol* **307**, 114–126.

Morikawa, Y., Dai, Y.-S., Hao, J., Bonin, C., Hwang, S. and Cserjesi, P. (2005). The basic helix-loop-helix factor Hand2 regulates autonomic nervous system development. *Dev Dyn* **234**, 613–621.

Morikawa, Y., Zehir, A., Maska, E., Deng, C., Schneider, M. D., Mishina, Y. and Cserjesi, P. (2009). BMP signaling regulates sympathetic nervous system development through Smad4-dependent and -independent pathways. *Development* **136**, 3575–3584.

Morin-Kensicki, E. M. and Eisen, J. S. (1997). Sclerotome development and peripheral nervous system segmentation in embryonic zebrafish. *Development* **124**, 159–167.

Morioka, Y., Monypenny, J., Matsuzaki, T., Shi, S., Alexander, D. B., Kitayama, H. and Noda, M. (2009). The membrane-anchored metalloproteinase regulator RECK stabilizes focal adhesions and anterior-posterior polarity in fibroblasts. *Oncogene* **28**, 1454–1464.

Morris, J. K., Lin, W., Hauser, C., Marchuk, Y., Getman, D. and Lee, K. F. (1999). Rescue of the cardiac defect in ErbB2 mutant mice reveals essential roles of ErbB2 in peripheral nervous system development. *Neuron* **23**, 273–283.

Morrison, S. J., White, P. M., Zock, C. and Anderson, D. J. (1999). Prospective identification, isolation by flow cytometry, and in vivo self-renewal of multipotent mammalian neural crest stem cells. *Cell* **96**, 737–749.

Mu, X., Silos-Santiago, I., Carroll, S. L. and Snider, W. D. (1993). Neurotrophin receptor genes are expressed in distinct patterns in developing dorsal root ganglia. *J Neurosci* **13**, 4029–4041.

Mueller, T. D. and Nickel, J. (2012). Promiscuity and specificity in BMP receptor activation. *FEBS Lett* **586**, 1846–1859.

Mundell, N. A. and Labosky, P. A. (2011). Neural crest stem cell multipotency requires Foxd3 to maintain neural potential and repress mesenchymal fates. *Development* **138**, 641–652.

Muraguchi, T., Takegami, Y., Ohtsuka, T., Kitajima, S., (null), Omura, A., Miki, T., Takahashi, R., Matsumoto, N., Ludwig, A., et al. (2007). RECK modulates Notch signaling during cortical neurogenesis by regulating ADAM10 activity. *Nat Neurosci* **10**, 838–845.

Nakamura, S., Senzaki, K., Yoshikawa, M., Nishimura, M., Inoue, K. I., Ito, Y., Ozaki, S. and Shiga, T. (2008). Dynamic regulation of the expression of neurotrophin receptors by Runx3. *Development* **135**, 1703–1711.

Noda, M. and Takahashi, C. (2007). Recklessness as a hallmark of aggressive cancer. *Cancer Sci* **98**, 1659–1665.

Oh, J., Takahashi, R., Kondo, S., Mizoguchi, A., Adachi, E., Sasahara, R. M., Nishimura, S., Imamura, Y., Kitayama, H., Alexander, D. B., et al. (2001). The membrane-anchored MMP inhibitor RECK is a key regulator of extracellular matrix integrity and angiogenesis. *Cell* **107**, 789–800.

Paratore, C., Goerich, D. E., Suter, U., Wegner, M. and Sommer, L. (2001). Survival and glial fate acquisition of neural crest cells are regulated by an interplay between the transcription factor Sox10 and extrinsic combinatorial signaling. *Development* **128**, 3949–3961.

Parlier, D., Ariza, A., Christulia, F., Genco, F., Vanhomwegen, J., Kricha, S., Souopgui, J. and Bellefroid, E. J. (2008). Xenopus zinc finger transcription factor IA1 (Insm1) expression marks anteroventral noradrenergic neuron progenitors in Xenopus embryos. *Dev Dyn* **237**, 2147–2157.

Parr, B. A., Shea, M. J., Vassileva, G. and McMahon, A. P. (1993). Mouse Wnt genes exhibit discrete domains of expression in the early embryonic CNS and limb buds. *Development* **119**, 247–261.

Parras, C. M. (2002). Divergent functions of the proneural genes Mash1 and Ngn2 in the specification of neuronal subtype identity. *Genes Dev* **16**, 324–338.

Patterson, G. H. and Lippincott-Schwartz, J. (2004). Selective photolabeling of proteins using photoactivatable GFP. *Methods* **32**, 445–450.

Pattyn, A., Guillemot, F. and Brunet, J.-F. (2006). Delays in neuronal differentiation in Mash1/Ascl1 mutants. *Dev Biol* **295**, 67–75.

Pattyn, A., Morin, X., Cremer, H., Goridis, C. and Brunet, J. F. (1997). Expression and interactions of the two closely related homeobox genes Phox2a and Phox2b during neurogenesis. *Development* **124**, 4065–4075.

Pattyn, A., Morin, X., Cremer, H., Goridis, C. and Brunet, J. F. (1999). The homeobox gene Phox2b is essential for the development of autonomic neural crest derivatives. *Nature* **399**, 366–370.

Peirano, R. I. and Wegner, M. (2000). The glial transcription factor Sox10 binds to DNA both as monomer and dimer with different functional consequences. *Nucleic Acids Res* **28**, 3047–3055.

Peirano, R. I., Goerich, D. E., Riethmacher, D. and Wegner, M. (2000). Protein zero gene expression is regulated by the glial transcription factor Sox10. *Molecular and Cellular Biology* **20**, 3198–3209.

Perez, S. E., Rebelo, S. and Anderson, D. J. (1999). Early specification of sensory neuron fate revealed by expression and function of neurogenins in the chick embryo. *Development* **126**, 1715–1728.

Perron, M., Opdecamp, K., Butler, K., Harris, W. A. and Bellefroid, E. J. (1999). X-ngnr-1 and Xath3 promote ectopic expression of sensory neuron markers in the neurula ectoderm and have distinct inducing properties in the retina. *Proc Natl Acad Sci USA* **96**, 14996–15001.

Peters, R. (1986). Fluorescence microphotolysis to measure nucleocytoplasmic transport and intracellular mobility. *Biochim Biophys Acta* **864**, 305–359.

Pfaff, S. L., Mendelsohn, M., Stewart, C. L., Edlund, T. and Jessell, T. M. (1996). Requirement for LIM homeobox gene Isl1 in motor neuron generation reveals a motor neuron-dependent step in interneuron differentiation. *Cell* **84**, 309–320.

Pinco, O., Carmeli, C., Rosenthal, A. and Kalcheim, C. (1993). Neurotrophin-3 affects proliferation and differentiation of distinct neural crest cells and is present in the early neural tube of avian embryos. *J Neurobiol* **24**, 1626–1641.

Pingault, V., Bondurand, N., Kuhlbrodt, K., Goerich, D. E., Préhu, M. O., Puliti, A., Herbarth, B., Hermans-Borgmeyer, I., Legius, E., Matthijs, G., et al. (1998). SOX10 mutations in patients with Waardenburg-Hirschsprung disease. *Nat Genet* **18**, 171–173.

Pisano, J. M., Colón-Hastings, F. and Birren, S. J. (2000). Postmigratory Enteric and Sympathetic Neural Precursors Share Common, Developmentally Regulated, Responses to BMP2. *Dev Biol* **227**, 1–11.

Pomeranz, H. D. and Gershon, M. D. (1990). Colonization of the avian hindgut by cells derived from the sacral neural crest. *Dev Biol* **137**, 378–394.

Prendergast, A., Linbo, T. H., Swarts, T., Ungos, J. M., McGraw, H. F., Krispin, S., Weinstein, B. M. and Raible, D. W. (2012). The metalloproteinase inhibitor Reck is essential for zebrafish DRG development. *Development* **139**, 1141–1152.

Puente, X. S. and López-Otín, C. (2004). A genomic analysis of rat proteases and protease inhibitors. *Genome Res* **14**, 609–622.

Rabien, A., Burkhardt, M., Jung, M., Fritzsche, F., Ringsdorf, M., Schicktanz, H., Loening, S. A., Kristiansen, G. and Jung, K. (2007). Decreased RECK expression indicating proteolytic imbalance in prostate cancer is associated with higher tumor aggressiveness and risk of prostate-specific antigen relapse after radical prostatectomy. *Eur Urol* **51**, 1259–1266.

Radeke, M. J. and Feinstein, S. C. (1991). Analytical purification of the slow, high affinity NGF receptor: identification of a novel 135 kd polypeptide. *Neuron* **7**, 141–150.

Raible, D. W. and Eisen, J. S. (1994). Restriction of neural crest cell fate in the trunk of the embryonic zebrafish. *Development* **120**, 495–503.

Raible, D. W., Wood, A., Hodsdon, W., Henion, P. D., Weston, J. A. and Eisen, J. S. (1992). Segregation and early dispersal of neural crest cells in the embryonic zebrafish. *Dev Dyn* **195**, 29–42.

Rebelo, S., Reguenga, C., Osório, L., Pereira, C., Lopes, C. and Lima, D. (2007). DRG11 immunohistochemical expression during embryonic development in the mouse. *Dev Dyn* **236**, 2653–2660.

Reissmann, E., Ernsberger, U., Francis-West, P. H., Rueger, D., Brickell, P. M. and Rohrer, H. (1996). Involvement of bone morphogenetic protein-4 and bone morphogenetic protein-7 in the differentiation of the adrenergic phenotype in developing sympathetic neurons. *Development* **122**, 2079–2088.

Rickmann, M., Fawcett, J. W. and Keynes, R. J. (1985). The migration of neural crest cells and the growth of motor axons through the rostral half of the chick somite. *J Embryol Exp Morphol* **90**, 437–455.

Riethmacher, D., Sonnenberg-Riethmacher, E., Brinkmann, V., Yamaai, T., Lewin, G. R. and Birchmeier, C. (1997). Severe neuropathies in mice with targeted mutations in the ErbB3 receptor. *Nature* **389**, 725–730.

Rifkin, J. T., Todd, V. J., Anderson, L. W. and Lefcort, F. (2000). Dynamic Expression of Neurotrophin Receptors during Sensory Neuron Genesis and Differentiation. *Dev Biol* **227**, 465–480.

Rowe, A., Eager, N. S. and Brickell, P. M. (1991). A member of the RXR nuclear receptor family is expressed in neural-crest-derived cells of the developing chick peripheral nervous system. *Development* **111**, 771–778.

Ruberte, E., Dolle, P., Chambon, P. and Morriss-Kay, G. (1991). Retinoic acid receptors and cellular retinoid binding proteins. II. Their differential pattern of transcription during early morphogenesis in mouse embryos. *Development* **111**, 45–60.

Ruberte, E., Friederich, V., Morriss-Kay, G. and Chambon, P. (1992). Differential distribution patterns of CRABP I and CRABP II transcripts during mouse embryogenesis. *Development* **115**, 973–987.

Rubinstein, A. L., Lee, D., Luo, R., Henion, P. D. and Halpern, M. E. (2000). Genes dependent on zebrafish cyclops function identified by AFLP differential gene expression screen. *genesis* **26**, 86–97.

Ruit, K. G., Elliott, J. L., Osborne, P. A., Yan, Q. and Snider, W. D. (1992). Selective dependence of mammalian dorsal root ganglion neurons on nerve growth factor during embryonic development. *Neuron* **8**, 573–587.

Rychlik, J. L., Gerbasi, V. and Lewis, E. J. (2003). The interaction between dHAND and Arix at the dopamine β-hydroxylase promoter region is independent of direct dHAND binding to DNA. *J Biol Chem* **278**, 49652–49660.

Rychlik, J. L., Hsieh, M., Eiden, L. E. and Lewis, E. J. (2005). Phox2 and dHAND transcription factors select shared and unique target genes in the noradrenergic cell type. *Journal of molecular neuroscience* **27**, 281–292.

Sahin, U. (2004). Distinct roles for ADAM10 and ADAM17 in ectodomain shedding of six EGFR ligands. *J Cell Biol* **164**, 769–779.

Saint-Jeannet, J. P., He, X., Varmus, H. E. and Dawid, I. B. (1997). Regulation of dorsal fate in the neuraxis by Wnt-1 and Wnt-3a. *Proc Natl Acad Sci USA* **94**, 13713–13718.

Saito, T., Greenwood, A., Sun, Q. and Anderson, D. J. (1995). Identification by differential RT-PCR of a novel paired homeodomain protein specifically expressed in sensory neurons and a subset of their CNS targets. *Mol Cell Neurosci* **6**, 280–292.

Sasahara, R. M., Takahashi, C. and Noda, M. (1999). Involvement of the Sp1 site in ras-mediated downregulation of the RECK metastasis suppressor gene. *Biochem Biophys Res Commun* **264**, 668–675.

Sato, M. and Yost, H. J. (2003). Cardiac neural crest contributes to cardiomyogenesis in zebrafish. *Dev Biol* **257**, 127–139.

Sato, T., Takahoko, M. and Okamoto, H. (2006). HuC:Kaede, a useful tool to label neural morphologies in networks in vivo. *genesis* **44**, 136–142.

Schilling, T. F. and Kimmel, C. B. (1994). Segment and cell type lineage restrictions during pharyngeal arch development in the zebrafish embryo. *Development* **120**, 483–494.

Schimmelpfeng, K., Gögel, S. and Klämbt, C. (2001). The function of leak and kuzbanian during growth cone and cell migration. *Mech Dev* **106**, 25–36.

Schmidt, M., Lin, S., Pape, M., Ernsberger, U., Stanke, M., Kobayashi, K., Howard, M. J. and Rohrer, H. (2009). The bHLH transcription factor Hand2 is essential for the maintenance of noradrenergic properties in differentiated sympathetic neurons. *Dev Biol* **329**, 191–200.

Schneider, C., Wicht, H., Enderich, J., Wegner, M. and Rohrer, H. (1999). Bone morphogenetic proteins are required in vivo for the generation of sympathetic neurons. *Neuron* **24**, 861–870.

Schoenwolf, G. C. and Smith, J. L. (1990). Mechanisms of neurulation: traditional viewpoint and recent advances. *Development* **109**, 243–270.

Schreiner, S., Cossais, F., Fischer, K., Scholz, S., Bösl, M. R., Holtmann, B., Sendtner, M. and Wegner, M. (2007). Hypomorphic Sox10 alleles reveal novel protein functions and unravel developmental differences in glial lineages. *Development* **134**, 3271–3281.

Schweizer, G., Ayer-Le Lièvre, C. and Le Douarin, N. M. (1983). Restrictions of developmental capacities in the dorsal root ganglia during the course of development. *Cell Differ.* **13**, 191–200.

Serbedzija, G. N., Bronner-Fraser, M. and Fraser, S. E. (1989). A vital dye analysis of the timing and pathways of avian trunk neural crest cell migration. *Development* **106**, 809–816.

Serbedzija, G. N., Burgan, S., Fraser, S. E. and Bronner-Fraser, M. (1991). Vital dye labelling demonstrates a sacral neural crest contribution to the enteric nervous system of chick and mouse embryos. *Development* **111**, 857–866.

Serbedzija, G. N., Fraser, S. E. and Bronner-Fraser, M. (1990). Pathways of trunk neural crest cell migration in the mouse embryo as revealed by vital dye labelling. *Development* **108**, 605–612.

Shah, N. M., Groves, A. K. and Anderson, D. J. (1996). Alternative neural crest cell fates are instructively promoted by TGFbeta superfamily members. *Cell* **85**, 331–343.

Shah, N. M., Marchionni, M. A., Isaacs, I., Stroobant, P. and Anderson, D. J. (1994). Glial growth factor restricts mammalian neural crest stem cells to a glial fate. *Cell* **77**, 349–360.

Sharom, F. J. and Lehto, M. T. (2002). Glycosylphosphatidylinositol-anchored proteins: structure, function, and cleavage by phosphatidylinositol-specific phospholipase C. *Biochem Cell Biol* **80**, 535–549.

Shepherd, I. T. (2004). Roles for GFR 1 receptors in zebrafish enteric nervous system development. *Development* **131**, 241–249.

Shepherd, I. T. (2012). The boundaries of enteric neural crest definition in zebrafish.

Shoval, I., Ludwig, A. and Kalcheim, C. (2006). Antagonistic roles of full-length N-cadherin and its soluble BMP cleavage product in neural crest delamination. *Development* **134**, 491–501.

Sieber-Blum, M. and Cohen, A. M. (1980). Clonal analysis of quail neural crest cells: they are pluripotent and differentiate in vitro in the absence of noncrest cells. *Dev Biol* **80**, 96–106.

Sieber-Blum, M. and Sieber, F. (1984). Heterogeneity among early quail neural crest cells. *Brain Research* **316**, 241–246.

Silos-Santiago, I., Molliver, D. C., Ozaki, S., Smeyne, R. J., Fagan, A. M., Barbacid, M. and Snider, W. D. (1995). Non-TrkA-expressing small DRG neurons are lost in TrkA deficient mice. *J Neurosci* **15**, 5929–5942.

Silveira Corrêa, T. C., Massaro, R. R., Brohem, C. A., Taboga, S. R., Lamers, M. L., Santos, M. F. and Maria-Engler, S. S. (2010). RECK-mediated inhibition of glioma migration and invasion. *J Cell Biochem* **110**, 52–61.

Simizu, S., Takagi, S., Tamura, Y. and Osada, H. (2005). RECK-mediated suppression of tumor cell invasion is regulated by glycosylation in human tumor cell lines. *Cancer Res* **65**, 7455–7461.

Sliwkowski, M. X., Schaefer, G., Akita, R. W., Lofgren, J. A., Fitzpatrick, V. D., Nuijens, A., Fendly, B. M., Cerione, R. A., Vandlen, R. L. and Carraway, K. (1994). Coexpression of erbB2 and erbB3 proteins reconstitutes a high affinity receptor for heregulin. *J Biol Chem* **269**, 14661–14665.

Smeyne, R. J., Klein, R., Schnapp, A., Long, L. K., Bryant, S., Lewin, A., Lira, S. A. and Barbacid, M. (1994). Severe sensory and sympathetic neuropathies in mice carrying a disrupted Trk/NGF receptor gene. *Nature* **368**, 246–249.

Solnica-Krezel, L., Schier, A. F. and Driever, W. (1994). Efficient recovery of ENU-induced mutations from the zebrafish germline. *Genetics* **136**, 1401–1420.

Sommer, L., Ma, Q. and Anderson, D. J. (1996). neurogenins, a novel family of atonal-related bHLH transcription factors, are putative mammalian neuronal determination genes that reveal progenitor cell heterogeneity in the developing CNS and PNS. *Mol Cell Neurosci* **8**, 221–241.

Sommer, L., Shah, N., Rao, M. and Anderson, D. J. (1995). The cellular function of MASH1 in autonomic neurogenesis. *Neuron* **15**, 1245–1258.

Song, Q., Mehler, M. F. and Kessler, J. A. (1998). Bone morphogenetic proteins induce apoptosis and growth factor dependence of cultured sympathoadrenal progenitor cells. *Dev Biol* **196**, 119–127.

Song, S. Y., Son, H. J., Nam, E., Rhee, J. C. and Park, C. (2006). Expression of reversion-inducing-cysteine-rich protein with Kazal motifs (RECK) as a prognostic indicator in gastric cancer. *Eur J Cancer* **42**, 101–108.

Sonnenberg-Riethmacher, E., Miehe, M., Stolt, C. C., Goerich, D. E., Wegner, M. and Riethmacher, D. (2001). Development and degeneration of dorsal root ganglia in the absence of the HMG-domain transcription factor Sox10. *Mech Dev* **109**, 253–265.

Soppet, D., Escandon, E., Maragos, J., Middlemas, D. S., Reid, S. W., Blair, J., Burton, L. E., Stanton, B. R., Kaplan, D. R., Hunter, T., et al. (1991). The neurotrophic factors brain-derived neurotrophic factor and neurotrophin-3 are ligands for the trkB tyrosine kinase receptor. *Cell* **65**, 895–903.

Southard-Smith, E. M., Kos, L. and Pavan, W. J. (1998). Sox10 mutation disrupts neural crest development in Dom Hirschsprung mouse model. *Nat Genet* **18**, 60–64.

Span, P. N., Sweep, C. G. J., Manders, P., Beex, L. V. A. M., Leppert, D. and Lindberg, R. L. P. (2003). Matrix metalloproteinase inhibitor reversion-inducing cysteine-rich protein with Kazal motifs: a prognostic marker for good clinical outcome in human breast carcinoma. *Cancer* **97**, 2710–2715.

Squinto, S. P., Stitt, T. N., Aldrich, T. H., Davis, S., Bianco, S. M., Radziejewski, C., Glass, D. J., Masiakowski, P., Furth, M. E. and Valenzuela, D. M. (1991). trkB encodes a functional receptor for brain-derived neurotrophic factor and neurotrophin-3 but not nerve growth factor. *Cell* **65**, 885–893.

Stanke, M., Junghans, D., Geissen, M., Goridis, C., Ernsberger, U. and Rohrer, H. (1999). The Phox2 homeodomain proteins are sufficient to promote the development of sympathetic neurons. *Development* **126**, 4087–4094.

Steinthorsdottir, V., Stefansson, H., Ghosh, S., Birgisdottir, B., Bjornsdottir, S., Fasquel, A. C., Olafsson, O., Stefansson, K. and Gulcher, J. R. (2004). Multiple novel transcription initiation sites for NRG1. *Gene* **342**, 97–105.

Sternlicht, M. D. and Werb, Z. (2001). How matrix metalloproteinases regulate cell behavior. *Annu Rev Cell Dev Biol* **17**, 463–516.

Sun, Y., Dykes, I. M., Liang, X., Eng, S. R., Evans, S. M. and Turner, E. E. (2008). A central role for Islet1 in sensory neuron development linking sensory and spinal gene regulatory programs. *Nat Neurosci* **11**, 1283–1293.

Sun, Y., Nadal-Vicens, M., Misono, S., Lin, M. Z., Zubiaga, A., Hua, X., Fan, G. and Greenberg, M. E. (2001). Neurogenin promotes neurogenesis and inhibits glial differentiation by independent mechanisms. *Cell* **104**, 365–376.

Szabo, A., Dalmau, J., Manley, G., Rosenfeld, M., Wong, E., Henson, J., Posner, J. B. and Furneaux, H. M. (1991). HuD, a paraneoplastic encephalomyelitis antigen, contains RNA-binding domains and is homologous to Elav and Sex-lethal. *Cell* **67**, 325–333.

Takahashi, C., Sheng, Z., Horan, T. P., Kitayama, H., Maki, M., Hitomi, K., Kitaura, Y., Takai, S., Sasahara, R. M., Horimoto, A., et al. (1998). Regulation of matrix metalloproteinase-9 and inhibition of tumor invasion by the membrane-anchored glycoprotein RECK. *Proc Natl Acad Sci USA* **95**, 13221–13226.

Takemoto, N., Tada, M., Hida, Y., Asano, T., Cheng, S., Kuramae, T., Hamada, J.-I., Miyamoto, M., Kondo, S. and Moriuchi, T. (2007). Low expression of reversion-inducing cysteine-rich protein with Kazal motifs (RECK) indicates a shorter survival after resection in patients with adenocarcinoma of the lung. *Lung Cancer* **58**, 376–383.

Takenaka, K., Ishikawa, S., Kawano, Y., Yanagihara, K., Miyahara, R., Otake, Y., Morioka, Y., Takahashi, C., Noda, M., Wada, H., et al. (2004). Expression of a novel matrix metalloproteinase regulator, RECK, and its clinical significance in resected non-small cell lung cancer. *Eur J Cancer* **40**, 1617–1623.

Takenaka, K., Ishikawa, S., Yanagihara, K., Miyahara, R., Hasegawa, S., Otake, Y., Morioka, Y., Takahashi, C., Noda, M., Ito, H., et al. (2005). Prognostic significance of reversion-inducing cysteine-rich protein with Kazal motifs expression in resected pathologic stage IIIA N2 non-small-cell lung cancer. *Ann Surg Oncol* **12**, 817–824.

Takeuchi, T., Hisanaga, M., Nagao, M., Ikeda, N., Fujii, H., Koyama, F., Mukogawa, T., Matsumoto, H., Kondo, S., Takahashi, C., et al. (2004). The membrane-anchored matrix metalloproteinase (MMP) regulator RECK in combination with MMP-9 serves as an informative prognostic indicator for colorectal cancer. *Clin Cancer Res* **10**, 5572–5579.

Tamarin, A. and Boyde, A. (1977). Facial and visceral arch development in the mouse embryo: a study by scanning electron microscopy. *J Anat* **124**, 563–580.

Teng, L., Mundell, N. A., Frist, A. Y., Wang, Q. and Labosky, P. A. (2008). Requirement for Foxd3 in the maintenance of neural crest progenitors. *Development* **135**, 1615–1624.

Tessarollo, L., Tsoulfas, P., Martin-Zanca, D., Gilbert, D. J., Jenkins, N. A., Copeland, N. G. and Parada, L. F. (1993). trkC, a receptor for neurotrophin-3, is widely expressed in the developing nervous system and in non-neuronal tissues. *Development* **118**, 463–475.

Tessarollo, L., Vogel, K. S., Palko, M. E., Reid, S. W. and Parada, L. F. (1994). Targeted mutation in the neurotrophin-3 gene results in loss of muscle sensory neurons. *Proc Natl Acad Sci USA* **91**, 11844–11848.

Theiler, K. (2007). *The house mouse: atlas of embryonic development*. New York.

Thisse, C. and Thisse, B. (2008). High-resolution in situ hybridization to whole-mount zebrafish embryos. *UNKNOWN* **3**, 59–69.

Thisse, C., Thisse, B. and Postlethwait, J. H. (1995). Expression of snail2, a second member of the zebrafish snail family, in cephalic mesendoderm and presumptive neural crest of wild-type and spadetail mutant embryos. *Dev Biol* **172**, 86–99.

Tiveron, M. C., Hirsch, M. R. and Brunet, J. F. (1996). The expression pattern of the transcription factor Phox2 delineates synaptic pathways of the autonomic nervous system. *J Neurosci* **16**, 7649–7660.

Tojo, H., Kaisho, Y., Nakata, M., Matsuoka, K., Kitagawa, M., Abe, T., Takami, K., Yamamoto, M., Shino, A. and Igarashi, K. (1995). Targeted disruption of the neurotrophin-3 gene with lacZ induces loss of trkC-positive neurons in sensory ganglia but not in spinal cords. *Brain Research* **669**, 163–175.

Tsarovina, K., Pattyn, A., Stubbusch, J., Müller, F., van der Wees, J., Schneider, C., Brunet, J.-F. and Rohrer, H. (2004). Essential role of Gata transcription factors in sympathetic neuron development. *Development* **131**, 4775–4786.

Tsutsui, H., Karasawa, S., Shimizu, H., Nukina, N. and Miyawaki, A. (2005). Semi-rational engineering of a coral fluorescent protein into an efficient highlighter. *EMBO Rep* **6**, 233–238.

Udenfriend, S. and Kodukula, K. (1995). How glycosylphosphatidylinositol-anchored membrane proteins are made. *Annu. Rev. Biochem.* **64**, 563–591.

Ungos, J. M., Karlstrom, R. O. and Raible, D. W. (2003). Hedgehog signaling is directly required for the development of zebrafish dorsal root ganglia neurons. *Development* **130**, 5351–5362.

Vaessen, M. J., Meijers, J. H., Bootsma, D. and Van Kessel, A. G. (1990). The cellular retinoic-acid-binding protein is expressed in tissues associated with retinoic-acid-induced malformations. *Development* **110**, 371–378.

Vaglia, J. L. and Hall, B. K. (1999). Regulation of neural crest cell populations: occurrence, distribution and underlying mechanisms. *Int J Dev Biol* **43**, 95–110.

Valarché, I., Tissier-Seta, J. P., Hirsch, M. R., Martinez, S., Goridis, C. and Brunet, J. F. (1993). The mouse homeodomain protein Phox2 regulates Ncam promoter activity in concert with Cux/CDP and is a putative determinant of neurotransmitter phenotype. *Development* **119**, 881–896.

Van den Steen, P. E., Husson, S. J., Proost, P., Van Damme, J. and Opdenakker, G. (2003). Carboxyterminal cleavage of the chemokines MIG and IP-10 by gelatinase B and neutrophil collagenase. *Biochem Biophys Res Commun* **310**, 889–896.

van der Jagt, M. F. P., Sweep, F. C. G. J., Waas, E. T., Hendriks, T., Ruers, T. J. M., Merry, A. H. H., Wobbes, T. and Span, P. N. (2006). Correlation of reversion-inducing cysteine-rich protein with kazal motifs (RECK) and extracellular matrix metalloproteinase inducer (EMMPRIN), with MMP-2, MMP-9, and survival in colorectal cancer. *Cancer Lett* **237**, 289–297.

Varley, J. E. and Maxwell, G. D. (1996). BMP-2 and BMP-4, but not BMP-6, increase the number of adrenergic cells which develop in quail trunk neural crest cultures. *Exp Neurol* **140**, 84–94.

Varley, J. E., McPherson, C. E., Zou, H., Niswander, L. and Maxwell, G. D. (1998). Expression of a constitutively active type I BMP receptor using a retroviral vector promotes the development of adrenergic cells in neural crest cultures. *Dev Biol* **196**, 107–118.

Varley, J. E., Wehby, R. G., Rueger, D. C. and Maxwell, G. D. (1995). Number of adrenergic and islet-1 immunoreactive cells is increased in avian trunk neural crest cultures in the presence of human recombinant osteogenic protein-1. *Dev Dyn* **203**, 434–447.

Villanueva, S., Glavic, A., Ruiz, P. and Mayor, R. (2002). Posteriorization by FGF, Wnt, and retinoic acid is required for neural crest induction. *Dev Biol* **241**, 289–301.

Vincentz, J. W., VanDusen, N. J., Fleming, A. B., Rubart, M., Firulli, B. A., Howard, M. J. and Firulli, A. B. (2012). A Phox2- and Hand2-Dependent Hand1 cis-Regulatory Element Reveals a Unique Gene Dosage Requirement for Hand2 during Sympathetic Neurogenesis. *J Neurosci* **32**, 2110–2120.

Vize, P. D., McCoy, K. E. and Zhou, X. (2009). Multichannel wholemount fluorescent and fluorescent/chromogenic in situ hybridization in Xenopus embryos. *UNKNOWN* **4**, 975–983.

Wagner, M., Han, B. and Jessell, T. M. (1992). Regional differences in retinoid release from embryonic neural tissue detected by an in vitro reporter assay. *Development* **116**, 55–66.

Weinstein, B. M., Stemple, D. L., Driever, W. and Fishman, M. C. (1995). Gridlock, a localized heritable vascular patterning defect in the zebrafish. *Nat Med* **1**, 1143–1147.

Westerfield, M. *The zebrafish book. A guide for the laboratory use of zebrafish (Danio rerio)*. 4(null) ed. Eugene.

Weston, J. A. and Butler, S. L. (1966). Temporal factors affecting localization of neural crest cells in tbe chicken embryo. *Dev Biol* **14**, 246–266.

White, J. M. (2003). ADAMs: modulators of cell–cell and cell–matrix interactions. *Curr Opin Cell Biol* **15**, 598–606.

Wiedenmann, J., Ivanchenko, S., Oswald, F., Schmitt, F., Röcker, C., Salih, A., Spindler, K.-D. and Nienhaus, G. U. (2004). EosFP, a fluorescent marker protein with UV-inducible green-to-red fluorescence conversion. *Proc Natl Acad Sci USA* **101**, 15905–15910.

Wildner, H., Gierl, M. S., Strehle, M., Pla, P. and Birchmeier, C. (2008). Insm1 (IA-1) is a crucial component of the transcriptional network that controls differentiation of the sympatho-adrenal lineage. *Development* **135**, 473–481.

Wohl, S. G., Schmeer, C. W. and Isenmann, S. (2012). Neurogenic potential of stem/progenitor-like cells in the adult mammalian eye. *Progress in Retinal and Eye Research* **31**, 213–242.

Woldeyesus, M. T., Britsch, S., Riethmacher, D., Xu, L., Sonnenberg-Riethmacher, E., Abou-Rebyeh, F., Harvey, R., Caroni, P. and Birchmeier, C. (1999). Peripheral nervous system defects in erbB2 mutants following genetic rescue of heart development. *Genes Dev* **13**, 2538–2548.

Wright, D. E. and Snider, W. D. (1995). Neurotrophin receptor mRNA expression defines distinct populations of neurons in rat dorsal root ganglia. *J Comp Neurol* **351**, 329–338.

Wright, E. M., Snopek, B. and Koopman, P. (1993). Seven new members of the Sox gene family expressed during mouse development. *Nucleic Acids Res* **21**, 744.

Wright, E. M., Vogel, K. S. and Davies, A. M. (1992). Neurotrophic factors promote the maturation of developing sensory neurons before they become dependent on these factors for survival. *Neuron* **9**, 139–150.

Wu, X. and Howard, M. J. (2001). Two signal transduction pathways involved in the catecholaminergic differentiation of avian neural crest-derived cells in vitro. *Mol Cell Neurosci* **18**, 394–406.

Xiang, M., Gan, L., Zhou, L., Klein, W. H. and Nathans, J. (1996). Targeted deletion of the mouse POU domain gene Brn-3a causes selective loss of neurons in the brainstem and trigeminal ganglion, uncoordinated limb movement, and impaired suckling. *Proc Natl Acad Sci USA* **93**, 11950–11955.

Xu, H., Firulli, A. B., Zhang, X. and Howard, M. J. (2003). HAND2 synergistically enhances transcription of dopamine-β-hydroxylase in the presence of Phox2a. *Dev Biol* **262**, 183–193.

Xu, J., Wu, S. and Shi, X. (2010). Expression of matrix metalloproteinase regulator, RECK, and its clinical significance in osteosarcoma. *J Orthop Res* **28**, 1621–1625.

Yamamoto, M., Ko, L. J., Leonard, M. W., Beug, H., Orkin, S. H. and Engel, J. D. (1990). Activity and tissue-specific expression of the transcription factor NF-E1 multigene family. *Genes Dev* **4**, 1650–1662.

Yang, C., Kim, H. S., Seo, H. and Kim, K. S. (1998). Identification and characterization of potential cis-regulatory elements governing transcriptional activation of the rat tyrosine hydroxylase gene. *J Neurochem* **71**, 1358–1368.

Yang, H.-J., Wang, K.-C., Chi, J. G., Lee, M.-S., Lee, Y.-J., Kim, S.-K., Lee, C. S. and Cho, B.-K. (2006). Cytokinetics of secondary neurulation in chick embryos: Hamburger and Hamilton stages 16–45. *Childs Nerv Syst* **22**, 567–571.

Yoshida, D., Nomura, R. and Teramoto, A. (2008). Regulation of cell invasion and signalling pathways in the pituitary adenoma cell line, HP-75, by reversion-inducing cysteine-rich protein with kazal motifs (RECK). *J Neurooncol* **89**, 141–150.

Yoshikawa, M., Senzaki, K., Yokomizo, T., Takahashi, S., Ozaki, S. and Shiga, T. (2007). Runx1 selectively regulates cell fate specification and axonal projections of dorsal root ganglion neurons. *Dev Biol* **303**, 663–674.

Zellmer, E., Zhang, Z., Greco, D., Rhodes, J., Cassel, S. and Lewis, E. J. (1995). A homeodomain protein selectively expressed in noradrenergic tissue regulates transcription of neurotransmitter biosynthetic genes. *J Neurosci* **15**, 8109–8120.

Zhang, D., Sliwkowski, M. X., Mark, M., Frantz, G., Akita, R., Sun, Y., Hillan, K., Crowley, C., Brush, J. and Godowski, P. J. (1997). Neuregulin-3 (NRG3): a novel neural tissue-enriched protein that binds and activates ErbB4. *Proc Natl Acad Sci USA* **94**, 9562–9567.

Zhou, X. F. and Rush, R. (1995). Sympathetic neurons in neonatal rats require endogenous neurotrophin-3 for survival. *J Neurosci* **15**, 6521–6530.

Zirlinger, M., Lo, L., McMahon, J., McMahon, A. P. and Anderson, D. J. (2002). Transient expression of the bHLH factor neurogenin-2 marks a subpopulation of neural crest cells biased for a sensory but not a neuronal fate. *Proc Natl Acad Sci USA* **99**, 8084–8089.

Zou, M., Li, S., Klein, W. H. and Xiang, M. (2012). Brn3a/Pou4f1 regulates dorsal root ganglion sensory neuron specification and axonal projection into the spinal cord. *Dev Biol* **364**, 114–127.